

FINAL REPORT

on

SMELT-WATER EXPLOSIONS

to

FOURDRINIER KRAFT BOARD INSTITUTE, INC.

January 31, 1973

by

H. H. Krause, R. Simon, and A. Levy

Copyright© 1973
FOURDRINIER KRAFT BOARD INSTITUTE, INC.

BATTELLE
Columbus Laboratories
505 King Avenue
Columbus, Ohio 43201

Battelle is not engaged in research for advertising, sales promotion, or publicity purposes, and this report may not be reproduced in full or in part for such purposes.

24/10

MANAGEMENT SUMMARY

Previous work has shown that the violent and frequently damaging explosions that may occur when water contacts smelt in a recovery furnace, as a result of pressure-part failure or other cause, are physical explosions resulting from the rapid expansion of steam. Investigation of this type of explosion phenomenon has been the purpose of this program.

The particular objective of this research was to identify the properties of the smelt-water system that are important to the explosion process and to devise means for reducing the risk or severity of explosions by methods technically and economically compatible with the kraft process. For this purpose, a laboratory experimental program was conducted both with synthetic smelts of various compositions and with kraft-mill smelts in an effort to correlate physical properties and chemical composition of smelts with the frequency and violence of explosions resulting from smelt-water interactions. A computer model of a probable explosion mechanism also was developed.

Reproducible results were obtained from explosion experiments performed with laboratory equipment designed to introduce small amounts of water into molten smelts by different methods. These experiments demonstrated that, for a given smelt temperature and composition, a high incidence of explosion will result when the water is trapped beneath the smelt. It should be pointed out that the experimental results reported in this program are all derived from small-scale smelt-water explosions carried out in the laboratory. Although the same explosion mechanism appears to be involved in both laboratory and furnace explosions, the extent to which the laboratory result can be extrapolated to full-scale recovery furnace-operations is not yet known.

The laboratory experiments showed that both kraft-mill smelts and synthetic smelts can be exploded under the same water-injection conditions. It has been possible to relate chemical composition to the incidence of explosions. These results can be summarized as follows:

- The major smelt component, Na_2CO_3 , is not in itself explosive, according to all available evidence.
- The incidence of explosion increases with increasing amounts of Na_2S in the smelt.
- Smelts containing relatively small amounts of Na_2S can be greatly sensitized to explosion by the minor smelt components: NaCl or NaOH .
- Other minor smelt components, K_2CO_3 , Na_2SO_4 , and Na_2SO_3 , in decreasing order, are mild sensitizers for explosion.
- The addition of calcium carbonate or sodium aluminate, which are not ordinarily in smelt, reduces explosion incidence when added to smelt in a small amount (5 wt %). The inhibitive effect increases with temperature and appears to be related to the release of CO_2 in the smelt.

No single physical property of smelt (measured in the laboratory program or considered in the computer model of the explosion) changes rapidly enough with composition to account for the large differences in explosiveness that have been observed for different compositions.

However, smelt compositions with higher rates of CO₂ gas release from the Na₂CO₃ in the smelt are less explosive. This observation is in agreement with the requirements of the computer model developed to explain the explosion mechanism.

The computer model simulates the behavior of a body of water immersed in smelt. This model takes into account the pertinent physical characteristics of water, steam, and smelt of different compositions, as well as the effects of various concentrations of CO₂ gas in the steam. The computations show that only extremely rapid and thorough mixing of smelt and water can produce the very high initial rates of heat input needed for the explosively rapid steam generation. This rapid mixing may be the result of high-velocity jets of fluid formed during the process of growth and the collapse of small steam-vapor cavities near the water body. The computer model predicts that those conditions resulting in a greater flow of CO₂ gas into the steam-water body will inhibit this hypothesized mechanism for the smelt-water explosion.

Consideration of the basic equations of the computer model has resulted in the formulation of two critical dimensionless parameters that can be applied to smelt-water interactions. One involves the rate of heat input to the water, and, the other, the rate of gas input. The amount of mechanical energy developed by smelt-water explosions under various conditions also has been computed. A typical result is that a pound of water with an initial heat input rate equivalent to 2×10^6 Btu/sec per square foot of outer surface area would generate about as much explosive mechanical energy as 1/2 pound of TNT.

To obtain this high initial rate of heat input requires a much expanded surface contact area between the water and the smelt. The calculations showed that the collapse of a steam-filled cavity in the smelt is capable of producing the high velocity jets of smelt needed to mix with the water and to cause an explosion. The collapse of the steam-filled cavity can be inhibited by the presence of sufficient gas in the cavity. Increased CO₂ gas release from the smelt may thus account for the action of explosion-inhibiting smelt additives.

The results of this research program suggest that the likelihood of completely eliminating the possibility of smelt-water explosions in the kraft process is small. The variables which control and influence the triggering and the explosion mechanisms are extremely complex. It does not appear that a single or simple combination of physical or chemical smelt parameters controls the explosion process either in the laboratory or in the plant.

Even accepting the premise that the achievement of a complete practical solution is remote, reduced incidence or severity of explosion would be beneficial to the kraft industry. Additional understanding of the explosion phenomenon may ultimately lead to such a partial solution of the problem.

On this basis, additional laboratory and explosion-model research utilizing new approaches is recommended to investigate:

- The inhibition of explosion by gas release from the smelt.
- The mode of contact of smelt and the water phase.
- The validity of the two explosion-controlling parameters suggested by the analytical model of the explosion process.
- The further development of the analytical model for the explosion mechanism.

TABLE OF CONTENTS

	Page
INTRODUCTION	1
Background	1
Objectives	3
SUMMARY	3
CONCLUSIONS	6
RECOMMENDATIONS FOR FUTURE WORK	6
DISCUSSION OF EXPERIMENTAL RESULTS	8
Laboratory Techniques	8
Influence of Smelt Composition on Explosiveness	9
Major Smelt Components	9
Minor Smelt Components	11
Sodium Chloride	11
Sodium Sulfate	12
Sodium Hydroxide	13
Potassium Carbonate	14
Sodium Sulfite	14
Kraft-Mill Smelts	15
AID Analysis	18
Correlation of Explosiveness With Smelt Composition	19
Explosion Inhibitors	19
Influence of Physical Properties of Smelt on Explosiveness	22
Viscosity	22
Surface Tension	24
Density	26
Sound Velocity	27
Electrical Conductivity	27
Carbonate Decomposition Studies	29
Cavitation Experiments	29
Vacuum Decomposition Experiments	30
Pressure-Transducer Experiments	31
DISCUSSION OF COMPUTER MODEL	32
Nature of Physical Explosions	32
Qualitative Description of Smelt-Water Explosion Model	35
Results of Model Computations	36
The Main Explosion	36
The Initiating Mechanism	39
Explosion Damage Considerations	42
Critical Parameter Analysis	44
REFERENCES	47

TABLE OF CONTENTS
(Continued)

	Page
APPENDIXES	
APPENDIX A. EXPERIMENTAL TECHNIQUES AND DATA	A-1
APPENDIX B. SMELT-WATER EXPLOSION MODEL COMPUTER PROGRAM	B-1
APPENDIX C. LIMITATIONS OF THE PRESENT MODEL	C-1
APPENDIX D. FORMULATION OF DIMENSIONLESS PARAMETERS	D-1

LIST OF TABLES

Table 1. Incidence of Reported Critical Exposures and Smelt-Water Explosions	2
Table 2. Effect of NaCl on Smelt Explosiveness	11
Table 3. Maximum Explosion Temperatures of Smelt Compositions at Various Injection Pressures	12
Table 4. Effect of Na ₂ SO ₄ on Smelt Explosiveness	13
Table 5. Effect of K ₂ CO ₃ on Smelt Explosiveness	14
Table 6. Effects of Na ₂ SO ₃ on Smelt Explosiveness	15
Table 7. Explosion Threshold Values for Water Injection Into Kraft-Mill Smelts	16
Table 8. Results of Water-Injection Explosion Experiments and Chemical Analyses of Typical Kraft-Mill Smelts	17
Table 9. Explosion Incidence With NaAlO ₂ or CaCO ₃ in Smelt Mixtures, Using the Water-Injection Method	20
Table 10. Explosion Incidence With Carbonate Additives in Smelt, Using the Dropped-Tube Method	21
Table 11. Effect of Various Salts on the Decomposition Rate of Na ₂ CO ₃ at 1830 F	30
Table 12. Known Physical Explosion Systems	33
Table A-1. Explosion Intensities	A-6
Table A-2. Attenuation of Ultrasonic Energy in Molten Salt Compositions Over a Path Length of 1 Inch	A-10

LIST OF TABLES
(Continued)

	Page
Table A-3. Vacuum Decomposition of Na_2CO_3	A-15
Table A-4. Reduction of Na_2CO_3 Decomposition by Sensitizers	A-15
Table B-1. Listing of Molten Salts – Water Explosion Model Computer Program	B-6

LIST OF FIGURES

Figure 1. Maximum Temperatures for Which High Explosion Probability was Observed in Na_2CO_3 – Na_2S Mixtures	10
Figure 2. Comparison of Water Injections and Sodium Chloride Additions Required to Explode Kraft-Mill Smelts	16
Figure 3. Automatic Interaction Detector Analysis of Kraft-Mill Smelts	19
Figure 4. Viscosities of Molten Salts	23
Figure 5. Surface Tension of Molten Salts as a Function of Temperature	25
Figure 6. Densities of Molten Salts	26
Figure 7. Velocity of Sound in Molten Salts	28
Figure 8. Pressure Waves From Explosions as Detected by a Transducer	32
Figure 9. Development of Smelt-Water Explosion With 1 Pound of Water, for an Initial Heat-Input of 2 Million Btu/Ft ² /Sec	37
Figure 10. Dependent Variables of Explosion of 1 Pound of Water as Functions of Initial Rate of Heat Input	39
Figure 11. Pressure as a Function of Time for Triggering Globule, no Added CO_2 Input	41
Figure 12. Pressure as a Function of Time for Triggering Globule With CO_2 Gas Added	41
Figure A-1. Diagram of Piston-Type Water Injection Apparatus	A-2
Figure A-2. Detail of the Piston-Type Water Injection Apparatus	A-2
Figure A-3. Schematic of Direct Gas-Pressure Injection Apparatus	A-3

LIST OF FIGURES
(Continued)

	Page
Figure A-4. Electrical Circuit for Controlling Short-Pulse Water Injection	A-4
Figure A-5. Apparatus Used for Dropped-Tube Explosion Experiments	A-5
Figure A-6. Schematic of Apparatus for Ultrasonic Measurements	A-8
Figure A-7. Apparatus Used for Cavitation Experiments	A-12
Figure A-8. Apparatus for Vacuum Decomposition Experiments	A-14
Figure A-9. Infrared Spectrum of Typical Kraft Mill Smelt	A-16
Figure A-10. Apparatus for Pressure Transducer Experiments	A-17
Figure A-11. Schematic of Apparatus for Physical-Property Measurements	A-18
Figure B-1. Direct and Cavitation-Collapse Pressure Pulses for Ambient Pressure and for a Superimposed Variable Pressure	B-5

FINAL REPORT
SMELT-WATER EXPLOSIONS

by

H. H. Krause, R. Simon, and A. Levy

INTRODUCTION

The research program described in this report is a fundamental investigation of the smelt-water explosion phenomenon. Previous research on smelt-water explosions demonstrated that the explosion process is physical rather than chemical. Although chemical processes in the smelt-water system may affect certain critical physical phenomena such as the rate of energy build up in the water, the forces generated result primarily from rapid formation of steam. Explosion probability is known to depend on smelt composition and on that of the aqueous phase. As a consequence, this research program was aimed at developing understanding of the explosion mechanism and means of reducing explosion frequency by investigating both experimentally and theoretically the effects of the physical properties of the systems on its explosiveness.

This is the final report on the project and the work performed from October 1, 1969, through September 30, 1972.

Background

Explosions have occurred from time to time throughout the history of recovery furnaces, but many of these explosions were the result of improper handling of the auxiliary fuel system rather than the result of smelt-water interactions. In 1962, as a result of concern about the frequency and severity of recovery furnace explosions, the Black Liquor Recovery Boiler Advisory Committee was formed. The purpose of this committee was to contribute to the safety of operations by collecting and disseminating information on problems affecting recovery furnace operation. One of the major results of this Committee's activities has been the formulation of recommendations relative to the design, control, and operation of auxiliary fuel systems. Since the advent of these recommendations on the handling of auxiliary fuels, the frequency of auxiliary fuel explosions has dramatically decreased.

In addressing smelt-water explosions, the Committee has reconstructed the record of recovery furnace explosions as far back as 1948. Since 1965, the Committee has also attempted to record critical exposures — defined as contacts between water and smelt in recovery furnaces that did not result in an explosion. The number of critical exposures and smelt-water explosions that have been reported in the kraft industry are shown in Table 1. While the table shows only a few explosions from 1948 to 1958, this low frequency probably results because only major explosions during this period were uncovered when the history of past explosions was investigated. From 1958 through 1964, only two or three smelt-water explosions occurred each year.

However, from 1965 through 1971, 28 of the 50 smelt-water explosions that have been reported since 1948 took place. From 1965, 51 critical exposures were reported which means that over all about one third of the reported smelt-water contacts since 1965 resulted in explosions.

TABLE 1. INCIDENCE OF REPORTED CRITICAL EXPOSURES AND SMELT-WATER EXPLOSIONS

Year	Exposures	Explosions
1948	No record	2
1951	Ditto	3
1955	"	1
1958	"	2
1959	"	2
1960	"	2
1961	"	3
1962	"	2
1963	"	2
1964	"	3
1965	1	4
1966	6	6
1967	3	2
1968	10	1
1969	12	5
1970	13	2
1971	6	8

The Smelt-Water Research Group, formed in 1963 by a large number of companies that produce kraft pulp in the United States and Canada was organized for the purpose of conducting research on smelt-water explosions. This group contracted to have the research carried out in the laboratories of The Babcock & Wilcox Company and Combustion Engineering, Inc. The Institute of Paper Chemistry coordinated the two research projects. The results of these investigations showed convincingly that the forces generated in the smelt-water explosion result from explosively rapid steam generation. Thus the explosion is physical, rather than chemical, although chemical processes in the smelt-water system may affect certain critical physical phenomena such as the rate of energy build-up in the water. It was demonstrated in the laboratory that the incidence and intensity of explosion varies with smelt composition and the composition of the aqueous phase.

With a view to complementing and extending the Babcock & Wilcox and Combustion Engineering investigations conducted for the Smelt-Water Research Group, directions for future research were sought by the Fourdrinier Kraft Board Institute, Inc. Studies were conducted in 1967-1968 by both Arthur D. Little, Incorporated, and the Battelle-Columbus Laboratories on the feasibility of further research in the area of smelt-water explosions. Both organizations indicated that additional research was warranted and suggested programs for fundamental research into the mechanism of smelt-water explosions, with the intent that knowledge of the mechanism would suggest means of preventing the explosions.

The research program summarized in this report is an outgrowth of these feasibility studies, and had available as a starting point all of the information developed for the Smelt-Water

Research Group and the FKI. At that point in time the major unexplained aspect of the explosion process was the primary mechanism by which the explosion process was initiated. Extremely high rates of heat transfer from the smelt into the water were deemed to be necessary to generate steam at an explosive rate. Turbulent mixing that serves to increase the contact area between the smelt and the water and to remove the insulating layer of steam was hypothesized as the most likely mechanism for smelt-water explosions.

Objectives

The specific objectives of this research program were: (1) to identify the physical properties of the smelt-water system that are important in determining explosive tendencies, (2) to evaluate quantitatively the relationships of these properties to the incidence of explosion, and (3) to devise methods for reducing explosion incidence that are technically and economically compatible with the kraft process.

A general objective was to achieve an understanding of explosions from laboratory-scale experiments, with the hope that this information could in turn be related to recovery-furnace operations.

SUMMARY

This research program has consisted of three concurrent efforts: (1) a detailed laboratory study of the incidence of explosion in smelt-water contacts as influenced by the composition of the molten salt mixture, (2) measurement of those properties of the smelt-water system that were deemed to be most significant in the explosion process, and (3) a computer model of the explosion mechanism, based on the physical properties of the smelt-water system.

Laboratory-scale explosion experiments were performed with equipment designed either for injection of small amounts of water into molten smelts or for trapping it under the smelt. The major and the minor components of kraft smelts were studied for their effects on smelt explosiveness, and sufficient data were obtained to permit ranking of these components as to their contribution to the explosiveness of smelts. Of the major smelt components, Na_2CO_3 could not be exploded. The other major smelt component, Na_2S , proved to be an explosion sensitizer. The explosion incidence of a smelt mixture increased as the amount of Na_2S in the mixture was increased. Of the minor smelt components, NaCl and NaOH were found to be strong explosion sensitizers. Weight for weight, these compounds ranked above Na_2S in this respect. Other minor smelt components that proved to be mild sensitizers for explosion were, in descending order: K_2CO_3 , Na_2SO_4 , and Na_2SO_3 .

Selected kraft-mill smelts studied in this program were found to be explosive under the same laboratory conditions as those employed with the synthetic smelt mixtures. The laboratory data on the explosiveness of the kraft-mill smelts, as obtained by injection of water, were correlated with the chemical composition of these smelts. For this purpose a mathematical treatment known as "automatic interaction detector analysis" was used. This analysis showed that the 12 smelts studied could be ranked as to relative explosiveness on the basis of three of

the eight components in the smelt composition: NaCl, Na₂S, and K₂O, in that order. Experiments with synthetic smelt mixtures further support these results.

Investigation of explosion inhibitors showed that the addition of either CaCO₃ or NaAlO₂ reduced the explosion incidence in molten smelt compositions regardless of the method by which water was introduced. The inhibitive effect increases with increasing temperature and, for CaCO₃, it appears to be related to the CO₂ released by decomposition of the carbonate. NaAlO₂ may catalyze the release of CO₂ from the Na₂CO₃ of the smelt, to achieve the same result.

Four physical properties of smelt expected to be of significance to the explosion process were measured: (1) viscosity, (2) surface tension, (3) density, (4) sound velocity. Viscosity values for typical smelt compositions were found to range from about 4 centipoises at 1500 F down to 1 centipoise at 1800 F. As the amount of Na₂S in the mixture increased, the viscosity decreased. The slope of the viscosity-versus-temperature curve proved to be very steep, and the changes in viscosity with temperature are as great as the changes with composition.

The surface tension of the smelt mixtures decreased as the Na₂CO₃ in the mixture was replaced by NaCl, but the effect of Na₂S was slight compared to that of NaCl. Values ranged from about 200 dynes per centimeter for pure Na₂CO₃ and a mixture containing 30 weight percent* Na₂S, down to about 180 dynes per centimeter for a smelt containing 5 percent NaCl. The surface tension of the molten salts was found to decrease only slightly with temperature, and compositional effects were greater than temperature effects for this property.

The densities of the molten smelt mixtures ranged from about 1.95 g/cm³ at 1500 F to about 1.85 g/cm³ at 1800 F. The effect on density of replacing Na₂CO₃ with NaCl was greater than that resulting from substitution by Na₂S. Compositional effects on density were about the same magnitude as temperature effects.

Sound-velocity measurements in the molten salts showed that the value for Na₂S lies about midway between those of Na₂CO₃ and NaCl. Typical smelt composition values would lie between Na₂S and Na₂CO₃, ranging from about 7500 feet per second at 1500 F down to about 7100 feet per second at 1800 F. The effect of varying composition on sound velocity was about as great as that of temperature.

To test the hypothesis that the release of CO₂ from the Na₂CO₃ in the smelt plays a part in the explosion mechanism, two types of decomposition experiments were performed. The near-vacuum conditions that would exist in an expanding bubble of steam were simulated by cavitation experiments in which the molten smelt was stirred rapidly. The CO₂ release from the Na₂CO₃ in the smelt increased by a factor of two at a stirring speed of 3700 to 3900 rpm. This sudden increase indicated the onset of cavitation, which would affect the explosion mechanism.

The second type of experiment consisted of vacuum decomposition in which the rate of release of CO₂ from the Na₂CO₃ was measured. It was observed that the explosion sensitizers, Na₂S and NaCl, caused a significant reduction in the rate of CO₂ evolution. On the other hand, the explosion inhibitors, CaCO₃ and NaAlO₂, provided an increase in the rate of CO₂ released. These effects were both in the right direction to support the hypothesized effect on the explosion mechanism.

*All smelt compositions given in this report are weight percent.

The time scale of the laboratory explosions was investigated by attaching a pressure transducer to an alumina rod inserted into the molten salt during the explosion. When the explosion occurred, the shock wave generated in the smelt was picked up by the rod, sensed by the transducer, and registered on an oscilloscope. The explosion was found to occur within 1 or 2 milliseconds after the injection of water. Peaks as high as 40 psi were recorded during these experiments. However, the pressure variations so obtained cannot be directly related to the actual pressures developed by the explosion.

The infrared spectra of various smelt mixtures were investigated to determine whether or not differences in composition between explosive and nonexplosive smelts could be so detected. However, as the same components appeared in the infrared spectra of both, the only differences were in the relative quantities of some of the components. Hence this technique could not be used as a screening device to detect explosive smelts.

A computer model has been developed to describe the physical explosion of steam resulting from the interaction of molten smelt and water. This model has taken into account the pertinent physical characteristics of water, steam, and smelt of different compositions, as well as the effects of various concentrations of CO_2 gas resulting from the decomposition of the Na_2CO_3 . The computations showed that only extremely rapid and thorough mixing of smelt and water could produce the very high rates of heat input needed for the generation of violent steam explosions. Consideration of the triggering mechanism showed that the energy needed to form the required contact surface between the smelt and a pound of water is much less than 1 Btu, which is negligibly small. To obtain the necessary heat transfer, sufficient smelt must be injected rapidly into the pound of water. The kinetic energy required could be provided by the cooperative action of several small triggering globules around the main water body. Small steam globules in smelt, which are imploding and at the same time moving toward the main body of water, can introduce jets of smelt into the main water body and thereby produce the rapid mixing needed to achieve a heat-transfer rate great enough to produce the main explosion.

Computations on the main explosion showed that the physical explosion of 1 pound of water at a heat input rate of 2×10^6 Btu/ft² per second will generate 300,000 to 400,000 ft-lb of mechanical energy in the surrounding smelt, and is equivalent to the mechanical energy of explosion of about 1/2 pound of TNT immersed in water.

The analysis also has resulted in the derivation of two critical dimensionless parameters whose factors consist of physical constants, dynamic variables, and length dimensions. One parameter, involving the rate of heat influx into the water, is applicable primarily to the main explosion. The second parameter, involving the rate of gas influx to the steam globule, pertains to the triggering mechanism, i.e., the rapid injection of smelt into the water body as a result of the collapse of nearby small steam and gas cavities in the smelt.

The computations also revealed that the presence of enough CO_2 in the small collapsing steam globule will dampen the fluctuations of pressure, temperature, and radius and also stabilize the radial symmetry of the bubble motion. The effect is to inhibit the triggering of the main explosion. According to the explosion model, the most effective way to inhibit the explosion is to interfere with the triggering mechanism by introducing carbon dioxide into the steam globule. The experimental program demonstrated that the most effective way of introducing CO_2 was through the decomposition of CaCO_3 added to the smelt.

CONCLUSIONS

On the basis of the laboratory data and the computer model of the explosion mechanism, the following conclusions can be drawn:

- Smelt composition is of major importance in determining explosiveness. Sulfide and chloride concentrations exert the greatest influence.
- The mode of contact between water and smelt is of major importance in determining explosiveness. The degree of confinement of water within the smelt, the relative velocity of the two phases, and the relative amounts of smelt and water involved are significant.
- No single physical property of the smelt varies sufficiently with composition to be the determinant factor in explosiveness. However, two dimensionless parameters appear to be significant:
 - (a) One whose value is influenced predominantly by the rate of gas input to the steam globule (influences the triggering mechanism)
 - (b) Another whose value is influenced predominantly by the initial rate of heat input to the water (controls the main explosion).
- The release of sufficient carbon dioxide from the smelt to minimize the collapse of the steam globule, which has been hypothesized as the triggering mechanism during smelt-water contact, could prevent the explosion.
- Extremely intimate mixing of water and smelt is required to achieve an initial heat-transfer rate great enough to result in explosion. Smelt and water must mix rapidly enough to generate about a thousandfold increase in contact surface in about a millisecond during the initial phase of the explosion. Once this condition is achieved, each pound of water involved can exert the explosive force of about 1/2 pound of TNT.

RECOMMENDATIONS FOR FUTURE WORK

The information obtained from this program suggests that the likelihood of eliminating smelt-water explosions in the kraft process is small. The variables that control and influence the triggering and explosion mechanisms are extremely complex. No single or simple combination of physical or chemical smelt parameters appears to control the explosion process either in the laboratory or in the plant.

Although a complete practical solution appears remote, a reduction in the incidence or severity of explosion would be beneficial to the kraft industry. Additional understanding of the explosion phenomenon could lead to such a partial solution of the problem. For example, obtaining an understanding of why pure Na_2CO_3 and water do not explode could result in recommendations for operating conditions that would reduce the incidence or severity of explosions.

If additional research to solve the smelt-water-explosion problem were to be found desirable, several new avenues of approach are recommended. Both an experimental program and analytical modeling of the explosion are considered important. The laboratory research to be carried out in a short-range program would comprise:

- Investigating the role of gas evolution in reducing explosion incidence. This work would emphasize materials that may catalyze decomposition of the carbonate in smelt when in contact with water.
- Investigating the influence of contact mode between water and smelt in causing explosions. This would require studying such factors as the relative motion between water and smelt, the wettability of the smelt, and superheat effects in the water.

The analytical modeling considered most likely to yield practical benefits as a result of improved understanding in a relatively short period of time would be:

- An approach to the explosion-triggering mechanism which would investigate the thermodynamics of the interface layer between the water body and the smelt, and consider superheating, the mechanisms of heat and mass transfer, CO_2 gas generation, and the effects of the motional instabilities in the expansion of the interface layer as steam is generated.
- The effects of a given amount of initially hot smelt with a specified degree of fragmentation within the main water body, after injection by the triggering mechanism. This approach should permit the rates of heat and gas generation to be inferred rather than assumed. A more accurate analysis of the thermodynamics of the explosion to be made would enable relating presently assumed factors in the dimensionless parameter analysis to additional physical and chemical properties of the smelt.

The long-range research program would be aimed at a full understanding of the smelt-water explosion phenomenon. For this purpose, differences between molten Na_2CO_3 , which is not explosive, and sensitized mixtures containing NaCl or Na_2S would be studied. Smelt compositions as such would be used as needed to verify the applicability of the results. The experimental program would consist of the following:

- Determination of the range and combination of molten salt properties that lead to critical values of the two suggested explosion-controlling parameters.
 - a. Measurement of the relationship between heat-transfer rates and smelt composition. By measuring heat transfer from jets of molten salts injected into water, the rate of heat input to the water can be determined.
 - b. Measurement of the rate of gas evolution as a function of molten salt composition.
- Laboratory experiments designed to study the possible role of smelt-water interface phenomena in the development of the small vapor-filled cavities whose collapses presumably trigger the main explosion. Among the phenomena to be studied are superheating and various means of nucleation to prevent superheat, heat- and

mass-transfer across the interface, and gas-bubble generation. Particular attention would be paid to development of suitable instrumentation for detection and measurement of the presumed collapsing steam cavities at or near this interface.

The long-range development of the analytical model would obtain a more accurate representation of the main explosion, incorporating model boundary conditions that simulate those for a smelt bed of finite thickness in a recovery furnace. In addition, a much-more-complete model for the triggering mechanism would be developed.

For the main explosion, the model would incorporate:

- The effects of the upper free surface and of the bottom of the smelt bed on the development of the explosion. This would entail revising the model to accommodate axially symmetric motion rather than being limited, as at present, to spherically symmetric motion.
- The effects of nonuniform temperature, pressure and composition within the water body.

The more complete development of the triggering mechanism would entail:

- The details of the collapse of the steam globules and the resulting injection of smelt into the main water body. This consideration would require both axially symmetric geometry for the shape variations and rectilinear motions for the globule.
- Revisions of the triggering mechanism model to encompass possible means other than cavity collapse for obtaining rapid intermixing of smelt and water.

DISCUSSION OF EXPERIMENTAL RESULTS

Laboratory Techniques

For the explosion experiments the smelt was contained in a graphite crucible having a conical interior to provide access to a relatively large surface for the small volume of smelt used in each experiment. A high-frequency power-supply unit was used to energize an induction heating coil that surrounded the crucible. About 70 grams of smelt were used in each experiment to provide a melt surface of about 2-inch diameter near the top of the crucible. The temperature of the molten salt was measured with a platinum-rhodium thermocouple. The device for the introduction of the water was mounted above the heating coil. During an experiment the crucible was heated until the molten smelt was at the desired temperature. The injector was positioned above the crucible and actuated to introduce the water into the molten smelt. The crucible was blanketed with an inert gas during the experiment to prevent oxidation of the Na_2S in the mixture.

Water was introduced into the molten smelt by injection and by a dropped-tube method. Either a piston-type injector or a direct-gas-pressure injector was used (see details in

Appendix A). With the injection systems the velocity of the injected water ranged from .70 to 100 feet per second. The injection velocity was controlled by the gas pressure applied to the injector, and the amount of water introduced could be varied by changing the size of the needle on the injector. In the dropped-tube method, a ceramic tube on the end of which was suspended a large drop of water, was dropped into the molten smelt. The amount of water introduced in experiments was varied by using ceramic tubes of different diameters.

Influence of Smelt Composition on Explosiveness

A large number of laboratory-scale explosion experiments were carried out in order to determine the effects of smelt composition on the explosiveness of molten salt mixtures when water is introduced. These experiments involved both injection and dropped-tube introduction of water into the molten salt mixtures. The amounts of water introduced were purposely kept small, ranging from 30 to 1000 mg, in order to minimize damage to the experimental equipment and thereby make possible a large number of experiments. Although relatively small amounts of water were used, the results agreed in general with those found by previous investigators who used substantially larger amounts of water. The many experiments made possible under these conditions have provided a base for quantitative observation on the explosion incidence as a function of smelt composition. The major components of smelt and the most significant minor components were studied individually on this program. Synthetic and actual kraft-mill smelts also were investigated. The explosion-inhibiting effects of two compounds, CaCO_3 and NaAlO_2 , were studied as well.

Major Smelt Components

The component present in all smelts in the largest amount is Na_2CO_3 . There are no reports of any one ever having been able to obtain an explosive interaction of sodium carbonate and water. Attempts to explode sodium carbonate by the various techniques developed on this research program also were unsuccessful. The explosion mechanism hypothesized in this work suggests that the release of CO_2 gas from the Na_2CO_3 , which is enhanced by interaction with water, is responsible for the lack of explosions. However, only a small amount of NaCl is needed to sensitize Na_2CO_3 to explosion. For example, the composition 95 Na_2CO_3 -5 NaCl had an explosion incidence of 10 percent by the dropped-tube method.

The other major component of smelt is Na_2S , which may be present in amounts ranging from 10 to 30 weight percent in the kraft smelt. Pure Na_2S is very reactive with water, and explosions resulted more than 90 percent of the time in our work when water was introduced into molten Na_2S . Both methods of introducing water produced these high-explosion-incidence values.

Most of the explosion experiments on this program were carried out with compositions having a Na_2S content in the range normally found in kraft-mill smelts. However, to determine effects of smelt temperature and injection velocity, the concentration of Na_2S was 50 weight percent in some experiments. The results of experiments with Na_2CO_3 - Na_2S mixtures are shown in Figure 1. The temperature range in which a given smelt composition had a high explosion incidence when water was injected during these experiments depended on the operating pressure of the injector, which in turn determined the water injection velocity. The temperature ranges for which explosions occurred at least 90 percent of the time at the different operating pressures

are shown in the figure. The minimum temperature for explosion was the freezing point of the molten salt mixture. The maximum temperature for high explosion incidence increased with the operating pressure and injection velocity. As noted in Figure 1, a higher content of Na_2S in the mixture resulted in a higher maximum explosion temperature for a given pressure. The highest temperature used in these experiments was 1800 F, but no explosions were obtained above a temperature of 1725 F, at water injector pressures up to 150 psi. When higher velocity injections were used with the particular experimental equipment, the smelt was splashed from the container rather than exploded, so efforts to use greater pressures were not continued.

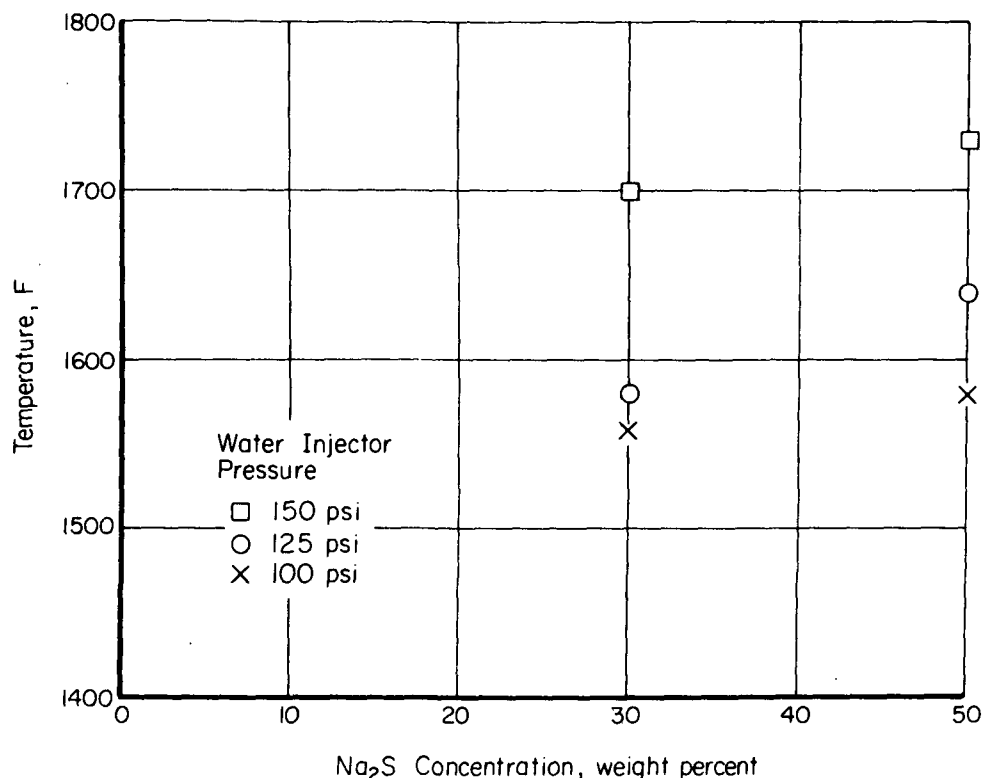


FIGURE 1. MAXIMUM TEMPERATURES FOR WHICH HIGH EXPLOSION PROBABILITY WAS OBSERVED IN $\text{Na}_2\text{CO}_3 - \text{Na}_2\text{S}$ MIXTURES

It also was observed that as the Na_2S concentration was reduced, with all the other variables of the system being held constant, the incidence of explosion also was reduced. Depending on the smelt temperature and the method of introducing water, explosion incidence values ranged from 100 percent for a composition consisting of 70 Na_2CO_3 -30 Na_2S down to an incidence of 10 percent for a mixture containing 20 percent Na_2S . With the methods employed on this program, no explosions were obtained when the Na_2S concentration was less than 20 percent. However, in some of the work done by Combustion Engineering, Inc., in which repeated injections were made into the same smelt mixture, an occasional explosion occurred with compositions down to 9 percent Na_2S after a relatively large amount of water had been injected. Although the frequency of explosion is reduced when the Na_2S concentration is lowered, no absolute lower limit for the concentration has been established. This fact stems from the observation that, in contact with water, Na_2S can react to generate NaOH , which is a strong sensitizer for smelt-water explosions. Consequently, if enough water is in contact with Na_2S for a sufficient length of time, a highly explosive composition may be reached. In the work with kraft-mill smelts on this program, the most explosive smelt contained only 11.7 percent Na_2S , and its explosiveness was attributed to relatively large amounts of the sensitizers NaCl and potassium compounds.

Minor Smelt Components

Most of the minor smelt components are sulfur compounds present in the smelt as a result of incomplete reduction of the Na_2SO_4 to Na_2S . As a consequence, some sulfate, sulfite, and thiosulfate will always be present in the smelt in small amounts. Other minor components of smelt are NaCl , NaOH , and potassium compounds. Of the minor components, the only ones present in quantities greater than 1 percent are sulfate, chloride, hydroxide, and the potassium compounds. The potassium in smelt is probably distributed among the various anions of the mixture in some steady-state distribution. However, in the analysis of smelts, it is customary to group the potassium compounds together and express them in terms of the K_2O content of the mixture. In the explosion experiments carried out on this program, the potassium was added as K_2CO_3 ; it is presumed that the bulk of the potassium would be present in this form because carbonate is the anion that predominates in the smelt.

Sodium Chloride. NaCl has been found to be a powerful explosion sensitizer in smelts. Thus, as shown in Table 2, increasing the NaCl concentration from zero to 5 weight percent in a smelt mixture containing Na_2CO_3 and Na_2S , increased the explosion incidence from 10 percent to 100 percent. The data were obtained using the dropped-tube method at a temperature of 1400 F.

TABLE 2. EFFECT OF NaCl ON SMELT EXPLOSIVENESS^(a)

Composition, weight percent			Explosion Incidence, percent
Na_2CO_3	Na_2S	NaCl	
75	25	0	10
74	25	1	25
73	25	2	35
72	25	3	45
71	25	4	90
70	25	5	100

(a) Experiments with dropped-tube at 1400 F.

Increasing the amount of NaCl in the mixture increases the maximum temperature for high incidence of explosion, much the same as does increasing the amount of Na_2S . The important difference that less injection velocity is required for explosion with NaCl suggests that less turbulence would be required during a smelt-water contact to bring about an explosive interaction. Explosions also can occur down to lower temperatures when NaCl is present, because the freezing point of the mixture is lower when the NaCl is present. A comparison of maximum explosion temperatures and injector operating pressures for various smelt compositions is presented in Table 3. These data are for injections made over the temperature range from the melting point of the mixture up to 1500 F. As these experiments were carried out with injection volumes of only 35 milligrams of water, it was necessary to use relatively high percentages of NaCl in the mixture in order to obtain explosions. However, the data illustrate the wide range of temperatures over which an explosion can be obtained, provided a sufficiently sensitized mixture is used.

TABLE 3. MAXIMUM EXPLOSION TEMPERATURES OF SMELT COMPOSITIONS AT VARIOUS INJECTION PRESSURES

Smelt Composition, weight percent			Maximum Explosion Temperatures, F, at Indicated Injection Pressure, psi				
Na ₂ CO ₃	Na ₂ S	NaCl	50	75	100	125	150
50	50		x	x	1580	1640	1730
70	30		x	x	1560	1580	1700
50	30	20	1310	—	—	—	—
50	25	25	1350	1800	—	—	—
46	23	31	1510	—	—	—	—

x = No explosion at any temperature.

— = No experiments tried at this pressure.

In the course of these explosion experiments with NaCl in the smelt, it was noted that explosions occurred when the water impinged obliquely onto a thin film of molten smelt adhering to the sloping wall of the graphite crucible. This result has provided additional support for the hypothesis that the explosions involved rapid heat transfer promoted by shearing away the insulating steam blanket from water in contact with molten smelt. The oblique impingement provided such shearing action, and sharp explosions occurred even though there was no significant depth of smelt under which the water could be trapped. The importance of this shearing action became apparent when the sloping wall of the cone-shaped smelt container was replaced by a flat graphite surface and the water was impinged at a 90-degree angle. No explosions could be obtained with a thin film of molten smelt on the flat surface, although the composition and temperature conditions were such that it produced more than 95 percent explosion incidence in the conical container.

When a cylindrical graphite crucible having the same depth as the cone-shaped container was used, explosions were obtained 60 percent of the time under thin-film conditions which produced almost 100 percent incidence of explosion in the conical container. The shearing effect resulting from the impingement of water droplets on the container wall appears to be an important factor in the explosion mechanism as it occurred in the laboratory apparatus.

Sodium Sulfate. Analyses of various kraft-mill smelts have shown that there is always 1 to 2 percent of Na₂SO₄ present. Low sulfidity smelts often contain significant amounts of Na₂SO₄, and among those smelts analyzed on this program levels of 4 to 6 percent were found in some cases. Previous investigators of smelt-water explosions have concluded that Na₂SO₄ could be a contributor to the explosiveness of the smelt. Accordingly, experiments were carried out on this program with Na₂SO₄ substituted for NaCl in a composition which is highly explosive over a wide range of temperatures. These experiments were done by injection of water, at a smelt temperature of 1400 F. As shown in Table 4, the explosion incidence dropped from 95 percent to 30 percent as the Na₂SO₄ content of the smelt mixture was increased from zero to 25 weight percent.

TABLE 4. EFFECT OF Na_2SO_4 ON SMELT EXPLOSIVENESS^(a)

Na_2CO_3	Composition, weight percent			Explosion Incidence, percent
	Na_2S	NaCl	Na_2SO_4	
50	25	25	0	95
50	25	20	5	93
50	25	15	10	89
50	25	10	15	50
50	25	5	20	48
50	25	0	25	30

(a) 35 mg water injected at 1400 F.

Additional experiments were performed with the Na_2SO_4 concentrations at 10 weight percent to determine the effect of temperature on the explosiveness. In approximately 200 experiments the explosion incidence remained about 90 percent up to 1400 F. However, from 1400 to 1500 F, the explosion incidence dropped to 47 percent. Hence, at the higher temperature, Na_2SO_4 did not sensitize the mixture as much as did NaCl . For mill smelts having both low sulfidity and low chloride content, it appeared that the Na_2SO_4 in the mixture contributed significantly to its explosiveness.

From the various experiments conducted it was concluded that, under the experimental water-injection conditions, Na_2SO_4 is a moderate sensitizer for smelt-water explosions. Its effect as an explosion sensitizer is less than that of Na_2S , and considerably less than that of NaCl .

Sodium Hydroxide. Although NaOH is usually present in smelt in concentrations of less than 1 weight percent, the action of water with the carbonate and sulfide components of smelt will produce NaOH . In the work by Babcock & Wilcox for the Smelt-Water Research Committee, significant amounts of NaOH were formed in this fashion. Combustion Engineering, Inc., also noted that NaOH appeared to sensitize the molten smelt to explosion with water. Consequently, the effect of NaOH on explosiveness was examined during this program. Initially 5 weight percent NaOH was used to replace the same amount of NaCl in a highly explosive mixture. Both the original mixture and the one containing NaOH exploded 95 to 97 percent of the time when water was injected in the temperature range 1200 to 1600 F. The mixture containing NaOH began to foam, presumably evolving CO_2 , at about 1600 F, however, and above this temperature no explosions were obtained. The mixture without NaOH did not decompose as readily and could be exploded up to 1800 F.

In additional experiments, 10, 15, 20, and 25 percent NaOH replaced equivalent amounts of NaCl in the base mixture. In all of these compositions, explosion incidence was greater than 90 percent up to 1350 F. From 1350 to 1450 F, explosion incidence dropped to about 30 percent and above 1450, foaming of the mixture prevented explosion. It was concluded that NaOH sensitizes smelt to explosions as much as does NaCl , but the NaOH narrows the temperature range of stability for the smelt mixtures.

Potassium Carbonate. In the average mill smelt, potassium is the only metal other than sodium which is present in any significant amount. As pointed out earlier, potassium is probably present primarily as K_2CO_3 , but it has become customary in mill-smelt analyses to express the potassium content as K_2O . Typically 2 to 3 percent K_2O will be found in a mill smelt, although amounts up to 5.8 weight percent were found in the mill smelts analyzed on this program.

When the explosiveness of pure K_2CO_3 was examined by the dropped-tube method, which is considered a most severe test, an explosion incidence of 10 percent was observed. Consequently, this material has inherent explosiveness that Na_2CO_3 does not, and can obviously contribute to sensitizing smelt. The effect on smelt explosiveness was investigated by injections into synthetic smelt mixtures containing K_2CO_3 in place of Na_2CO_3 . The results of 50 injections at each concentration are shown in Table 5 and are compared to similar experiments with Na_2CO_3 . These experiments showed that the K_2CO_3 sustained the explosiveness of the mixture even at low NaCl concentrations.

TABLE 5. EFFECT OF K_2CO_3 ON SMELT EXPLOSIVENESS^(a)

Composition, weight percent			Explosion Incidence, percent	Explosion Incidence With Na_2CO_3 , percent
K_2CO_3	Na_2S	NaCl		
55	25	20	90	95
60	25	15	60	65
65	25	10	62	50
70	25	5	60	30

(a) Injections of 35 mg H_2O at 1400 F.

In mixtures not containing NaCl, the sensitizing effect of K_2CO_3 was observed also. Thus, for example, in carbonate-sulfide mixtures containing 15 percent Na_2S , the explosion incidence went from 0 to 100 percent when Na_2CO_3 was replaced by K_2CO_3 in the mixture. However, when the Na_2S concentration was only 10 percent, the explosion incidence went from 0 to only 10 percent when the K_2CO_3 was substituted.

From these results it was concluded that K_2CO_3 is an explosion sensitizer in smelt mixtures, whereas Na_2CO_3 does not contribute to the explosiveness of the smelt. As to its rank as an explosion sensitizer, K_2CO_3 appears to be less of a sensitizer than Na_2S , but probably greater than Na_2SO_4 .

Sodium Sulfite. The question of the contribution of Na_2SO_3 to explosiveness was raised by one of the mill smelts which had not undergone complete reduction, and contained about 3.2 percent Na_2SO_3 and 6.5 percent Na_2SO_4 . A series of experiments was performed with Na_2SO_3 substituted for NaCl in a highly explosive mixture. The experiments were carried out by injections of small amounts of water (35 milligrams). As shown in Table 6, the explosion incidence dropped significantly with each substitution of Na_2SO_3 for NaCl.

The explosiveness of the compositions containing 5, 10, 15 percent Na_2SO_3 was about the same as that found earlier for similar mixtures containing Na_2SO_4 . The Na_2SO_3 mixtures were less explosive than those with Na_2SO_4 at the 20 and 25 percent concentration level. From these results it was concluded that Na_2SO_3 is a weak explosion sensitizer, and it ranks after Na_2SO_4 in that respect.

TABLE 6. EFFECTS OF Na_2SO_3 ON SMELT EXPLOSIVENESS(a)

Composition, weight percent				Explosion Incidence, percent
Na_2CO_3	Na_2S	NaCl	Na_2SO_3	
50	25	25	0	100
50	25	20	5	100
50	25	15	10	82
50	25	10	15	62
50	25	5	20	30
50	25	0	25	0

(a) Injection of 35 mg H_2O at 1400 F.

Kraft-Mill Smelts

Explosion experiments were carried out with smelts obtained from kraft mills located in different areas, as designated by the members of the technical committee. The purpose of these experiments was to relate the results of the explosion experiments with synthetic smelts to actual mill smelts, and to correlate mill-smelt compositions with explosiveness. For the first series of experiments, the water was injected into the smelts, and increasing amounts of water from 35 up to 1000 milligrams were used in the course of these experiments. The injections were made at temperatures from 30 to 100 F above the melting point of the smelts, which range from 1250 F to 1350 F. The results obtained with 100 injections into each of the 12 mill smelts employed on this program are presented in Table 7. Five of the mill smelts exploded with the injection of the minimum amount of water (35 milligrams). The explosion incidence under these circumstances was about the same, 4 or 5 percent, for all but one of these five smelts. Smelt K, which ultimately proved to be the most explosive of the group, had an incidence of 30 percent in this first set of experiments. The remaining seven smelts did not explode with the injection of the 35-milligram quantity of water. When the amount of water was increased to 75 milligrams, three additional smelts underwent explosion, with an incidence of from 3 to 6 percent. Increasingly larger amounts of water were required to obtain explosions with the other four smelts. However, once explosions did occur, the incidence at which they occurred was rather large compared to the others except for Smelt I.

To provide additional basis for ranking the 12 mill smelts as to explosiveness, NaCl was added to each of them in 5 percent increments until the explosion incidence reached 50 percent. In these experiments, by injection of 35 milligrams of water, NaCl additions from 5 to 25 percent were required for the different smelts to reach the 50 percent explosion level. The results are shown in Table 8, in which the smelts are listed in decreasing order of explosiveness on the basis of the amount of NaCl required.

The remaining columns of the table show the chemical analyses of the original smelts, to provide comparison of smelt composition with explosiveness. As seen from the table, the two most explosive smelts required only 5 percent additional NaCl to reach the 50 percent level of explosion incidence, while the others required increasing amounts up to 25 percent. Within each group, the explosive ranking was determined on the basis of the amount of water required to obtain explosions when no NaCl had been added. In general, there was good agreement between the amounts of NaCl which had to be added to achieve 50 percent explosion incidence, and the amount of water needed to explode the smelts without NaCl addition as shown by Figure 2.

TABLE 7. EXPLOSION THRESHOLD VALUES FOR WATER INJECTION INTO KRAFT-MILL SMELTS

Smelt Designation	Explosion Incidence, percent ^(a) , for Indicated Injection mg H ₂ O				
	35	75	300	600	1000
K	30	—	—	—	—
C	5	—	—	—	—
A	4	—	—	—	—
B	4	—	—	—	—
J	4	—	—	—	—
D	0	6	—	—	—
E	0	6	—	—	—
L	0	3	—	—	—
H	0	0	18	—	—
F	0	0	0	18	—
G	0	0	0	0	25
I	0	0	0	0	4

(a) Based on 100 injections.

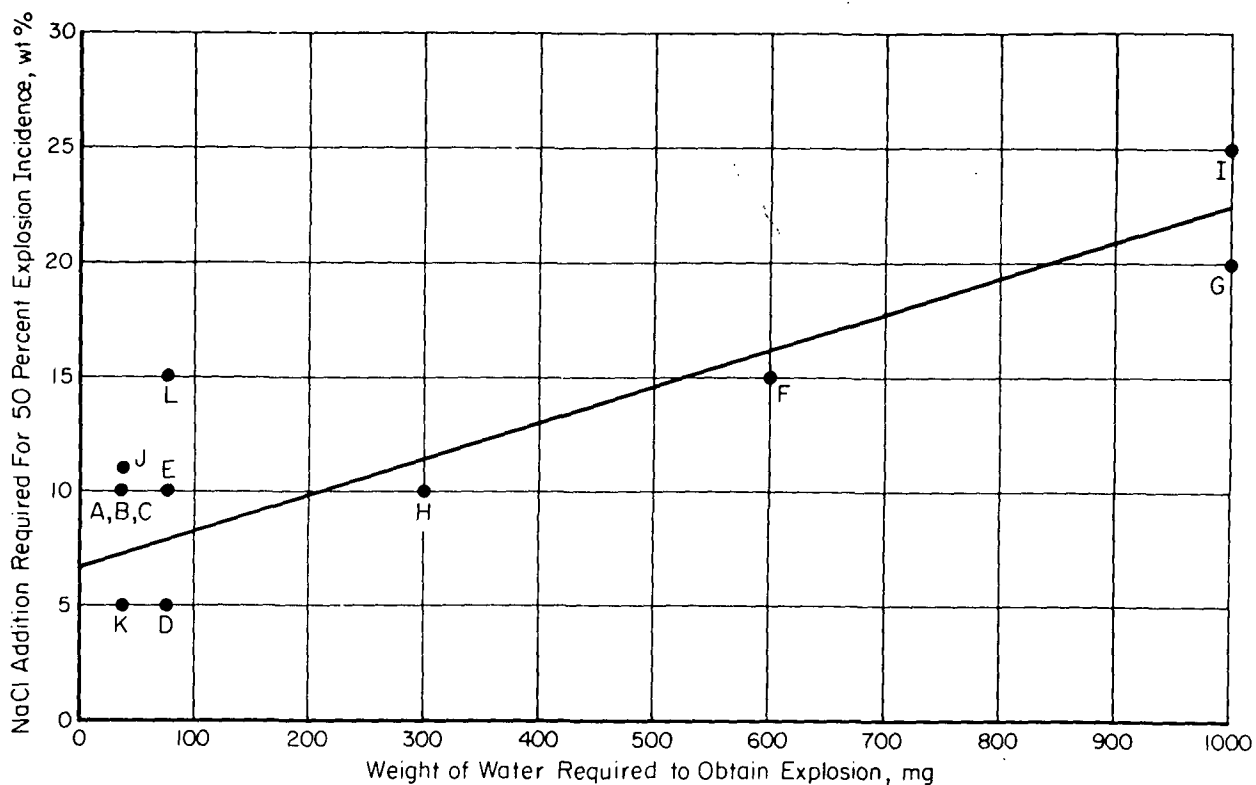


FIGURE 2. COMPARISON OF WATER INJECTIONS AND SODIUM CHLORIDE ADDITIONS REQUIRED TO EXPLODE KRAFT-MILL SMELTS

Letters designate smelts.

TABLE 8. RESULTS OF WATER-INJECTION EXPLOSION EXPERIMENTS AND CHEMICAL ANALYSES OF TYPICAL KRAFT-MILL SMELTS

Smelt	Source	Wt % NaCl Addition Required(a)	Chemical Analysis of Original Smelts, wt %								K ₂ O	Total
			Na ₂ CO ₃	Na ₂ S	NaCl	Na ₂ SO ₄	Na ₂ S ₂ O ₃	Na ₂ SO ₃	NaOH			
K	West coast	5	73.6	11.7	4.55	4.05	0.89	nil	nil	4.72	99.5	
D	West coast	5	68.9	24.8	1.40	1.08	0.55	nil	nil	2.11	98.8	
A	East coast	10	75.8	16.5	1.02	1.81	0.95	nil	0.64	5.80	102.5	
B	South	10	66.4	24.8	2.58	1.98	0.51	nil	nil	3.36	99.6	
C	Southeast	10	72.0	19.0	1.17	2.74	0.85	0.63	nil	2.66	99.1	
E	South	10	75.5	18.6	1.32	1.23	0.45	nil	nil	2.42	99.5	
H	South	10	80.6	12.9	1.52	2.07	0.38	nil	nil	1.96	98.6	
J	South	12	73.0	15.2	4.60	2.06	0.38	nil	nil	4.45	99.7	
L	South	15	74.2	9.9	2.39	5.23	0.38	nil	nil	1.91	94.0	
F	West coast	15	61.2	12.3	5.61	6.47	2.33	3.15	nil	1.93	93.0	
G	Southeast	20	72.1	21.4	0.48	1.69	0.32	nil	0.32	4.14	100.4	
I	South	25	74.1	18.7	1.35	1.91	0.42	nil	nil	3.86	100.3	

(a) For 50 percent explosion incidence with 35 mg H₂O injection.

Examination of the chemical analysis of the smelts in view of the explosiveness observed shows that high Na_2S content is not required for smelt to be especially sensitive to explosion, provided the quantities of some of the other sensitizing ingredients is sufficiently great. Thus Smelt K, which contained only 11.7 percent Na_2S , was the most explosive of the group, undoubtedly as the result of the presence of fairly large amounts of chloride, sulfate, and potassium. On the other hand, the sulfide content of the second most explosive, Smelt D, was great enough to make up for the relatively small amount of the other explosion sensitizers.

When the dropped-tube method was used to explode the kraft-mill smelts, it was not possible to distinguish among the various smelts as had been the case with water injection. Of course the amount of water used in the dropped-tube experiments (300 milligrams) was larger than that used in most of the injection experiments. As a consequence, 10 of the 12 mill smelts exploded every time, so that this method was not as sensitive in distinguishing small differences as was the injection technique.

In order to be sure that the chemical analysis of the mill smelts included all of the components that are important to its explosiveness, synthetic mill smelts were prepared on the basis of the analyses shown in Table 8. These synthetic mill smelts showed the same explosion incidence as did the actual mill smelts, confirming that the chemical analyses included the explosive components.

AID Analysis

A mathematical treatment known as "automatic interaction detector" analysis was applied to the data on the composition of the 12 kraft-mill smelts and their explosiveness. The explosive ranking of the mill smelts and chemical composition as given in Table 8 were used in this computer analysis. The AID program provides a technique to evaluate qualitatively the interaction of a large number of independent variables and choose which are most significant in predicting the dependent variable. The analysis showed that the explosive ranking of the 12 smelts could be determined on the basis of three of the eight components in the smelt composition: NaCl , Na_2S , and potassium (expressed as K_2O), in that order. The AID analysis graphic tree is shown in Figure 3. The mill smelts fall into four groups, which are in decreasing order of explosiveness:

- | | |
|---------|----------------|
| Group 1 | A, K |
| Group 2 | D, C, B, and E |
| Group 3 | H |
| Group 4 | L, F, J, G, I. |

According to this analysis the NaCl content of a smelt is the most important determinant of its explosiveness. On this basis, the five least explosive smelts L, F, J, G, and I are separated. The other seven smelts are then further separated on the basis of their Na_2S content: Smelts D, B, G, and E going into the more explosive group. Finally on the basis of the K_2O content, Smelts A and K are separated into the more explosive group and Smelt H falls into the less explosive group.

The fact that NaCl , Na_2S , and K_2CO_3 are the most important contributors to the explosiveness of the mill smelts also has been established by the explosion experiments that have been done on this program. The same ranking as explosion sensitizers for these three materials also has been established in the work with the synthetic smelt mixtures.

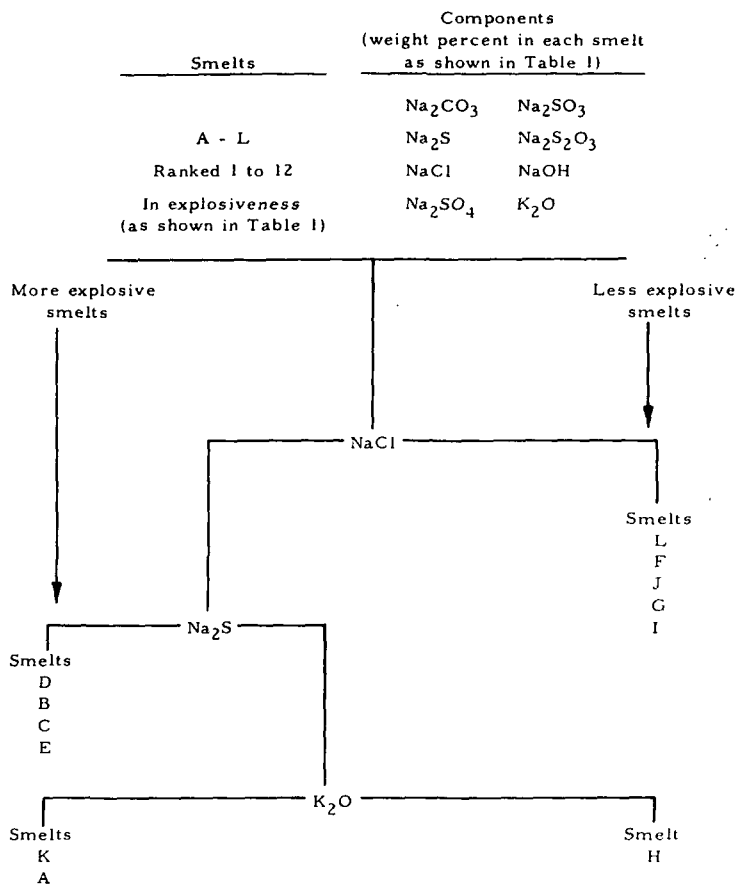


FIGURE 3. AUTOMATIC INTERACTION DETECTOR ANALYSIS OF KRAFT-MILL SMELTS

Correlation of Explosiveness With Smelt Composition

Attempts were made to obtain mathematical relationships between the incidence of explosions, as measured either by the water-injection or dropped-tube methods, and the percentage compositions of the sensitizing compounds Na₂S, NaCl, and K₂CO₃. In these attempts standard regression analysis was used to obtain the optimum values of the coefficients in the linear and the quadratic expressions relating explosion incidence and the concentrations of the three compounds in the smelt. However, there was poor correlation between the observed explosion-incidence values and those predicted by the results of the regression analysis.

It appears that a reasonably good fit for the experimental data could be obtained by applying the error function, in which the value of the explosion index follows a so-called "S-shaped curve". This curve is characterized by a very rapid increase in the explosion index over a narrow range of composition.

Explosion Inhibitors

Previous work for the smelt-water research group by Combustion Engineering, Inc., had demonstrated that NaAlO₂ and CaCO₃ reduced the probability of explosion when one to three

grams of water were injected through a hypodermic syringe into about 500 grams of molten salt. To study the effects of these compounds on smelt-water explosiveness under the experimental conditions being used on this program, the NaAlO_2 and the CaCO_3 were substituted in turn for part of the Na_2CO_3 in a smelt mixture with a high incidence of explosion. A composition containing 25 weight percent of Na_2S and 20 weight percent NaCl was selected as the base mixture for these experiments because it had an explosion incidence of 90 percent in the temperature range 1100 to 1600 F, when the injection method was used. The solubility of both NaAlO_2 and CaCO_3 in smelt mixtures is limited to about 1 or 2 percent by weight, so that the desensitizing effects took place with a portion of the NaAlO_2 or CaCO_3 in suspension in the melt. As the mixture melted, the undissolved portion remained on the bottom of the crucible at first; but, as the temperature was increased, the particles were dispersed by convection currents in the liquid.

The reduced explosion-incidence values that occurred for the smelt mixtures containing NaAlO_2 or CaCO_3 for the injection experiments are shown in Table 9. Approximately 100 injection experiments were carried out for each composition in each temperature range. As shown in the table, the base mixture maintained an explosion incidence greater than 90 percent from 1100 to 1500 F, which then decreased substantially from 1500 F to 1750 F, at which point the decomposition of the mixture caused foaming in the crucible. Both the NaAlO_2 and the CaCO_3 reduced the explosion incidence, and were more effective as the temperature was increased. At the lower temperatures investigated, the 5 percent CaCO_3 was somewhat more effective in reducing explosion than was the 5 percent NaAlO_2 . Except for this difference, the two performed with approximately the same effectiveness, and the differences noted in the table probably are as much the effect of experimental variations as they are of performance of the two materials. The CaCO_3 has the advantage of being effective to a higher temperature than does the NaAlO_2 .

TABLE 9. EXPLOSION INCIDENCE WITH NaAlO_2 OR CaCO_3 IN SMELT MIXTURES, USING THE WATER-INJECTION METHOD

Substituted Constituent ^(a)	Explosion Incidence ^(b) , percent				
	1100- 1200 F	1200- 1300 F	1300- 1400 F	1400- 1500 F	1500 F - (Decomposition Temp, F)
None	90	92	95	90	35 (1750)
5% NaAlO_2	64	57	16	12	10 (1650)
10% NaAlO_2	45	25	20	15	10 (1650)
5% CaCO_3	39	31	24	6	0 (1800)
10% CaCO_3	46	31	25	11	12 (1800)

(a) Substituted for Na_2CO_3 in $55\text{Na}_2\text{CO}_3\text{-}25\text{Na}_2\text{S}\text{-}20\text{NaCl}$.

(b) Based on approximately 100 injections of 35 mg H_2O in each temperature range for each composition.

The performance of these two compounds in reducing the more violent explosions obtained in the dropped-tube method of injection also was investigated. The initial smelt mixture used contained 30 weight percent Na_2S , and had an explosion incidence of 100 percent at 1400 F. When 5 percent of the Na_2CO_3 in the mixture was replaced by CaCO_3 , no explosions were obtained. The same reduction in explosiveness was obtained when 5 percent of NaAlO_2 was substituted for the Na_2CO_3 in the mixture. Hence these two compounds proved to be very effective explosion inhibitors in mixtures containing only carbonate and sulfide.

In order to examine the dropped-tube technique with mixtures containing chloride, additional experiments were performed using a base mixture containing 25 percent Na_2S and 3 percent NaCl . This mixture had a moderate explosion incidence of 60 percent at 1400 F with the dropped-tube method. The results obtained with additions of 5 weight percent CaCO_3 (Table 10) showed that the explosion-inhibiting effect of CaCO_3 improves as the temperature increases, just as it had done with the injection method. The decrease was not quite as marked as it was for the previous set of experiments, but again the difference between the two sets may be the result of experimental variation. The table also contains data for additions of BaCO_3 and Li_2CO_3 to the same smelt mixture. These compounds, which decompose at higher temperatures than CaCO_3 , also were investigated as possible explosion inhibitors. In order to introduce the same amount of carbonate into the mixtures as obtained with 5 percent CaCO_3 , additions of 9.8 weight percent BaCO_3 were required. The explosion incidence of the base mixture increased to 100 percent over the temperature range 1400-1600 F with this addition.

TABLE 10. EXPLOSION INCIDENCE WITH CARBONATE ADDITIVES IN SMELT, USING THE DROPPED-TUBE METHOD (300 mg H_2O)

Temperature, F	Explosion Incidence, percent			
	Base Mixture ^(a)	Base Plus 5 wt % CaCO_3	Base Plus 9.8 wt % BaCO_3	Base Plus 3.6 wt % Li_2CO_3
1400	60	56	100	100
1500	50	20	100	100
1600	50	10	100	100

(a) $72\text{Na}_2\text{CO}_3$ - $25\text{Na}_2\text{S}$ - 3NaCl .

For the Li_2CO_3 additions, only 3.6 percent was required to obtain an amount of carbonate equivalent to 5 percent CaCO_3 . With the Li_2CO_3 additions, the explosion incidence of the base mixture also increased to 100 percent over the temperature range 1400-1600 F.

The explanation for the inhibitive effect of CaCO_3 had been suggested by the computer modeling study to be the high rate of CO_2 release from the carbonate, as discussed in detail elsewhere in this report. As CaCO_3 decomposes more readily on heating than does Na_2CO_3 , adding CaCO_3 to a molten mixture would result in a greater CO_2 release. Inasmuch as the barium and lithium carbonates increased the explosiveness of the base mixture rather than decreasing it, it appears that for a carbonate to be effective as an explosion inhibitor, it is necessary that its decomposition yield a substantial amount of CO_2 at the temperature of the smelt.

The mechanism by which NaAlO_2 reduces explosiveness of smelt mixtures must necessarily be different, because this compound does not decompose to generate a gas. However, in the course of the explosion experiments, the foaming noted at the surface, as the temperature of the smelt was increased, indicated gas generation from some source. It was hypothesized that the NaAlO_2 may catalyze the decomposition of the Na_2CO_3 in the smelt to generate CO_2 . This possibility was tested in the vacuum decomposition experiments described later in the report, and it was found that NaAlO_2 increased the evolution of CO_2 from Na_2CO_3 .

MgCO_3 decomposes to release CO_2 at a lower temperature than does CaCO_3 , so its potential in reducing explosions also was investigated. The explosion incidence of the base mixture remain unchanged in a series of 20 experiments with 5 percent additions of MgCO_3 . The lack of effect was attributed to the low decomposition temperature, leading to release of all its CO_2 below 1400 F. The material dolomite, which consists of magnesium and calcium carbonates in equal amounts in a mixed crystal, also was tried in the explosion experiments. This material decomposes to yield CO_2 over a wider temperature range than does the MgCO_3 , but 5 percent additions of dolomite were ineffective in reducing the explosion incidence of the base mixture.

Further consideration of CaCO_3 additions to smelt mixtures appears to be warranted. Among the questions to be answered would be whether the CaCO_3 would persist long enough in the recovery furnace so that a sufficient amount would always be present to inhibit explosions when water was introduced into the furnace. Another question to be answered would be the effect of the calcium in the system. As CaCO_3 it would be insoluble in the green liquor, and as CaO it would precipitate carbonate in the green liquor. Hence it could possibly be removed at that stage of the process.

Influence of Physical Properties of Smelt on Explosiveness

Once it had been established that smelt-water explosions are physical explosions rather than chemical, it became obvious that the physical properties of the system must play an important part in the explosion mechanism. As a consequence, an important aspect of this research program was to investigate the physical properties that could be important in the explosion process. The selection of the physical properties to be measured and the order in which they were determined was guided by the computer modeling of the explosion mechanism. Physical properties of both water and steam, which are of vital concern to the explosion process, are well known and have all been recorded in the scientific literature. Thus, for example, the densities and the specific heats of water and steam as functions of temperature and pressure are available. Changes in the boiling point of water, the heat of vaporization of water, and the sensible heat of steam with temperature and pressure also are well-known quantities. However, the properties of smelt are not as well documented. Examination of the literature showed that information was available for such properties as the density, viscosity, and surface tension of Na_2CO_3 , NaCl , NaOH , and Na_2SO_4 in the temperature range of interest. However, there was no information on Na_2S or on the mixtures of compounds which constitute typical smelts. Consequently, measurement of selected physical properties was necessary as part of this program. The properties studied are: (1) viscosity, (2) surface tension, (3) sound velocity, and (4) density. These properties were measured for various smelt compositions in the temperature range of the molten smelts.

Viscosity

Data from the literature show that the viscosity of molten Na_2CO_3 decreases rather rapidly from a value of 4.5 centipoises at the melting point (1570 F) to about 1.5 centipoises at 1800 F, as shown in Figure 4. By way of comparison, the viscosity of water is 1.0 centipoise at 70 F, and as the temperature of the water is raised to the boiling point its viscosity decreases to 0.28 centipoise. Values from the literature for the viscosities of molten NaCl and molten NaOH , the two most powerful explosion sensitizers, also are shown in the figure.

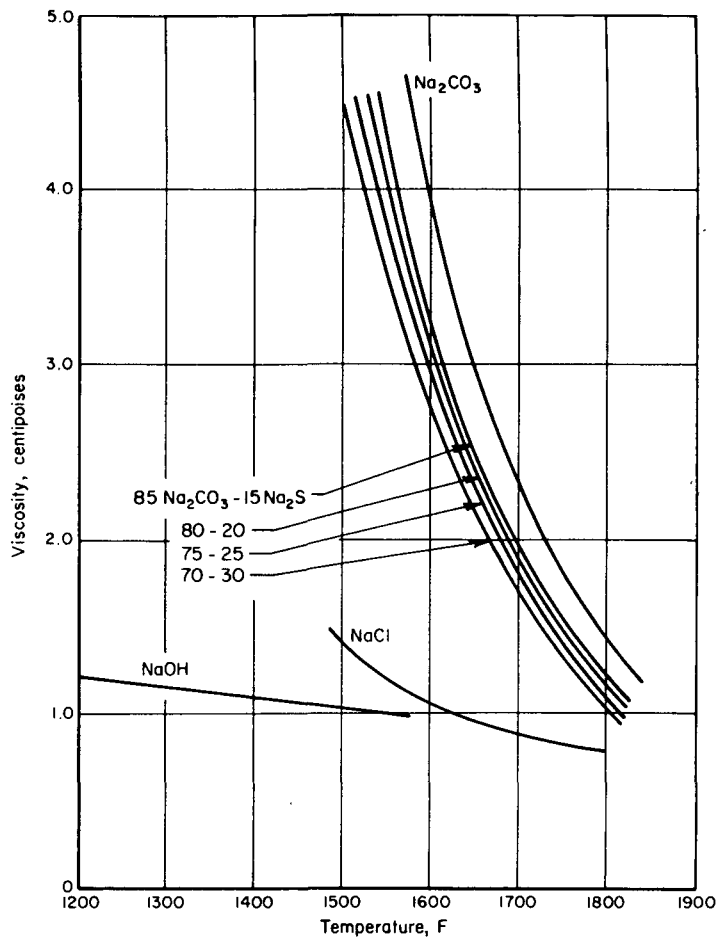


FIGURE 4. VISCOSITIES OF MOLTEN SALTS

Viscosities of molten salt mixtures were measured in this program by two methods. In the first method, a platinum bob suspended from one arm of an analytical balance was put in vertical motion in the molten salt, and the shear viscosity of the melt was determined from the rate of decay of movement of the bob. The apparatus was calibrated with liquids of known viscosity at room temperature and also with molten Na_2CO_3 . Because small differences in the viscosity proved difficult to measure by this technique, a second method also was employed. This method involved damping the rotational movement of a cylindrical crucible suspended by a steel wire. The molten salt was contained in the crucible and the rate at which its rotation decreased was used as a measure of the viscosity of the melt. Liquids with known viscosities were used to calibrate the equipment.

The results show that the viscosity of the smelt mixture decreases as the amount of Na_2S in the mixture is increased. The slope of the viscosity-versus-temperature curve for the mixtures of Na_2CO_3 and Na_2S approximates that for the pure Na_2CO_3 and is fairly steep with temperature, as shown in Figure 4.

The role viscosity may play in the smelt-water explosion mechanism is discussed further in a later section of the report. However, the relatively small changes in viscosity with composition which have been observed in this work would not account for the differences in explosiveness

which have been observed for the same range of compositions. Some kraft mills have reported that as the sulfidity of the smelt is lowered its viscosity increases to such an extent that the smelt flow is hindered and greater steam pressure is required at the shatter jets to break up the flow adequately. On the basis of this information, it appears that the increases in viscosity as the smelt composition approaches pure Na_2CO_3 are sufficient to affect the flow properties of the system significantly. In terms of the explosion model, however, these viscosity differences are not great enough to account for the difference in explosiveness.

Surface Tension

The surface tension of molten salts does not change as rapidly with temperature as does the viscosity. Surface-tension values reported in the literature for Na_2CO_3 range from 210 dynes per centimeter at 1600 F to 205 dynes per centimeter at 1800 F. For water, the surface tension changes from 72 to 59 dynes per centimeter in going from room temperature to the boiling point. In this program, the surface tension was measured with the equipment used for the density and the initial viscosity measurements. For the surface-tension work, a platinum rod was attached to the bottom of an alumina bob that was hung from the beam of an analytical balance and suspended in the molten salt. The force required to lift the rod from the surface of a liquid was readily detectable by the balance, and from this force the surface tension of the liquid could be calculated. The system was calibrated by using liquids of known surface tension, such as water at room temperature and molten Na_2CO_3 .

As shown in Figure 5, surface-tension was measured on two synthetic smelt compositions and on Smelt K by itself and with CaCO_3 added. The surface-tension values observed for the mixture containing 70 Na_2CO_3 -30 Na_2S were within experimental error the same as observed for Na_2CO_3 . However, substitution of 5 percent NaCl for the same amount of Na_2CO_3 resulted in a 10 percent drop in the surface tension. An additional 10 percent drop in surface tension was observed when water vapor was introduced into the inert atmosphere above the molten salt mixture.

Smelt K, the most explosive of those supplied by the Technical Committee, was found to have a surface tension only slightly lower than that for the synthetic mixture containing 5 weight percent NaCl , as shown in the figure. In view of the explosiveness of Smelt K and that for the synthetic mixture containing 5 percent NaCl , these results suggest that explosive compositions may have surface tension values about 20 percent lower than the nonexplosive Na_2CO_3 . When water vapor was introduced into the atmosphere above Smelt K, surface tension was found to be the same as that for the 5 percent chloride mixture under the same conditions.

The effect on surface tension of adding the explosion inhibitor, CaCO_3 , to Smelt K also was examined. The addition of 5 weight percent CaCO_3 raised the surface tension to a value about midway between that of the original Smelt K and that of pure Na_2CO_3 . When water vapor was introduced into the atmosphere above the smelt containing the 5 weight percent CaCO_3 , the surface tension was reduced to that of the original smelt before the CaCO_3 had been added.

These changes in surface tension are not large enough to account for the differences in explosiveness, but they do indicate that surface tension changes may play a part in the explosion mechanism as one of the factors in some parameter that reaches a critical value at a given smelt composition.

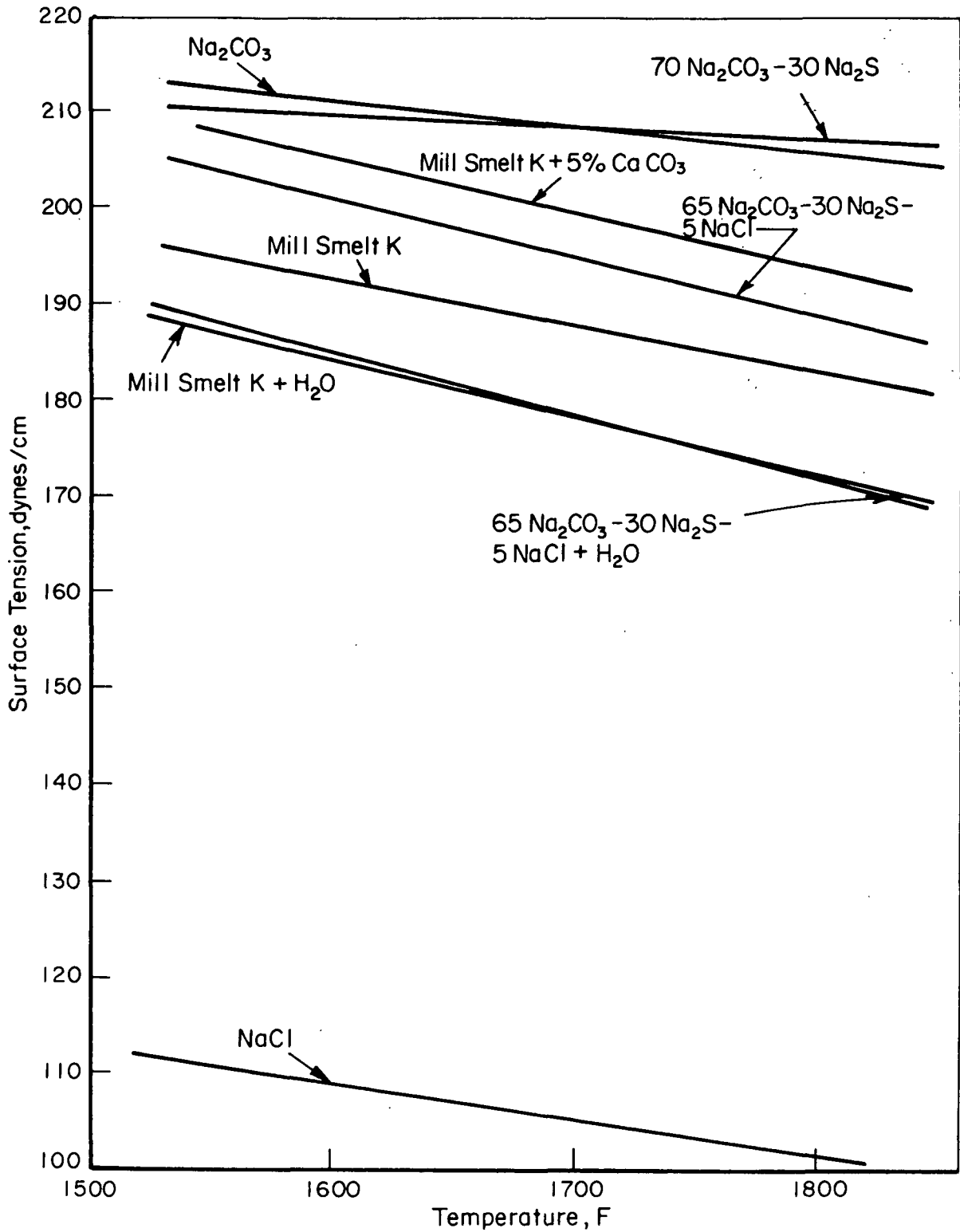


FIGURE 5. SURFACE TENSION OF MOLTEN SALTS AS A FUNCTION OF TEMPERATURE

Density

As was noted for viscosity and surface tension, the densities of the strongest explosion sensitizers, NaCl and NaOH, are appreciably lower than that of Na_2CO_3 . Data from the literature on the densities of these molten salts are shown in Figure 6, together with results of measurements made on this program. The mixture containing 30 percent Na_2S was found to have a density slightly less than that of the pure Na_2CO_3 . Substitution of 5 percent NaCl for the same amount of Na_2CO_3 resulted in the further reduction in density. Smelt K, the most explosive of the mill smelts examined on this program, was found to have a density lying between that of Na_2CO_3 and the mixture containing 30 percent Na_2S . The addition of 5 percent CaCO_3 to Smelt K increased the density to a value essentially equal to that of Na_2CO_3 , within experimental error.

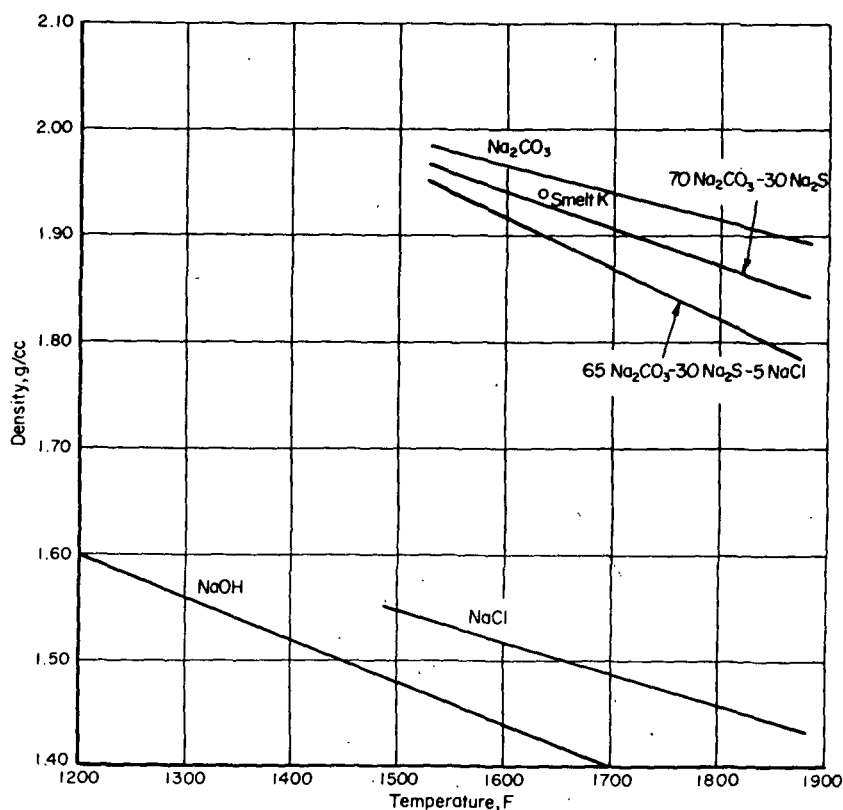


FIGURE 6. DENSITIES OF MOLTEN SALTS

These results show that there is not a very great difference in density between molten salt compositions that have a relatively high incidence of explosion and the nonexplosive Na_2CO_3 . However, on a percentage basis, the changes in density with composition are about the same as those observed for viscosity and surface tension. As stated before, no one property changes rapidly enough with composition to account for differences in explosiveness.

Sound Velocity

Changes in the density of smelt compositions as functions of pressure can be quite important to the explosion mechanism. This relationship is involved directly in determining the acoustic properties of the medium, through its bulk modulus (density times square of sound velocity). Consequently, the determination of the bulk modulus of the smelt from ultrasonic velocity measurements was undertaken as part of this program. The experimental method used was to pass a high-frequency signal through the molten smelt mixture and to record both the time required for the signal to pass through the melt, and the extent of the attenuation of the signal by the melt.

The values obtained for the velocity of sound are presented as a function of temperature in Figure 7. For the single-component melts, the velocity of sound was the greatest in Na_2CO_3 , intermediate in Na_2S , and lowest in NaCl . The sound velocities in the molten salt mixtures fell between those of their respective pure compounds. Addition of the explosion sensitizers, Na_2S and NaCl , to the Na_2CO_3 resulted in the lowering of the sound velocity and the properties calculated from it. All sound velocities decreased linearly as the temperature increased. The product of density and sound velocity is a quantity of major importance for the smelt-water explosion model. This quantity determines the magnitude of the pressure of the acoustic wave generated in the smelt from a given motion of the boundary between the water-steam globule and the surrounding smelt. The data from the ultrasonic measurements showed that this quantity is about three times that of water for normal smelt compositions and is decreased when NaCl is present in the mixture.

The bulk modulus (density times square of sound velocity) for normal smelt compositions proved to be about four times as great as that for water. The bulk modulus of smelt also was reduced appreciably by the addition of NaCl to the smelt. The differences in bulk moduli mean that, for a given pressure increment, the molten salts undergo a considerably smaller volume change than does water. These bulk moduli values were used for computations made with the computer model of the explosion mechanism.

The measurements of the attenuation of the ultrasonic waves in the molten salt compositions showed that only a small fraction of a decibel was absorbed over the short pathlength employed. Although this change proved to be too small to be measured accurately, the results of these experiments showed that neither the shear nor the bulk viscosity of molten smelts is an important factor in determining its acoustic wave propagation properties. However, the shear viscosity, which was discussed earlier in this section, could have an important influence on other factors that determine explosive tendency of smelts. For example, the rate of heat input to the water will depend on the rate of mixing of the smelt and water, which in turn may be greatly affected by small differences in shear viscosity.

Electrical Conductivity

Although the electrical conductivity of smelt was not determined, this physical property merits some consideration because of its relationship with thermal conductivity. If ' σ ' is the electrical conductivity, the ionic contribution to the thermal conductivity is $(k/e)^2 \sigma T/J$, where the ratio of Boltzmann's constant to the charge on the electron is $k/e = 86.3$ microvolts/degree, T is the absolute temperature, and J is the mechanical equivalent of heat.

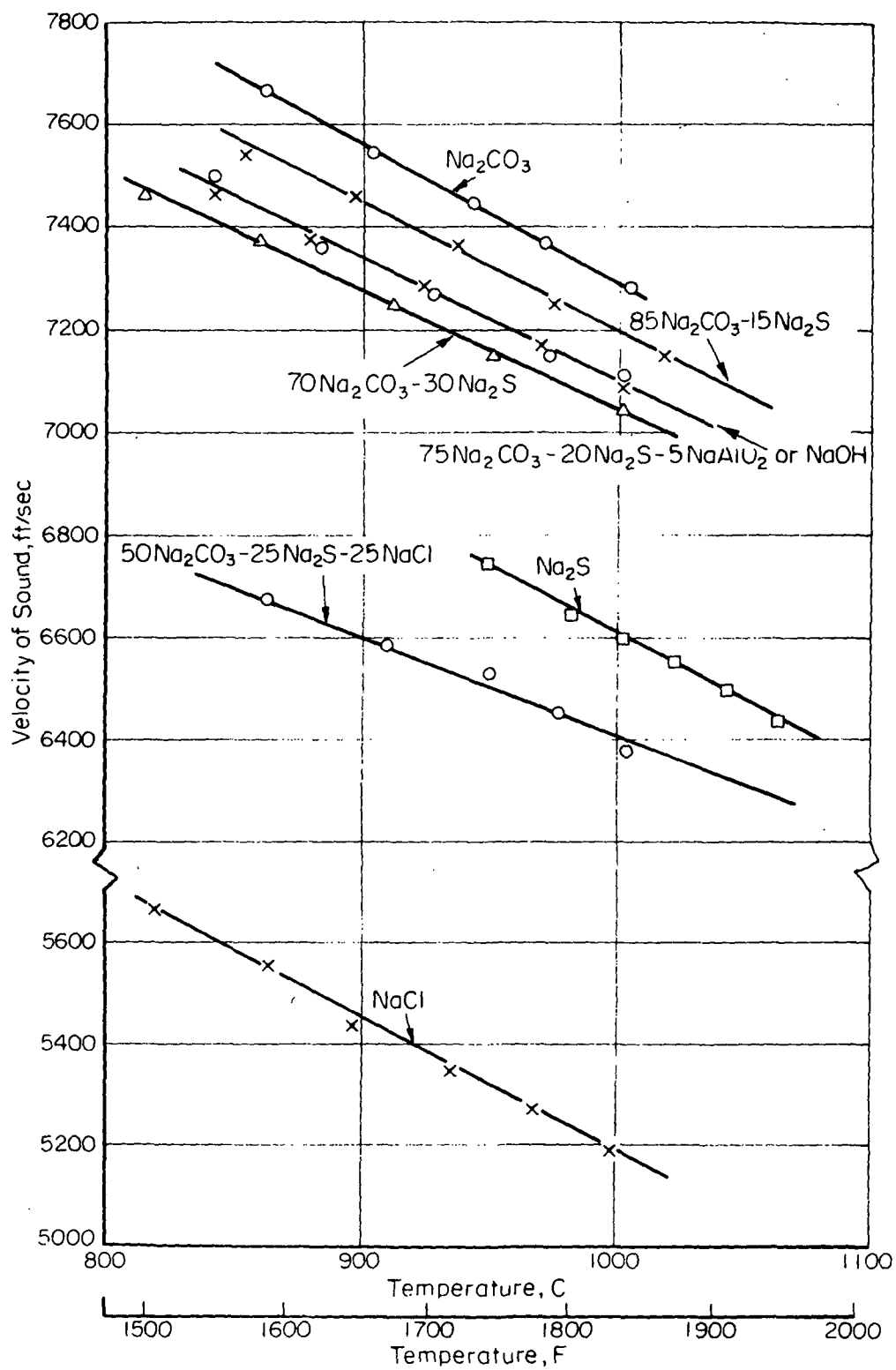


FIGURE 7. VELOCITY OF SOUND IN MOLTEN SALTS

The tabulated value of σ for molten Na_2CO_3 is about $3.0 \text{ ohm}^{-1} \text{ cm}^{-1}$, with a temperature coefficient of about $+0.004 \text{ ohm}^{-1} \text{ cm}^{-1}/\text{degree C}$. The tabulated value of σ for molten NaCl is about $3.8 \text{ ohm}^{-1} \text{ cm}^{-1}$, with a temperature coefficient of about $+0.003 \text{ ohm}^{-1} \text{ cm}^{-1}/\text{degree C}$. Measured values of σ for various compositions of the binary system $\text{Na}_2\text{CO}_3 - \text{NaCl}$ lie between the above values. Hence, electrical conductivity, and the associated thermal conductivity, are physical properties that do not differ significantly between explosive and nonexplosive compositions.

Carbonate Decomposition Studies

In the course of the development of the explosion model it became apparent that the evolution of a sufficient quantity of CO_2 gas from the decomposition of Na_2CO_3 into the steam globule during its expansion phase would inhibit the subsequent collapse of the globule and the generation of a high pressure pulse in the smelt. The rate of the carbonate decomposition would be enhanced by the lower-than-atmospheric pressure in the smelt in the neighborhood of the globule during its expansion phase. The conditions under which CO_2 gas is released and the extent to which it is generated were studied in two types of experiments: (1) cavitation experiments, and (2) vacuum decomposition experiments.

Cavitation Experiments

The steam cavitation model for initiation of smelt-water explosions requires very low pressure in the cavitation bubble at maximum expansion. The CO_2 formed by cavitation-induced decomposition of the Na_2CO_3 in molten smelt thus might be expected to inhibit explosion, so that smelt components that suppress decomposition would act as explosion sensitizers.

To test this hypothesis, experiments were carried out using a motor-driven stirrer capable of operating at speeds up to 10,000 rpm. The stirrer was designed to obtain cavitation in liquids having densities in the range of those of smelt components, from 1 to 3 grams per cubic centimeter. In transparent containers in liquid, cavitation can be detected visually by the formation of vapor bubbles in the liquid in the vicinity of the stirrer, and this technique presented no problems with ordinary liquids in glass containers. Cavitation was readily observed at stirring speeds of about 4000 rpm. When similar experiments were performed with molten smelt compositions contained in an alumina crucible in the resistance furnace, observation of the cavitation bubble phenomenon was uncertain. Consequently an alternative method was adopted. The change in CO_2 concentration over the melt produced by the cavitation was monitored by a continuous reading, nondispersive infrared CO_2 analyzer.

When molten Na_2CO_3 was maintained at 1600 F and the stirring speed was increased slowly, a sudden twofold increase in the CO_2 concentration was observed at a stirring speed of 3700 rpm. When the temperature of the molten sodium carbonate was raised to 1650 F, a comparable increase in CO_2 concentration occurred at a stirring speed of 3900 rpm.

Similar experiments were then carried out with two explosive smelt compositions, one containing 30 percent Na_2S and the other having 25 percent each of Na_2S and NaCl . With these compositions, under the same conditions as used for the Na_2CO_3 , no increase in the CO_2 concentration occurred at any stirring speed up to 10,000 rpm — the limit of the apparatus. These same results were obtained several times on different days when the experiments were repeated to verify the reproducibility.

From this series of experiments it was concluded that the Na_2S and the NaCl , which are explosion-sensitizing components in smelt, inhibit the decomposition of the Na_2CO_3 under the cavitation conditions.

Vacuum Decomposition Experiments

The purpose of the vacuum decomposition experiments was to obtain quantitative information on the effect of both explosion sensitizers and desensitizers on the rate of decomposition of Na_2CO_3 under near-vacuum conditions, such as would exist in a steam bubble at maximum expansion prior to cavitation.

These experiments were carried out by heating the molten salt mixture in a closed system under vacuum. When the desired temperature was reached, the CO_2 produced by decomposition of the Na_2CO_3 was collected in a trap at a temperature of minus 320 F (liquid nitrogen), then transferred to a vacuum line, where the amount obtained was measured.

When Na_2S and NaCl were substituted for part of the Na_2CO_3 , the decomposition rate of the Na_2CO_3 was decreased. This result was to be expected, because the mole fraction of Na_2CO_3 in the mixture was reduced by these substitutions. However, the amount by which the CO_2 yield was reduced was greater than would be anticipated on this basis. For a mixture containing 30 percent Na_2S , the amount of CO_2 obtained experimentally was only 59 percent of that calculated on the basis of the mole fraction of Na_2CO_3 in the mixture. With a mixture containing 25 percent Na_2S and 25 percent NaCl , the CO_2 collected was 71 percent of the theoretical amount. The data are presented in Table 11.

TABLE 11. EFFECT OF VARIOUS SALTS ON THE DECOMPOSITION RATE OF Na_2CO_3 AT 1830 F

Composition of Melt	Mole Fraction Na_2CO_3	CO_2 Evolved, mg/hr		Percent of Calculated Decomposition
		Experimental	Calc. from Mole Fraction	
Na_2CO_3	1.00	72.0	72.0	100
70 Na_2CO_3 -30 Na_2S	0.635	26.8	45.7	58.6
50 Na_2CO_3 -25 Na_2S -25 NaCl	0.385	19.6	27.7	70.7
45 Na_2CO_3 -25 Na_2S -20 NaCl -10 NaAlO_2	0.351	27.4	25.3	108
45 Na_2CO_3 -25 Na_2S -20 NaCl -10 CaCO_3	0.357	26.8	25.7	104

Vacuum decomposition experiments also were conducted with CaCO_3 and NaAlO_2 employed as explosion inhibitors. When either of these two compounds was introduced into the smelt mixture at a concentration of 10 weight percent, the rate of CO_2 release from the molten mixture was increased. The presence of the Na_2S and the NaCl in the mixture caused a reduction in the rate of CO_2 evolution, but this reduction was more than offset by the presence

of the CaCO_3 or the NaAlO_2 in the mixture. As a result there was a net increase in the rate of CO_2 evolution in the presence of the two explosion inhibitor compounds, as shown in the table.

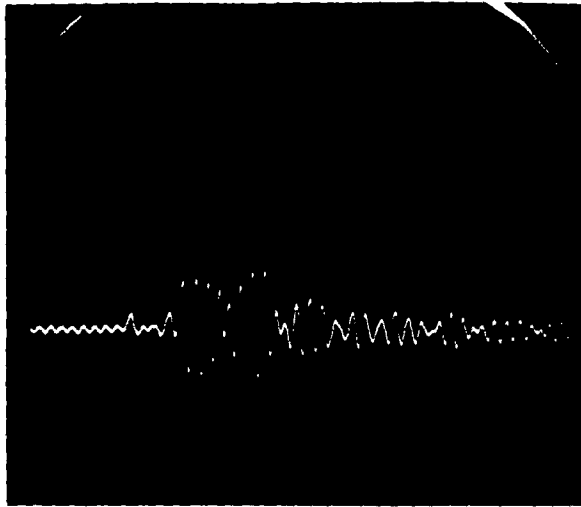
These data provide support for the proposed mechanism of the explosion in that compounds which sensitize the smelt to explosion reduce the rate at which CO_2 evolves, while those which desensitize the explosion increase the rate at which the gas is released from the carbonate in the smelt. These effects are in the right direction to fulfill the requirements of the explosion model.

Pressure-Transducer Experiments

To compare the relative magnitudes of smelt-water explosions obtained under different laboratory conditions, and to obtain data on the explosion characteristics for the model, pressure-transducer experiments were performed. In these experiments, a piezoelectric transducer was coupled to the smelt via an alumina rod immersed in the molten salt. The pressure wave from the explosion, picked up by the rod and sensed by the transducer, was recorded on an oscilloscope and photographed.

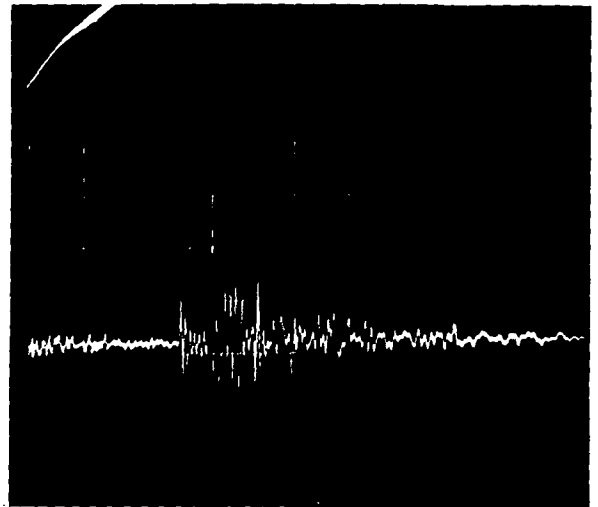
Oscilloscope traces of typical explosions using the smelt mixture containing 25 percent Na_2S and 25 percent NaCl are shown in Figure 8. The upper photograph shows the explosion with 35 milligrams of water injected from the piston type injector, and the lower photograph shows the effect of 75 milligrams of water, using the direct gas-pressure injector. A number of pressure pulses constituting the explosion occurred within a 2-millisecond interval. Typically from 6 to 10 pulses were detected. The amplitudes of the pressure waves varied, most of them being about 20 psi magnitude, but occasionally peaks up to 70 psi were observed. These peaks, of course, represent the particular response of the probe system used and do not represent the actual pressure variations within the exploding water body. This particular response is conditioned by the resonant frequency of the alumina rod, by certain characteristics of the transducer, and by the distance of the end of the rod from the center of the explosion and also from the wall of the crucible and the free surface of the smelt. These pressure-transducer experiments demonstrated that under the conditions of injection of water into smelt, the explosion occurred about 1 millisecond after the water-smelt contact. The duration of the explosion for the amounts of water involved in these experiments (35 to 75 milligrams) was approximately 2 milliseconds.

The results of these experiments are in reasonable agreement with those of other investigators who have attempted to instrument explosions resulting from introduction of water into molten salts. Investigators at the Argonne National Laboratory⁽¹⁾ observed delays of a few milliseconds between water injection and explosion with molten NaCl . The studies at Combustion Engineering, Inc., using larger amounts of water and of smelt, resulted in delay times of about 35 milliseconds between the injection of the water and the explosion. The shock waves detected a few inches above the smelt were also greater (100 to 180 psi). It can be concluded that once the required mixing is achieved and the smelt-water contact is made with large enough heat-transfer rate, the explosion is initiated within a time interval determined by the size of the water body, in agreement with the scaling laws obtained from the model studies, and possibly also as modified by the size and shape of the smelt body.



Scope Sweep →

Piston-type injector
 Horizontal scale: 1 millisecond/large division
 Vertical scale: 20 psi/large division



Scope Sweep →

Direct gas-pressure injector
 Horizontal scale: 2 millisecond/large division
 Vertical scale: 20 psi/large division

FIGURE 8. PRESSURE WAVES FROM EXPLOSIONS AS DETECTED BY A TRANSDUCER

DISCUSSION OF COMPUTER MODEL

Nature of Physical Explosions

Both chemical and physical explosions involve the generation of vapors or gases at a much more rapid rate than the system can absorb by expansion to accommodate the additional volume created. The term system includes not only the environment surrounding the exploding material but also the self-inertia of that material and its surroundings. The latter often furnishes the primary restraint to initial expansion. Because of the restraints, pressure at first builds up rapidly. The resultant potential energy is subsequently converted to kinetic energy of motion of the exploding gases and of their surroundings and to work done in moving or rupturing any restraining or confining structures.

In a chemical explosion, the gases or vapors are generated as a result of chemical reaction. The heat developed in exothermic chemical reactions serves to raise the temperature of the gas or vapor products and perhaps also to volatilize some of the products, thereby increasing the initial pressure pulse. The creation of vapors by volatilization may be considered to be a physical aspect of some chemical explosions. In a purely physical explosion, gases or vapors are not created by chemical action; they result only from volatilization of existing liquids because of a high rate of heat influx to these liquids from a hot environment or other sources. If an exothermic chemical reaction in the system contributes to this volatilizing heat flux, without producing gaseous reaction products, the explosion may be considered to be physical, but with chemical aspects.

The primary types of physical explosion systems that have been recognized are categorized and listed in Table 12. They involve the coming together of two liquids at an initial temperature difference of several hundred to a few thousand degrees. The lower temperature liquid boils at some intermediate temperature; its rapid vaporization causes the explosion. The higher temperature liquid may solidify at an intermediate temperature. For physical explosions to occur, it does not seem to matter substantially whether a relatively small body of the colder liquid is brought into contact with a relatively large body of the warmer one, or vice versa.

TABLE 12. KNOWN PHYSICAL EXPLOSION SYSTEMS

System	References
A. Molten salts – water	
1. Kraft smelts	(11)
2. NaCl	(11)
3. Na ₂ S	(11)
4. KI	(1)
5. AgCl	(1)
B. Molten metals – water	
1. Fe and Steel	(1,2)
2. Al	(1,2)
3. Na	(3)
4. Ti	(2)
5. Hg	(4)
6. Pb and Sn	(4,5)
7. Bi-Pb-Sn-Cd alloy, Pb-Sn alloy	(4)
C. Molten metals and oxides – sodium	
1. UO ₂	(1)
2. Zn	(1)
3. Ni	(1)
4. Steel	(1)
D. Cryogenic – ambient temperature liquids	
1. Liquified natural gas (LNG) – water	(6,7,8)
2. LNG – brine	(8)
3. LNG or liquid CH ₄ – n-pentane or n-hexane	(7,8)
4. Liquid ethane, propane, butane mixtures – water	(8)
5. Condensed pipeline gas (CPG) – coated water	(8)
6. CPG – coated Hg	(8)
E. Molten slag – water	(7)

As with all rules, there are exceptions. Solid sodium placed in contact with water will result in a physical explosion, as does liquid sodium. However, it is pointed out in Reference 3 that this explosion does not take place until after some or all of the sodium metal melts because of the heat generated by the chemical reaction at the Na-H₂O interface. Some of the molten sodium becomes finely divided and dispersed in the nearby water. The Na-H₂O explosion is thus a physical explosion with chemical aspects. The subsequent burning of the H₂ gas formed is not a part of the physical explosion. The sodium explosion occurs just as readily in a nitrogen

atmosphere.⁽³⁾ Likewise, the Al-H₂O explosion is a physical one with chemical aspects; it can occur with little oxidation of the aluminum⁽²⁾ and with no burning of the evolved H₂. While solidification of the hotter liquid after losing heat to the colder one is not necessary for the physical explosion to occur (e.g., the Hg-H₂O explosion), this solidification may contribute in some explosions to the rapid dispersion of one liquid into the other deemed necessary for the explosion to occur.

Investigators generally agree that volatilization of the colder liquid must occur at a very high rate for a physical explosion to occur. It is not generally agreed however, how this high rate of volatilization is obtained. For inertial restraint to expansion, an extremely high rate of heat transfer would be required, three and four orders of magnitude greater than the peak heat flux involved in the transition from nucleate to unstable violent boiling. This is in agreement with the conclusions of the smelt-water model computations.

Attaining a high rate of heat transfer is generally thought to involve a high degree of fragmentation of one liquid and its rapid dispersion into the other; this is in agreement with the considerations in this work regarding the initiation of the main smelt-water explosion. Some experimental evidence upholds this viewpoint. Molten lead dropped into water at 20 C explodes if its temperature ranges from 400 to 650 C or above 750 C.⁽⁵⁾ In these temperature ranges, the residual solidified lead bodies have a mossy or spongy appearance and are found to consist of finely divided particles loosely held together. Near its melting point (327 C) and around 700 C, no explosions occur and the solidified lead does not exhibit this evidence of fine fragmentation. Higgins⁽⁹⁾ developed a technique for intentionally fragmenting the molten metal. Intense explosions occurred for particle sizes of 200 microns or less and little explosive action occurred when the particle size was 1400 microns or greater. Rapid fragmentation and dispersion also seems to be necessary for liquid sodium to produce physical explosions in water⁽³⁾ and also for molten iron, aluminum, and other metals in water or molten sodium⁽¹⁾.

What produces the rapid fragmentation and dispersion of one liquid into the other is a more speculative matter. We have postulated that the instabilities in radial motion during the collapse phase of small water-vapor globules result in the rapid injection of hot smelt into the main water body. The possible role of collapsing vapor bubbles in producing fragmentation and dispersion is discussed also in the Argonne National Laboratory reports.⁽¹⁾ They observe vapor bulges and collapses on molten-metal surfaces in water before explosions occur.

Entrapment, with or without encapsulation, of small globules of the volatile colder liquid in the hotter one is considered by some investigators to be the precursor mechanism for the explosion. For explosions involving insertion of a relatively small amount of the hotter liquid into a large body of the colder, only a very small portion of the latter, comparable to or smaller than the mass of the inserted hotter liquid, can partake of the available heat input needed for the explosion. Some mechanism for essentially isolating this portion, such as entrapment within the hot liquid, seems to be required. There is ample evidence that small droplets of water become entrapped in molten metal^(5,10) and in molten smelt⁽¹¹⁾. Droplets of LNG also become entrapped in water^(6,8) and pieces of ice have been observed to be ejected in explosions. Rupture of solidified capsules, or at least the development of fissures in such capsules, has been proposed as one mechanism whereby the rapid intermixing of the hot and cold liquids can be obtained. Encapsulation by solidification is certainly not necessary for a physical explosion to take place, as seen from the mercury-water explosions. For any reasonable thicknesses of capsules that can be formed on the time scales involved, they can provide neither the mechanical rigidity nor the strength to contain the initial pressure rises computed to be needed for the main

explosion. Moreover, any small additional delay in expansion that may result from encapsulation would contribute to decreasing the initial rate of heat flow needed for the main explosion.

A largely unanswered question is how a small globule of water can become entrapped into a higher temperature body of smelt or metal that is immersed in a container of water. If the immersion is in the form of an injection, such as a jet, entrainment of water could take place by the development of the Helmholtz type of instability.^(2,3,4,6) This is an instability of the boundary between two fluids in relative motion parallel to the boundary. The onset of the instability is controlled primarily by the magnitude of the Weber number (density times square of velocity times radius divided by interfacial surface tension). Where no relative velocity has been deliberately introduced when the hot and cold liquids are brought together (such as by injection), it is generally presumed that motion instabilities associated with strong turbulences and convective flows in the violent boiling developed along the interface may be responsible for the globule entrapment. In our laboratory experiments involving injection of water into smelt, Helmholtz instabilities may be the cause of the rapid fragmentation and mutual dispersion of water into the smelt. On the other hand, the Taylor type of instability is involved in a collapsing vapor globule – the presumed initiating mechanism for the rapid fragmentation and intermixing in the model. This latter instability is associated with the acceleration of the boundary between two fluids in the direction perpendicular to the boundary. Both types of instability may be involved in many cases.

Another physical phenomenon postulated to initiate the main explosion is superheating of a thin layer of the volatile liquid that is in contact with the hot liquid.⁽⁷⁾ The sudden release of the superheat energy upon reaching the limit of superheat, the temperature at which spontaneous nucleation occurs, rapidly vaporizes a portion of the thin layer and results in the formation of a pressure pulse. Presumably, the rapid fragmentation and dispersion needed for the development of the main explosion are thus produced.

There are two difficulties with this initiation model: (1) how is induced nucleation avoided in the boundary layer despite the probable presence of nucleating sources such as solid particle contaminants, small pieces of frozen smelt, ions, and gas bubbles; and (2) how can the expected form of the pressure pulse in the two liquids cause any more than oscillations in the shape of the immersed body of liquid, rather than an appreciable extent of fragmentation and dispersion. However, it is shown later in the section entitled "The Initiating Mechanism" how the superheat phenomenon may be combined with the cavity-collapse phenomenon to form a very plausible picture of the initiating mechanism.

Qualitative Description of Smelt-Water Explosion Model

The computer model of the smelt-water physical explosion developed on this program, like any other model simulation, is an approximate representation of the actual phenomenon obtained by making some simplifying assumptions to facilitate the analysis. If the results of the model computations are in reasonable agreement with some of the main observable features of the actual phenomenon, the model is considered to be useful, since it permits insight to be gained concerning the trends of the changes in system behavior resulting from assumed changes in system properties and input variables. A series of computations made with the model may thus lead to suggestions for the optimization of the desirable aspects of the system behavior and for alleviation or prevention of the undesirable aspects.

The smelt-water model analysis begins with the assumption of the presence of a body in the form of a spherical globule within a pool of smelt of given pertinent physical characteristics (density and sound propagation velocity) and with given temperature and ambient pressure. The globule is composed of water together with a small amount of CO_2 in the gas phase. The computer determines what fraction of the water is initially in the vapor phase from the given ambient pressure, the CO_2 content, and the given initial water temperature. (The mathematical details of this and other computations are given in Appendix B. The limitations of the present computer model are discussed in Appendix C.)

Other initial conditions specified are the initial radial expansion velocity of the globule (nominally zero), the amplitude, phase, period, and degree of nonsinusoidal distortion of a variable component of the ambient pressure (to simulate approximately the effects of expansions and collapses of neighboring globules), the initial rate of heat input to the globule, and the initial rate of CO_2 influx to the globule resulting from decomposition of the smelt. As the computations proceed, the rate of heat input is modified in accordance with the value of the instantaneous temperature difference between the smelt and the globule, the globule radius, and the added insulation provided by the increasing steam and gas contents of the globule. The rate of gas influx is modified as computations proceed in accordance with the ratio of the partial pressure of the gas to the total pressure in the globule, the globule radius, and the globule temperature.

The computational process consists essentially of the stepwise integrations of a number of differential equations, as detailed in Appendix B. These differential equations were derived from the four basic sets of model equations, namely, (1) the conservation-of-energy equation, (2) the conservation-of-momentum equation, (3) the conservation-of-mass equation, and (4) the constitutive equations (equations of state) of liquid water, steam, and gas. The ideal gas law is a sufficiently accurate formulation of the equation of state of the gas (CO_2) under the conditions of interest. The pressure and temperature dependences of the various pertinent properties of liquid water and steam are represented by accurate analytical expressions, given in Appendix B. The derivations of these expressions and reference sources also are included in Appendix B.

Results of Model Computations

The Main Explosion

Figure 9 shows the results of a typical computation for the development of a main (high energy) steam explosion in smelt. The heat input, temperature increase, pressure, diameter, percent of steam, and conversion efficiency of thermal input energy to the globule into mechanical (kinetic) energy in the smelt are shown as functions of time. A log-log scale is used in Figure 9 for clarity in presentation, since changes in the variables occur rapidly at first and then more slowly. Although the zero point in time cannot be represented on the log-log scale, the initial values of the pressure, P_0 , and diameter, D_0 , are indicated on the left margin.

The amount of water involved in the Figure 9 calculations is 1 pound, with a CO_2 gas content of 10^{-5} pounds (0.6 percent gas content by volume) and no assumed increase in gas content with time. The development of the main explosion was found to be little influenced by gas content unless unrealistically high initial values of rates of increase are assumed. The action of the presumed triggering mechanism for the main explosion is much more sensitive to gas

content, as is seen later. The initial water temperature is 50 C (122 F), initial pressure is 1 atmosphere (with no assumed variation in ambient pressure), and initial heat input is 2×10^6 Btu/ft²/sec. The rate of heat input is expressed in terms of heat input rate per unit area of the outer surface of the spherical globule. However, as explained later, the actual contact area between smelt and water would have to be of the order of 1000 times the outer-surface area to obtain the high heat-transfer rates needed for the development of a main explosion.

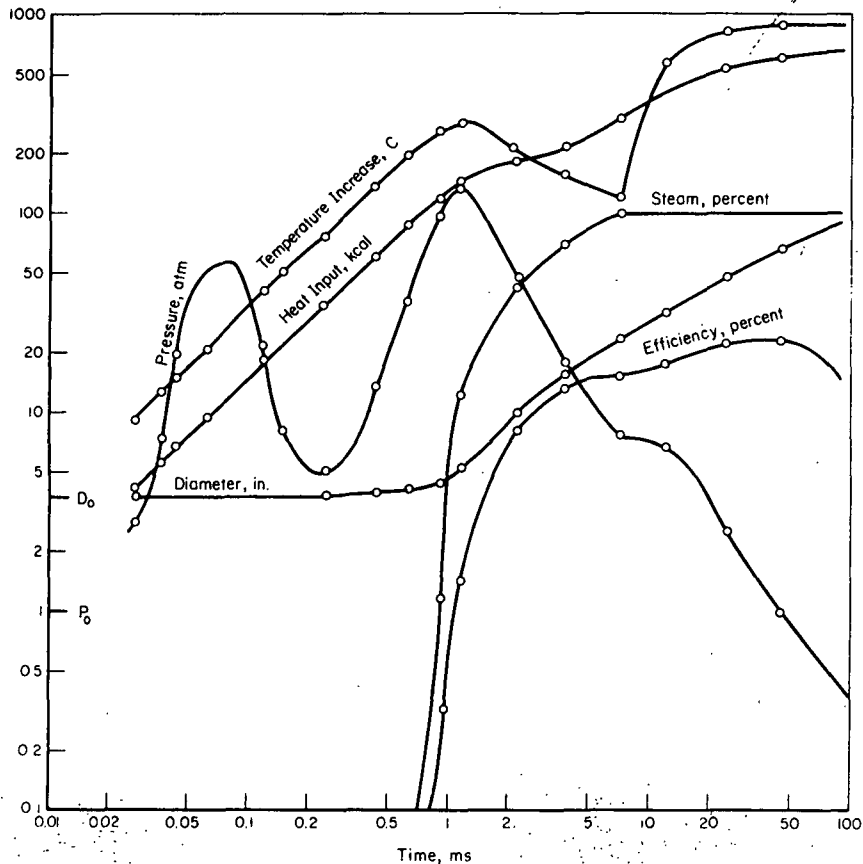


FIGURE 9. DEVELOPMENT OF SMELT-WATER EXPLOSION WITH 1 POUND OF WATER, FOR AN INITIAL HEAT-INPUT OF 2 MILLION BTU/FT²/SEC

For the first 0.7 millisecond after initiation of the main explosion, both the rate of heat input and the rate of rise of temperature of the globule (about 1/3 degree per microsecond) are almost constant. Less than 0.1 percent of the mass of the water has been converted to steam at the 0.7-millisecond point. The pressure peak of 57 atmospheres at 80 microseconds is the result of the inertial resistance of the smelt to the thermal expansion of the liquid water. The pressure drops to a minimum of 5 atmospheres at 240 microseconds as the smelt outward radial velocity increases. The amount of mechanical energy generated in the smelt by this water-expansion pulse is negligibly small, however. The diameter of the globule at 240 microseconds has increased by only 0.08 inch from its initial value of 3.75 inches.

Past the 240-microsecond point in time, the globule pressure begins to increase again as steam begins to be generated very rapidly and the expansion of the globule is again inhibited by the inertia of the surrounding smelt. The pressure reaches a peak value of 132 atmospheres at

1.15 milliseconds, when 12.2 percent of the water has been converted to steam. The globule temperature at this point is 334 C (633 F, a 511 F rise over its initial value) and its diameter is 5.28 inches (2.78 times the original volume). From then on the pressure of the globule (and the temperature also since the two are related by the assumed thermal equilibrium relationship between steam and liquid water) begins to decrease as the globule volume expands faster than steam can be generated to fill it. The heat input rate has also decreased considerably from its initial value because of the added insulation of the steam and the decreased difference between the smelt and globule temperatures (assumed smelt temperature is 950 C, 1742 F).

At 7.24 milliseconds all of the water has been converted to steam. The globule temperature begins to increase very rapidly at this point since input heat is no longer being used to vaporize water. As a consequence, the downward plunge in pressure is almost arrested for about 5 milliseconds as the globule continues to expand because of the kinetic energy imparted to the smelt. At 45 milliseconds the pressure has fallen back down to 1 atmosphere and, coincidentally, the steam temperature has risen to within 36 F of smelt temperature at this point. The total heat input at this point is 607 kilocalories (2410 Btu). Of this energy, 22.75 percent has been converted to kinetic energy of the smelt, at the peak of the efficiency curve. The maximum kinetic energy developed in the smelt is thus 410,000 ft-lb.

Note in Figure 9 that when the globule pressure is back down to 1 atmosphere at 45.2 milliseconds, its diameter is 66 inches (5.5 ft). Clearly, the development of the main explosion, in terms of generating kinetic energy in the smelt, would be essentially completed at some earlier time because of the limited depth of the smelt bed. Furthermore, at some earlier time, the results shown in Figure 9 would begin to become less accurate as the globule diameter approaches an appreciable fraction of the liquid smelt depth. The proximity of walls and bottom of the furnace and other temporary constraints to initial expansion would tend to augment the severity of the explosion, and the proximity of the upper free surface of the smelt to reduce it, as pointed out later in the critical parameter discussion. In the practical situation, therefore, all that can be concluded is that an explosion with a mechanical energy level of some small multiple of 100,000 ft-lb would be expected to develop for an initial heat input rate of 2×10^6 Btu/ft²/sec of outer surface area into a 1-pound globule of water in smelt. This is to be compared with the mechanical energy produced by an explosion of 1/2 pound of TNT in water, which is about 300,000 ft-lb.

The amount of heat energy required to change 1 pound of liquid water at 50 C (122 F) to steam at 930 C (1706 F) at a constant pressure of 1 atmosphere, in a thermodynamically reversible manner, is readily computed to be 475 kilocalories (1883 Btu). The energy input to the globule at 45.2 milliseconds, when the water has become all steam at 930 C (1706 F) and the pressure has dropped to 1 atmosphere, is given by the computer to be 607 kilocalories. Hence, the dynamic pressure-volume-temperature variations resulting from the high rate of heat input are such as to permit an additional heat input of 132 kilocalories up to this point, as compared with the reversible case. This additional heat is largely converted to the kinetic energy of motion of the smelt.

The values of the various quantities of interest for the main explosion are plotted in Figure 10 as functions of the initial rate of heat input, Q_0 . All other conditions are the same as for Figure 9. The maximum value of the pressure rise, in excess of the assumed 1 atmosphere ambient, is closely proportional to Q_0 , and the time after explosion initiation to reach this peak pressure is approximately inversely proportion to Q_0 . The kinetic energy developed in the smelt and the corresponding efficiency decrease rapidly as Q_0 decreases, down to only 23,000 ft-lb and 1.8 percent, respectively, at $Q_0 = 100,000$ Btu/ft²/sec. This point is considered to be about the lower limit for an effective main explosion.

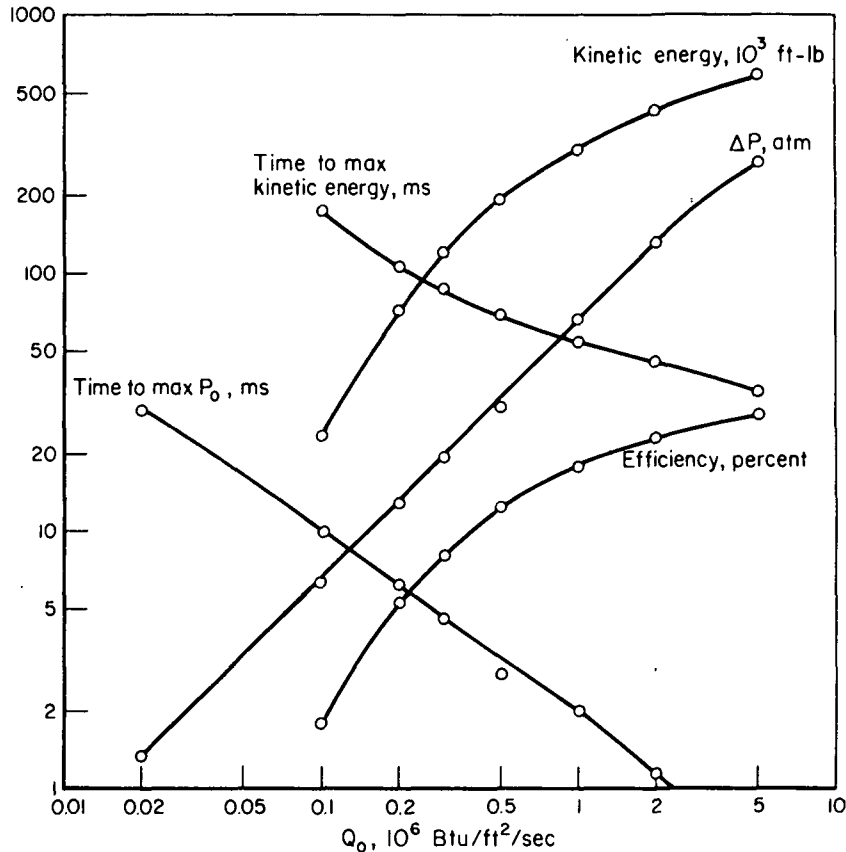


FIGURE 10. DEPENDENT VARIABLES OF EXPLOSION OF 1 POUND OF WATER AS FUNCTIONS OF INITIAL RATE OF HEAT INPUT

The particular characteristics of the smelt used in the computations illustrated above are a density of 1.86 g/cm^3 and sound velocity of 1985 m/sec , corresponding to a very explosive smelt composition of 50 weight percent Na_2CO_3 , 25 percent Na_2S , and 25 percent NaCl . No significant differences in results were obtained in computations using the measured values of these properties for a variety of smelt compositions, including pure Na_2CO_3 . Computed peak pressures, for example, may differ in value by as much as 25 percent or so, but the model computations result in no rapid transition from nonexplosive to explosive behavior as the concentration of NaCl , for example, is increased by a few percentage points. Surface tension and viscosity were not directly included in the model. As shown in Appendix B, it is only for extremely small globules (10 to 100 microns) that these physical properties would have any appreciable effects on the results. (The possible effects of viscosity and surface tension on the initiating mechanism for the main explosion are discussed below.)

The Initiating Mechanism

The initiating, or triggering, mechanism for the main explosion must, within about a millisecond, mix about a pound of smelt with each pound of water thoroughly enough to increase the area of the contact surface by several hundred to one thousand times the outer surface area of the assumed original sphere containing the water. This amount and rate of mixing is necessary to obtain the high initial heat-transfer rates that are needed for the development of a

severe explosion. One possible mechanism for achieving this mixing arises from the instabilities that accompany the collapses of small vapor-filled cavities surrounding or in contact with the main body of water. These instabilities may consist of large distortions in the shape of the surface, breakdowns into many smaller droplets, and formations of jets of smelt, all accompanied by much turbulence.

Figure 11 shows the globule pressure as a function of time for the same conditions as Figure 9, but for an initially 1-cm-radius globule with an initial rate of heat impact of only 1000 Btu/ft²/sec. (The same magnitude and waveform of pressure variation as shown in Figure 9 is obtained for any other initial globule radius if the time scale is changed in proportion to the radius, all other input parameters remaining the same.) The initial water-expansion pressure pulse is omitted since it is completed in microseconds, and, hence, cannot be suitably shown on the linear millisecond scale of Figure 11. The first pulse shown is the direct pressure pulse resulting from the initial rapid generation of steam, corresponding to the second pulse of Figure 9. It reaches a peak value of 2.0 atmospheres at 16 milliseconds and returns to 1 atmosphere at 21 milliseconds. Expansion continues because of the kinetic energy of the smelt, now against the retarding force of a greater ambient pressure than internal globule pressure. Expansion ceases at 30 milliseconds at a globule pressure of 0.61 atmosphere and a globule radius of 6.84 cm. Only 12 percent of the water has been converted to steam at this point. Collapse begins slowly at first and then with increasing speed, until halted by the build up of pressure to a peak value of 6.3 atmospheres at 42 milliseconds. The computer program provides for an increasing rate of heat transfer from the smelt to the globule during the phase of the globule collapse when the pressure is above 1 atmosphere and rising (the manner is explained in Appendix B). The globule-shape instabilities expected to develop in this region would lead to increased actual contact area with the smelt. Re-expansion occurs to a greater radius and lower pressure minimum (0.32 atmosphere) and to a higher second collapse pressure peak (12.9 atmospheres). The water has all turned to steam at this point and remains steam except for a minor amount of re-condensation near the subsequent pressure minimum. Subsequent pressure peaks are lower and broader, and eventually the pressure oscillations become sinusoidal as their amplitude becomes small compared with the ambient pressure. About 5 percent of the maximum kinetic energy in the smelt is lost per cycle of bubble oscillation in the form of radiated acoustic energy. (Although the amplitudes of successive peaks are seen to decrease by more than 5 percent in Figure 11, the energy is compensated for by their becoming "broader" in time.)

Figure 12 shows the effects of the CO₂ influx to the globule at the initial rate of 0.08 percent of the water mass per millisecond, but at an ever-decreasing rate as the gas partial pressure within the globule increases. All other conditions are the same as for Figure 11. The effect of the added gas on the pressure maxima and minima are seen to be quite pronounced. The third collapse pressure peak at 124 microseconds is now the highest one rather than the second, since the 100 percent steam point is not reached until about this later time.

The added CO₂, like the generated steam, serves primarily to reduce the rate of heat input by providing added thermal insulation. The thermal conductivities of steam and CO₂ gas are about the same. H₂ gas substituted for the CO₂ in the computations produced much less effect than CO₂ in reducing the pressure peaks of Figure 11, for the same volume (molal) rates of gas input. The thermal conductivity of H₂ is about 9 times that of CO₂, and its heat capacity per unit volume (specific heat times density) is about 21 percent greater than that of CO₂.

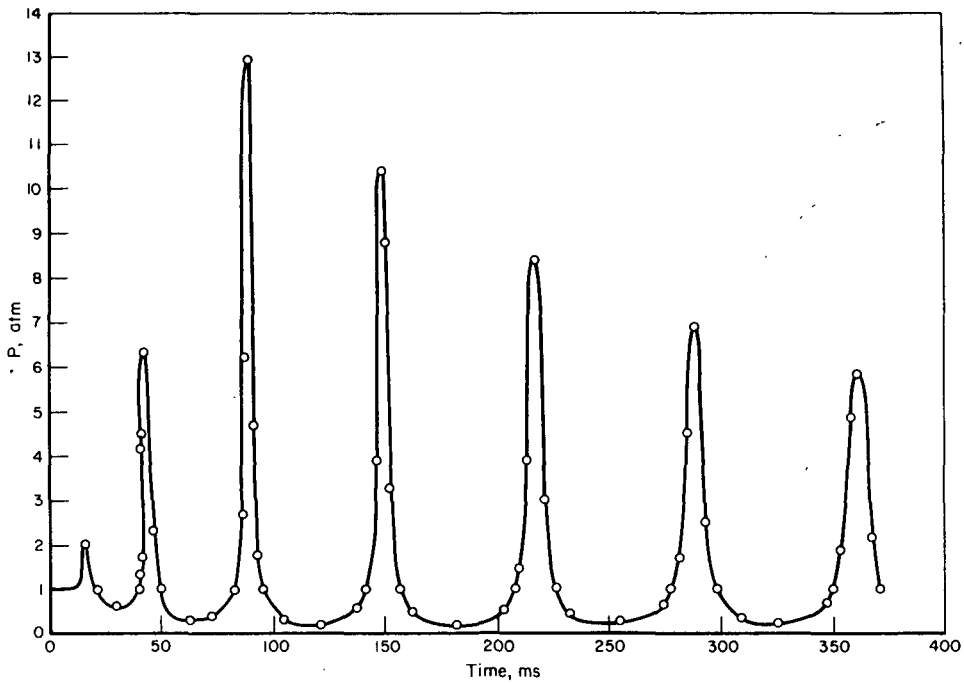


FIGURE 11. PRESSURE AS A FUNCTION OF TIME FOR TRIGGERING GLOBULE, NO ADDED CO_2 INPUT

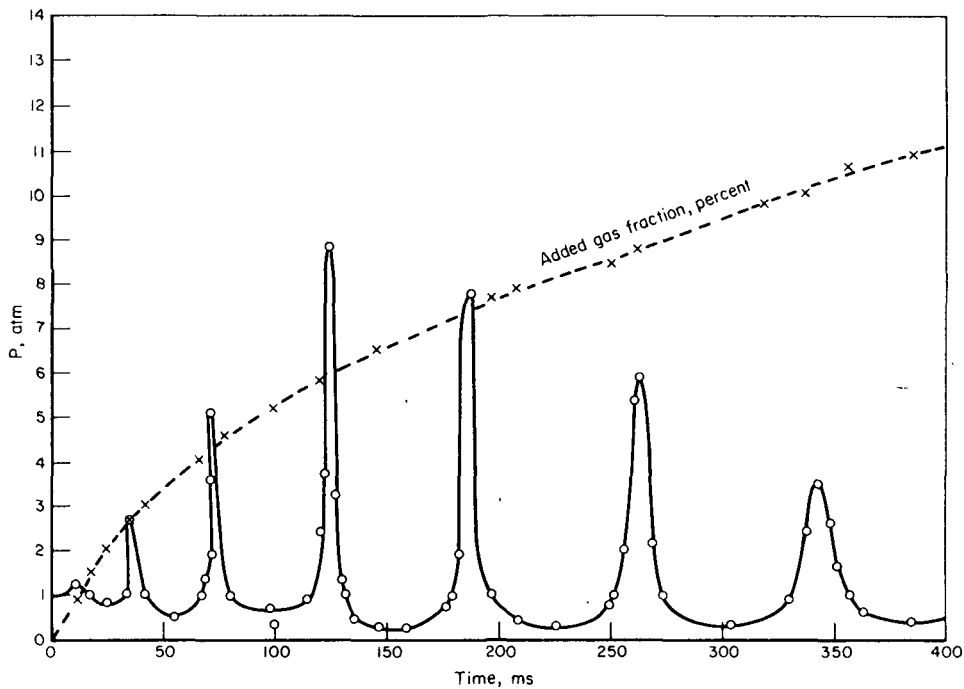


FIGURE 12. PRESSURE AS A FUNCTION OF TIME FOR TRIGGERING GLOBULE WITH CO_2 GAS ADDED

A series of computations was made on the effects of varying the ambient pressure. This variation simulates approximately the effects of neighboring globules. Ambient-pressure fluctuations at much greater, at about the same, and at much lower frequencies than the natural frequency of the globule expansion and collapse cycle (which is a nonlinear function of oscillation amplitude), different phase relationships between ambient and globule pressure variations, and different amplitudes and degrees of distortion of the ambient-pressure oscillations were "experimented with" on the computer. In most, but not all, attempts the amplitudes of one or more of the early globule pulsations were enhanced appreciably by the ambient-pressure variations. Although the amplitudes of the other pressure peaks remained about the same or were reduced, the effectiveness of the "triggering" action would, in general, be expected to be increased by the ambient-pressure variations, since the more energetic globule collapses are expected to result in greater radial motion instabilities. Thus gas influx would serve not only to reduce the pulsation amplitudes of the individual globules but also to reduce the enhancements of some of the amplitudes resulting from the interactions of neighboring globules.

The kinetic energy developed in the smelt by the expansions and contractions of several small triggering globules with initial radii of the order of millimeters, surrounding the main water body, is computed to be adequate to inject a sufficient amount of smelt rapidly enough into a main water body (1 pound of water) to cause an explosion. The amount of surface energy required to produce the approximately 1000-fold increase in contact surface area between the smelt and the water is computed to be negligible for surface tension values of the order of 200 dynes/cm.

Superheating of the boundary layer of the main water body in contact with the smelt could account for the formation of the small steam-filled cavities surrounding the main water body. The steam resulting from the release of the superheat cannot maintain its expansion in the form of a layer of ever-increasing thickness. Such accelerated motion of a less-dense fluid (the steam layer) toward a more-dense fluid (in both directions toward the water body and toward the smelt) is unstable.⁽¹²⁾ Any slight disturbance would tend to grow rapidly until the layer of steam degenerated into an array of pockets or globules of steam, thereby also resulting in recontacting of the smelt and liquid water between the globules for the process to repeat itself.

Each such expanding steam globule would expand more toward the water side because water is less dense than smelt. This equivalent rectilinear motion toward the smelt would accelerate as the globule subsequently collapsed, as required by the conservation of linear momentum of the surrounding fluid. Such accelerated motion becomes unstable, and results in the formation of jets of smelt that shoot through the globule into the water.⁽¹³⁾

Explosion Damage Considerations

The pressure curve of Figure 9 represents the assumed uniform absolute pressure within the globule. It is also the pressure in the smelt in immediate contact with the assumed spherical outer surface of the globule. Away from the globule, however, the excess pressure in the smelt (the smelt pressure minus the ambient pressure) decreases inversely as the distance from the center of the globule. Thus, at a distance of 2 globule radii from the surface of the globule, the smelt pressure is ambient pressure plus one-third the difference between the pressure shown in Figure 9 and ambient. The small time delay between a given pressure event in the globule and its

later appearance at some point in the smelt amounts to only about 5 microseconds per cm of distance from the globule surface, because of the finite value of the velocity of sound propagation in the smelt.

There are two components of the velocity of motion of the smelt at any point away from the globule. For the first component, the velocity is directly proportional to and in phase with the excess pressure (2.7 centimeters per second per atmosphere). For the second component, the radial acceleration is directly proportional to and in phase with the negative of the pressure gradient. The amplitude of the first component therefore, decreases inversely with distance from the source center and that of the second component inversely as the square of this distance, as is characteristic of radial incompressible fluid flow. The second velocity component is by far the dominant one at the surface of the globule, but the first one, called the "far-field" sound wave, becomes predominant at large distances from the globule. The kinetic and potential energies in the smelt associated with this second component interchange with the potential and thermal energies in the globule as the globule expands and contracts. All of the much smaller energy of the first component would be irreversibly radiated away into the smelt if the smelt were an essentially infinite body. However, some of this energy is reflected back to the globule from the various boundaries, obstacles, or pressure-release surfaces that may exist in the smelt.

The force produced by an explosion on a structure in contact with the smelt and the work done in deforming that structure cannot be computed in any simple manner from the pressures and energy flows in the smelt at the distance of the structure from the exploding globule in question. The mechanical characteristics, geometry, the various constraints on the motions of the structure, in combination with the pressure and duration of the incident wave all determine how much force is exerted on that structure by the acoustic wave and how much energy it absorbs from the wave. A thick steel plate at least 10 feet in diameter would initially reflect at least about 0.8 of the acoustic pressure wave, and so would experience a resultant pressure on its surface of at least 1.8 times the incident pressure from the explosion. This pressure-intensification factor would be greater over that portion of the plate that may be located in the "near field" of the globule. Within microseconds, the portion of the pressure wave that entered the steel plate would reflect from its far face and return such as to produce a small pulse of forward motion of the plate, thereby decreasing the above pressure ratio. As the plate forward velocity increases with successive reflections it would experience less force from the incident wave. Since the incident wave is also changing with time, since different portions of the plate are at different distances from the source, and since the edges of the plate and various points on the plate may be constrained from moving by structures having their own compliances, it would be difficult to predict without a great deal of detailed computation just how much force various portions of the plate would experience and how much permanent deformation the plate might suffer.

Although the structures of furnace floors and walls are much more complex than that of a steel plate, with embedded cooling tubes and added burdens of solid smelt layers and char beds, some estimate can be made as to the type of response to the smelt-water explosion shown in Figure 9. When the globule pressure has returned to 1 atmosphere at 45 milliseconds, the smelt surrounding the globule has attained an outward velocity of about 1000 cm/sec (33 ft/sec). In the direction toward the free surface of the smelt, which would about coincide with the surface of the globule at the termination of the explosion, the smelt would be thrown upward with this velocity, thereby rising to a height of as much as 1000 cm (33 ft) against gravity. The furnace floor immediately below the exploding globule would experience locally a pressure of tens of atmospheres for no more than about 2 milliseconds. This is estimated from the magnitude and duration of the initial steam-expansion pulse (132 atmospheres maximum), as decreased in

inverse ratio to the distance from the floor to the center of the exploding globule, as amplified by a factor of at least 1.8 from the initial reflection, and as decreased somewhat by the downward velocity of motion and deformation accumulated by the furnace floor during the 0.7-millisecond build-up time of this pressure pulse. Only a small fraction of the small amount of kinetic energy in the smelt at this point in time is available for doing work on the floor structure, because most of the acoustic wave is reflected from the floor. The high-pressure initial steam-expansion pulse could thus produce only some very local damage of an unknown extent to the furnace floor. It would also impart some downward momentum to the floor structure, which would eventually be opposed by elastic and possibly also some plastic deformation of the floor and its mounting structures. The main damage to the floor structure and its supports, however, should result from the sustained "stagnation" pressure level that results when the high outward velocity of the smelt following the initial steam-pressure pulse is essentially stopped by the floor. As previously mentioned, this outward velocity reaches 1000 cm/sec when the globule pressure has returned to 1 atmosphere. The value of the stagnation pressure resulting from stopping this smelt motion is just about an excess pressure of 1 atmosphere above ambient, but now spread over a much larger area. The resultant large force on the already previously weakened floor and its supports is sustained for about 100 milliseconds, allowing much of the energy in the smelt to be converted to work done in deforming the floor structure. Of the 400,000 ft-lb of energy developed in the smelt by the explosion shown in Figure 9, it is estimated that roughly one-fourth would be used up in throwing smelt up out of the smelt bed, roughly one-fourth into work done in deforming the floor and its supports, and roughly one-half in lateral motion of the smelt. If the explosion took place near a wall of the furnace, the added confinement would result in utilizing a larger portion of the available energy to damage the wall and the floor.

Critical Parameter Analysis

If the components or initial conditions of a physical system are changed, distinct changes in behavior of the system may occur when the numerical values of one or more dimensionless parameters reach certain critical values. Each such parameter consists of a dimensionless combination of dynamic or thermodynamic variables, material properties, and length dimensions of the system. A well-known example is the Reynold's number, $v\rho D/\eta$, whose numerical value determines whether a given fluid flow pattern is laminar or turbulent. The dynamic variable is v , the velocity; the material constant is the dynamic viscosity (ratio of viscosity, η , to density, ρ) and the critical system length dimension is D , the diameter or other pertinent linear measure of the conduit size. More than a dozen such dimensionless parameters are significant for various systems involving fluid flow, thermodynamics, and heat transfer.

The critical dimensionless parameters of a system may be obtained from the coefficients in the differential equations that govern the behavior of the system, after these equations have been properly reduced to dimensionless form. This reduction is accomplished by application of suitable scaling factors to both the dependent and independent variables in the equations. How this is done for the smelt-water explosion computer model is detailed in Appendix D.

The considerations given in Appendix D have resulted in the identification of two critical dimensionless parameters, A and B, and several other dimensionless parameters that are not thought to be critical for one reason or another. These critical parameters are

$$A = \frac{3Q_o \sqrt{\rho_{sm}/P_o}}{\rho_{wo} L_w(T_o)} \quad (1)$$

$$B = \dot{w}_g R_o \sqrt{\rho_{sm}/P_o} \quad (2)$$

where

Q_o = initial rate of heat input to the water globule per unit outer superficial area of the assumed spherical shape of the globule

ρ_{sm} = density of the smelt

ρ_{wo} = initial density of the liquid water

P_o = ambient pressure

$L_w(T_o)$ = latent heat of vaporization of water at the initial temperature = T_o

R_o = initial globule radius

\dot{w}_g = mass rate of gas influx relative to total mass of H_2O in the globule.

In order to examine the significance of Parameter A, it is written in the following form:

$$A = \left(\frac{3 Q_o}{R_o} t_c \right) / \rho_{wo} L_w(T_o) \quad (3)$$

where $t_c = R_o \sqrt{\rho_{sm}/P_o}$ is shown in Appendix D to represent the suitable time-scaling factor for the model explosion. Since $3 Q_o/R_o$ is the rate of heat input per unit volume of the globule, the term in the parentheses in the numerator of Equation (3) is the total amount of heat added to a unit volume of the globule in the characteristic time t_c . The quantity in the denominator is the latent heat of vaporization per unit volume of water. The Parameter A is thus the ratio of the amount of heat added to the globule over the period of time corresponding to a given amount of dynamic change to the total amount of heat required to vaporize the water in the globule. Therefore, it is not so much the rate of heat input that is responsible for the magnitude of the physical explosion, but the amount of heat added before any appreciable dynamic expansion can occur, whether limited by inertia, encapsulation, container walls, superheating, or other temporary restraints on expansion.

For $Q_o = 540,000 \text{ cal/cm}^2 \text{ sec}$ ($2 \times 10^6 \text{ Btu/ft}^2 \text{ sec}$), $\rho_{sm} = 2 \text{ g/cm}^3$, $\rho_{wo} = 1 \text{ g/cm}^3$, $P_o = 10^6 \text{ dynes/cm}^2$ (1 atmosphere), and $L_w = 540 \text{ cal/g}$, the value of the Parameter A is $3 \sqrt{2} = 4.23$, in accordance with Equation (1). The development of damaging physical explosions thus requires values of the dimensionless Parameter A of the order of unity. On the other hand, the development of sizable explosions by the collapse of vapor-filled small globules following their initial expansions, the presumed triggering mechanism for the main explosion, require Q_o values of the order of magnitude of only $1000 \text{ Btu/ft}^2 \text{ sec}$, corresponding to A-parameter values of the order of 0.002.

The influx of gas into the water-steam globule does not greatly affect the development of the main explosion unless this influx is much greater than can reasonably be accounted for. The value of Parameter B = $\dot{w}_g t_c$ is much more critical for the presumed triggering mechanism, however. For the example of Figure 12, $\dot{w}_g = 0.80/\text{sec}$, $t_c = 1.41$ milliseconds, and $B = 1.13 \times 10^{-3}$. Similar to the case for Parameter A, it is not how fast the gas enters the triggering globule that counts, but how much gas enters during the critical response time.

The factors in Parameter A include three physical properties of the smelt and water, one dynamic variable, the ambient pressure P_o , and one thermodynamic variable, Q_o , but no length variable. The absence of a length variable in A is in accord with the results of computations made with the model. The magnitudes of the pressure variations, temperature variations, and radial velocity of the globule wall depend primarily on the assumed value of Q_o , but not at all on the assumed value of the initial globule radius, R_o ; that is, on the size of the body of water. However, the time scale of all events is proportional to R_o , which factor appears in the definition of t_c . The value of Parameter B is thus proportional to R_o .

The magnitude of the thermodynamic variable Q_o in Parameter A must depend upon the mode of contact between the smelt and the water, in addition to the thermal properties of these materials such as thermal conductivity and specific heat. Its particular value in each case would depend upon the chance distributions in number, size, and phasing of the collapsing cavities surrounding the main water body that presumably initiate the main explosion. Parameter A would thus be expected to have some statistical distribution about a mean value in any given experimental situation. Explosive incidence is low or zero in a given situation if high enough values of A seldom occur, and explosions occur practically 100 percent of the time if most of the attained values of A are on the high side. Only the violence of the explosion would vary from case to case, depending on the particular magnitude of A. Practical experience tends to confirm the existence of such distributions in the magnitude of A, since only some of the known cases of smelt-water contact in recovery furnaces result in explosions. The variations in the degrees of violence of furnace explosions would depend not only on the statistical distributions in A but also on the size of the water body.

If dimensionless Parameter A is significant for physical explosions, it must be more generally applicable than to smelt-water explosions. For the explosion of water and liquefied natural gas, the density of water (1 g/cc) would replace that of smelt (1.86 g/cc) in Equation (1), and in the denominator would be the product of the density (0.415 g/cc) and latent heat of vaporization (138 cal/g) of LNG. To obtain the same value of $A = 4.23$ as computed for the particular case of the smelt-water explosion discussed above, would require a value of Q_o of only 156,000 Btu/ft² sec for the water-LNG explosion rather than 2×10^6 Btu/ft² sec. The temperature difference between LNG and water is about 160 C as compared with about 900 C for smelt and water. The required value of Q_o for the water-LNG explosion is thus about one-half of the ratio of the temperature differences times that for the comparable smelt-water explosion. This is a very reasonable result in view of other physical properties affecting heat transfer in the water - LNG system, and which are therefore expected to influence the value of Q_o . This reasonable value calculated for the Q_o of the water - LNG system tends to confirm the significance of Parameter A for physical explosions.

REFERENCES

- (1) Argonne National Laboratory, "Reactor Development Program Progress Report", ANL-7553 (February 1969) and ANL-7742 (September 1970).
- (2) L. C. Witte, J. E. Cox, and J. E. Bouvier, "The Vapor Explosion", *J. of Metals*, p. 39 (February 1970).
- (3) K. Flory and R. B. Mesler, "Sodium-Water Explosions", University of Kansas Report (March 18, 1970, Unpublished).
- (4) R. H. Bradley, L. C. Witte, and J. E. Cox, "The Vapor Explosion-Heat Transfer and Fragmentation. V. Investigation of the Vapor Explosion Phenomenon Using a Molten-Metal Jet Injected into Distilled Water", A.E.C. Technical Report No. ORO-3936-7, University of Houston (October, 1971).
- (5) R. M. Paoli and R. B. Mesler, "Explosion of Molten Lead in Water" Proceedings of the 8th International Congress on High Speed Photography, John Wiley & Sons (1968).
- (6) L. C. Witte and J. E. Cox, "Nonchemical Explosive Interaction of LNG and Water", presented at ASME Winter Annual Meeting, Washington, D.C., ASME preprint (1971).
- (7) D. L. Katz and C. M. Sliepceвич, "LNG/Water Explosions: Cause and Effect", *Hydrocarbon Processing*, p. 240 (November, 1971).
- (8) E. Nakanishi and R. C. Reid, "Liquid Natural Gas-Water Reactions", *Chem. Eng. Progress*, 67 (December 1971), p. 36.
- (9) H. M. Higgins, "The Reaction of Molten Uranium and Zirconium Alloys with Water", Aerojet General Report No. Agc-AE-7, p. 18 (April 30, 1965).
- (10) F. E. Brauer, N. W. Green, and R. B. Mesler, "Metal/Water Explosions", *Nuclear Science Eng.*, 31, p. 551 (March, 1968).
- (11) W. Nelson and E. H. Kennedy, "What Causes Kraft Tank Explosions?", *Paper Trade Journal*, 140, No. 29: 50-56; No. 30: 30-32 (July 16 and 23, 1956).
- (12) G. I. Taylor, "The Instability of Liquid Surfaces When Accelerated in a Direction Perpendicular to their Planes", *Proc. Royal Society London*, A201, p. 192 (1950).
- (13) L. Chincholle, "Bubbles and the Rocket Effect, *J. Applied Physics*, 41, p. 4532 (1970).

The work reported herein is carried out under contract with the Fourdrinier Kraft Board Institute, Inc., whose membership consists of the following companies

Alton Box Board Company
Boise Cascade Corporation
Chesapeake Corporation of Virginia
Container Corporation of America
Continental Can Company, Inc.
Crown Zellerbach Corporation
Georgia Kraft Company
Georgia-Pacific Corporation
Great Northern Paper Company
Hoerner-Waldorf Corporation
Inland Container Corporation
International Paper Company
MacMillan Bloedel United, Inc.

The Mead Corporation
Olinkraft, Inc.
Owens-Illinois, Inc.
Packaging Corporation of America
Pineville Kraft Corporation
St. Joe Paper Company
St. Regis Paper Company
Tennessee River Pulp and Paper Company
Union Camp Corporation
Western Kraft Corporation
Westvaco Corporation
Weyerhaeuser Company

The Project is also sponsored by the following companies which are not members of the Fourdrinier Kraft Board Institute, Inc.

U. S. COMPANIES

American Can Company
Arkansas Kraft Corporation
Bowers Southern Paper Corporation
Brown Company
The Buckeye Cellulose Corporation
Eastex, Inc.
P. H. Glatfelter Company
Gilman Paper Company
Groveton Papers Company
Gulf States Paper Corporation
Hammermill Paper Company
Hudson Pulp & Paper Corporation
ITT Rayonier, Inc.
Longview Fibre Company
Nekoosa-Edwards Paper Company
Oxford Paper Company
Potlatch Forest, Inc.

CANADIAN COMPANIES

Riegel Paper Corporation
Scott Paper Company
Simpson Lee Paper Company
Southwest Forest Industries
U.S. Plywood-Champion Papers, Inc.
Abitibi Paper Company, Ltd.
British Columbia Forest Products Ltd.
Canadian Forest Products Limited
Consolidated-Bathurst Limited
Domtar Pulp & Paper Products Ltd.
Dryden Paper Company, Ltd.
E. B. Eddy Company
Northwood Pulp Limited
The Price Company, Ltd.
Prince George Pulp & Paper Ltd.
Thurso Pulp and Paper Company

APPENDIX A

EXPERIMENTAL TECHNIQUES AND DATA

Explosion Experiments

Ultrasonic Measurements

Cavitation Experiments

Vacuum Decomposition Studies

Infrared Studies

Pressure Transducer Experiments

Other Physical Property Measurements

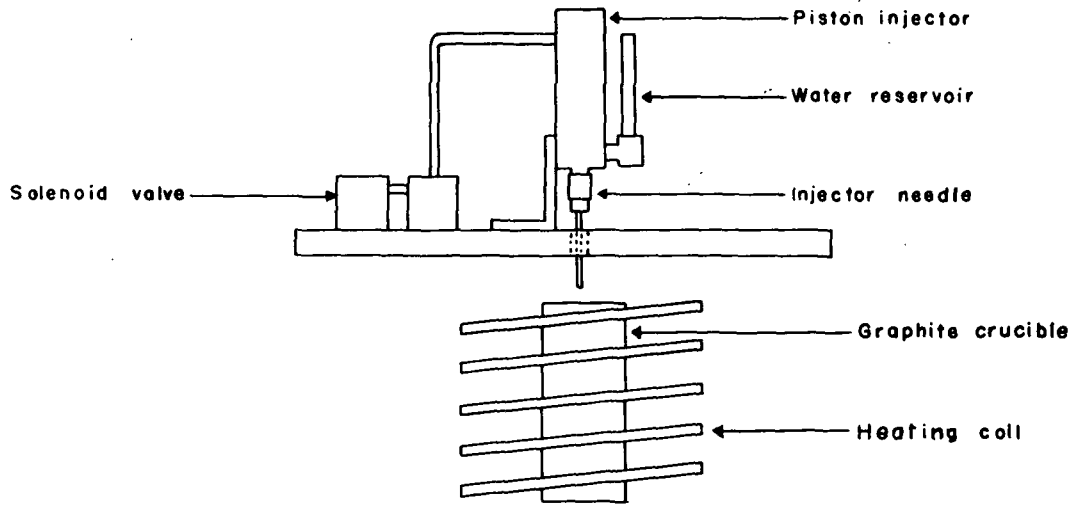


FIGURE A-1. DIAGRAM OF PISTON-TYPE WATER INJECTION APPARATUS

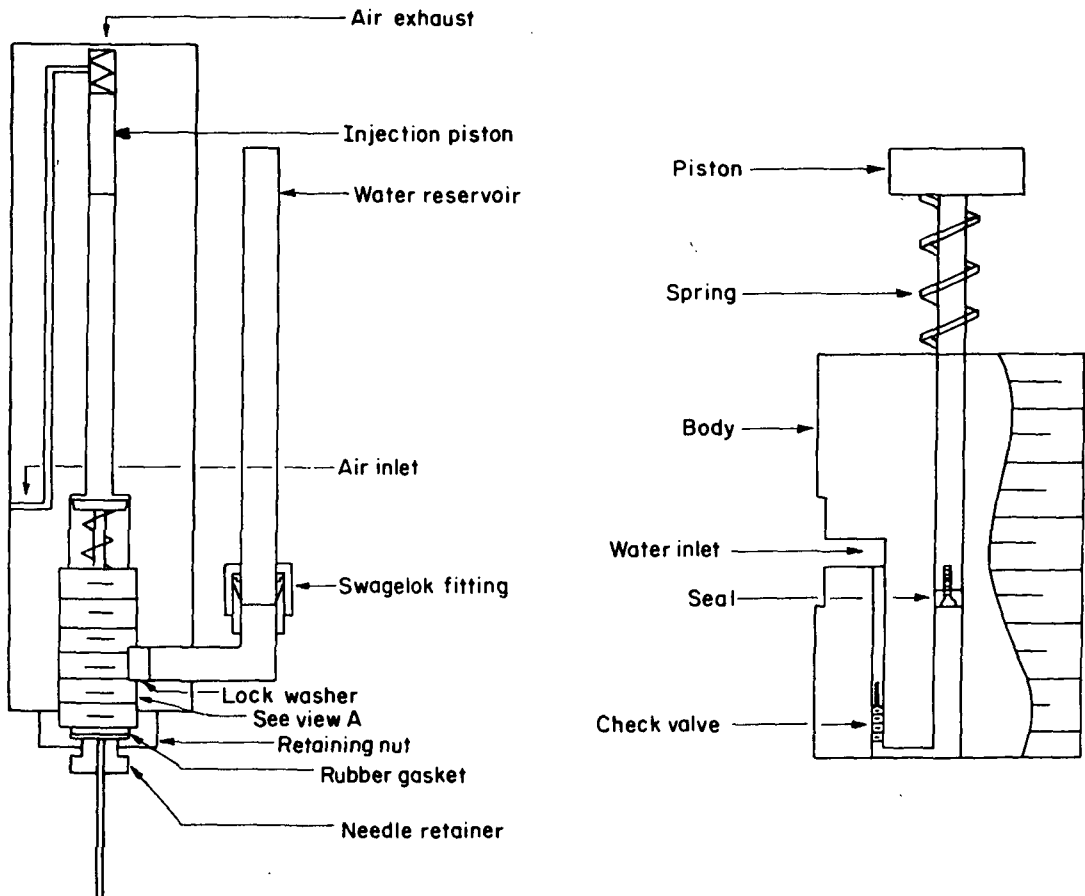


FIGURE A-2. DETAIL OF THE PISTON-TYPE WATER INJECTION APPARATUS

APPENDIX A

EXPERIMENTAL TECHNIQUES AND DATA

EXPLOSION EXPERIMENTS

The explosion studies were aimed at delineation of the ranges of smelt composition and other conditions that have a very high probability of explosion and those that are nonexplosive when water is injected. It was concluded in the feasibility study carried out at Battelle for the FKI in 1968 that neither heat conduction nor heat radiation could transfer energy from the smelt into the water nearly rapidly enough to cause explosion. Some type of turbulent mixing is required which will not allow a blanket of steam to insulate water that has been trapped within the smelt.

With this factor of turbulent mixing in mind, the laboratory apparatus for the explosion experiments was designed to permit very rapid injection of water into smelt. The design also provided several other features: (1) minimum equipment requirements, (2) rapid-heating capability, (3) versatility of water injection, (4) ease of instrumentation, (5) capability for use of high-speed photography, and (6) minimum hazard to personnel and equipment.

Apparatus and Procedure

The first apparatus used for the explosion experiments is shown schematically in Figures A-1 and A-2. The smelt is contained in a graphite crucible 5 inches high and 2 inches in diameter. The conical interior of the crucible provides sufficient surface for access to the small volume of smelt used in an experiment. The 70 grams of smelt normally used in each run provide a melt level about 0.5 inch from the top of the crucible. A 20-kw Lepel high-frequency power supply energizes the induction heating coil; the crucible is adjusted into position in the coil by a motor-driven screw. The smelt temperature is measured with a platinum-platinum 10 percent rhodium thermocouple.

The water is injected into the center of the surface of the smelt by a piston in a 1/8-inch cylinder to which a 1.5-inch length of hypodermic needle (No. 18, 1 mm) is attached. The piston is actuated by air pressure, controlled by a solenoid valve. The distance that the piston can traverse in its cylinder is controlled by a set screw, thus allowing some adjustment in the volume of water which is injected. This arrangement is capable of injecting 25 to 45 mg of water. The device is loaded for injection by reversing the air-inlet flow, thus driving the piston upward and drawing water from the reservoir into the injection cylinder.

During an experiment, the crucible, blanketed with inert gas to prevent oxidation, is heated until the molten smelt is at the desired temperature. The injector then is filled with distilled water, moved into place, and actuated to drive the water into the molten smelt. With nonexplosive smelt compositions a splash of smelt rising above the top of the crucible is observed when the water is injected. If the smelt is explosive, some or all of the smelt is blown out of the crucible, depending on the violence of the explosion. None of the explosions were violent enough to cause any damage to the equipment.

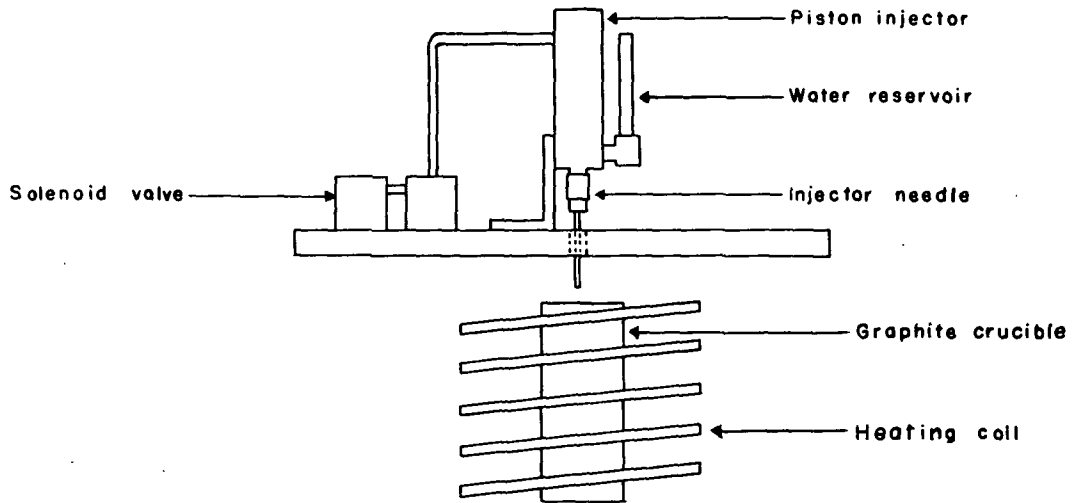


FIGURE A-1. DIAGRAM OF PISTON-TYPE WATER INJECTION APPARATUS

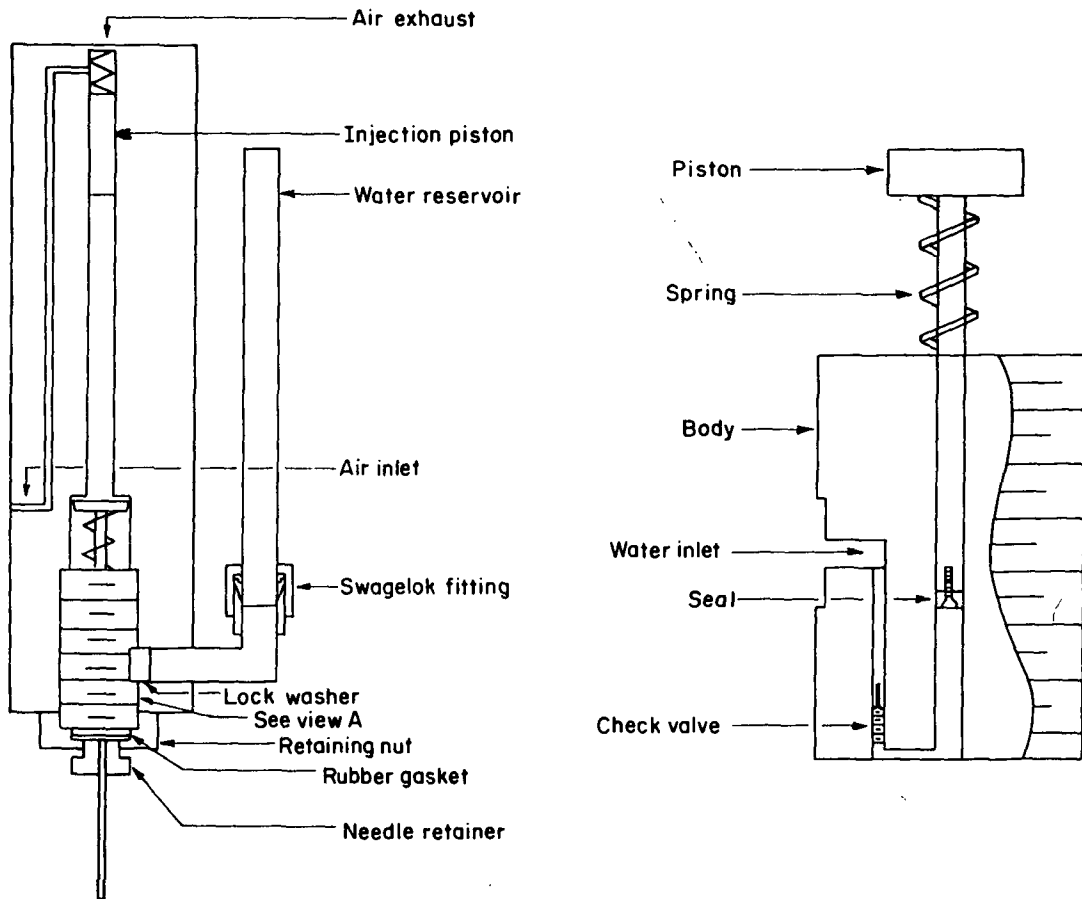


FIGURE A-2. DETAIL OF THE PISTON-TYPE WATER INJECTION APPARATUS

Experiments in which kraft-mill smelts were used demonstrated that a 35-mg portion of water was not sufficient to explode all of the smelts. Consequently, a larger diameter hypodermic needle was installed on the injector. This needle made possible injections of about 75 mg of water. However, the nature of the water stream emitted was changed substantially with this new arrangement. A spray rather than a relatively coherent stream of water resulted. As a result, a decrease rather than an increase in explosive incidence was observed, both with synthetic smelts and mill smelts.

In view of the importance of establishing conditions for exploding less-sensitive smelts, both synthetic and mill types, a new water injector was designed and built. Figure A-3 is a schematic of the injection system. This injector utilizes gas pressure directly on the water reservoir rather than on a piston. The amount of water injected can be controlled either by an electronic timer or a pulse generator, which opens a solenoid valve on the water supply line for a set time interval. This arrangement eliminates the spray effect that resulted with the original injector when the amount of water to be injected was increased.

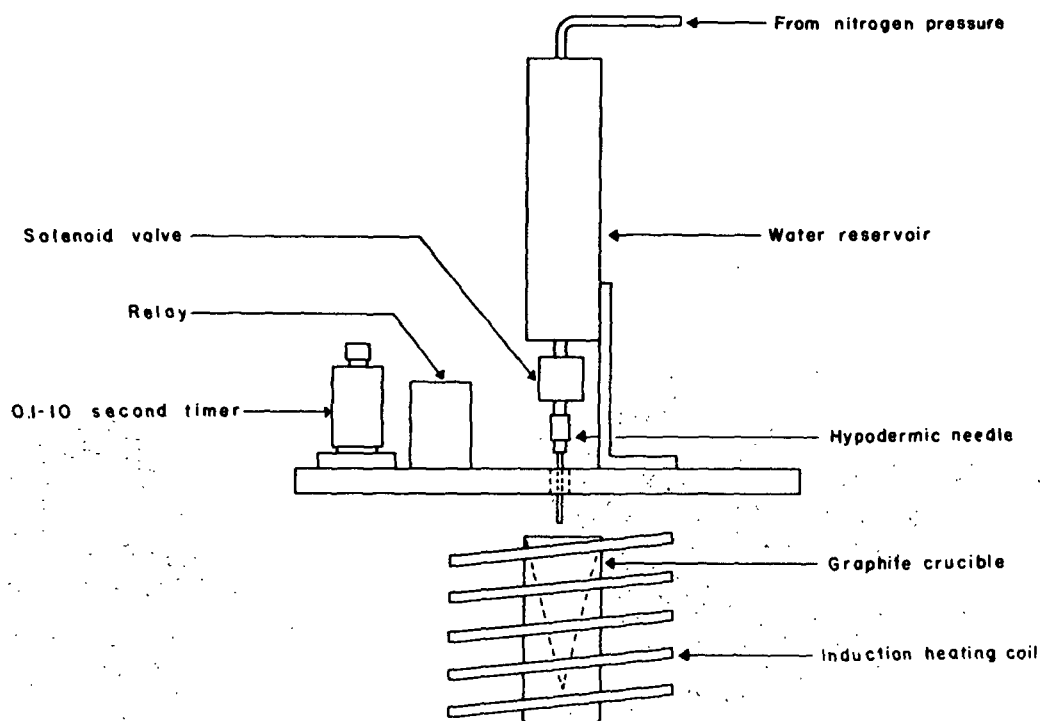


FIGURE A-3. SCHEMATIC OF DIRECT GAS-PRESSURE INJECTION APPARATUS

For relatively large amounts of water (250 mg to 2 g), the electronic timer proved to be adequate. However, for smaller amounts of water, requiring shorter injection periods, it was necessary to employ a variable-length pulse-generating system as shown in Figure A-4. A Wavetek square-wave generator capable of providing a 30 to 32-volt square-wave single pulse was used to drive a reed relay (400 ohm, 12 volt). A diode was included in the circuit to prevent multiple triggering of the square-wave generator. The response of the system dictated an upper limit of 180 cycles/sec, resulting in a minimum pulse of 5.6 milliseconds duration. With this arrangement water injections from 50 mg to 270 mg was possible.

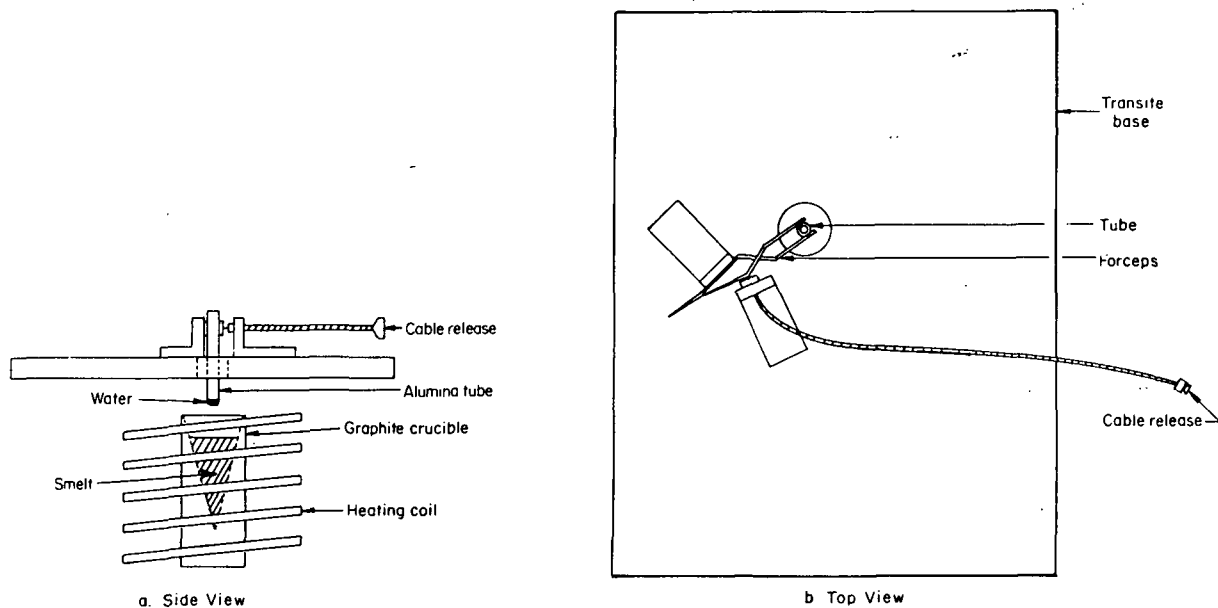


FIGURE A-5. APPARATUS USED FOR DROPPED-TUBE EXPLOSION EXPERIMENTS

- Hydrated sodium sulfide ($\text{Na}_2\text{S}\cdot 9\text{H}_2\text{O}$), reagent grade, from J. T. Baker Chemical Company – partially dehydrated in a vacuum oven, and then fused at 1750 F in an inert atmosphere to complete the removal of water and stored in a desiccator until used.
- Sodium chloride (NaCl), reagent grade, from the General Chemical Division, Allied Chemical Corporation, used as received.
- Sodium sulfate (Na_2SO_4), anhydrous, reagent grade, from Merck and Company, Inc., used as received.
- Sodium hydroxide (NaOH) reagent grade, from J. T. Baker Chemical Company, used as received.
- Sodium aluminate (NaAlO_2), purified, from Research Organic/Inorganic Chemical Company, used as received.
- Aluminum oxide (Al_2O_3), reagent grade, from J. T. Baker Chemical Company, used as received.
- Carbonates: K_2CO_3 , CaCO_3 , BaCO_3 , Li_2CO_3 – all reagent grade, J. T. Baker Chemical Co., used as received.

Effects of Tube Dimensions. The initial experiments with the dropped-tube method for introducing water into molten smelts were done with tubes having an OD of 0.312 in. (5/16) and an ID of 0.188 in. (3/16), which hold 300 mg of water as a large drop on the end of the tube. A series of experiments was performed with tubes of smaller diameter, which carry less water into the molten smelt. The smelt mixture consisted of 70 Na_2CO_3 -25 Na_2S -5 NaCl (weight percent),

and the temperature was 1400 F. The tube drops were made with the bottom of the tube 3 in. above the molten salt. As the amount of water introduced decreased with tube diameter, the explosion incidence also decreased, as shown below. Shortening the tube to 1 in. had no effect on explosion incidence, as the amount of water introduced remained the same.

Tube Dimensions, in.			Wt. of H ₂ O, mg	Explosion Incidence, percent (20 Experiments)
OD	ID	Length		
0.312	0.188	2	300	100
0.312	0.188	1	300	100
0.188	0.094	2	110	85
0.125	0.063	2	80	40

These results show that the explosion incidence in the dropped-tube method decreases with the amount of water introduced, just as it does with the rapid-injection techniques.

In another series of experiments, a 1/4-in. solid alumina rod was used to introduce the water into the molten-salt mixture. The amount of water introduced with this size rod was about 100 mg. The explosion incidence was 100 percent in 10 experiments, as compared to 85 percent with about the same amount of water on the alumina tube. The explosion incidence with the tube probably is lower because the water may occasionally be forced up the tube instead of being trapped in the smelt. Observations of the explosions showed that the rod was ejected in a random fashion and it would be very difficult to deduce any energy effects from its motion.

Explosion Intensities. A sound-level indicator was used in an effort to obtain a semiquantitative measure of the explosion intensities. The microphone for the instrument was placed 4 ft from the crucible containing the smelt. Explosions were produced under what are considered the temperature and injection pressure imparting the highest explosion probability for the compositions used. The loudest explosions obtained with the 70 Na₂CO₃-30 Na₂S composition reached 92 decibels. All of the explosions obtained with the 50 Na₂CO₃-25 Na₂S-25 NaCl composition were of greater intensity, the maximum being 109 decibels. The results are summarized in Table A-1.

TABLE A-1. EXPLOSION INTENSITIES

Composition	Injector Pressure, psi	Temperature, F	Maximum Sound Level, decibels
70 Na ₂ CO ₃ -30 Na ₂ S	125	1565	82
	125	1590	85
	150	1540	92
50 Na ₂ CO ₃ -25 Na ₂ S-25 NaCl	50	1225	109
	60	1225	104
	80	1245	108
	100	1400	96
	125	1210	98

These data are not directly relatable to explosive energy without additional information, but they do provide some feel for the relative violence of the explosions.

Experiments With Hot Water. Previous laboratory investigations of smelt-water explosions have noted a diminished explosiveness when hot water was introduced into molten smelt. This effect was investigated in our work both with the dropped-tube method and the piston-type injector. The composition $70\text{Na}_2\text{CO}_3\text{-}30\text{Na}_2\text{S}$ was used with the dropped-tube techniques for introducing water. In 10 experiments at each of 5 degree intervals, explosiveness was 100 percent from 50 C to 65 C. However, from 65 C to 92 C, which was the highest temperature used, no explosions were obtained with the dropped-tube technique.

In another set of experiments, the piston-type injector was used at 150 psi to inject 30-mg portions of water. The composition $65\text{Na}_2\text{CO}_3\text{-}25\text{Na}_2\text{S}\text{-}10\text{NaCl}$ was used to study the effect of hot water because this composition has moderate explosiveness with water at room temperature. The explosion incidence in 50 injections at each of three temperatures was as follows:

<u>Temperature, C</u>	<u>Explosion Incidence, percent</u>
25	55
55	26
70	0

The two methods of introducing water gave similar results in that the explosion incidence became zero in the range 65 to 70 C.

The relation of this hot-water effect to the proposed explosion mechanism is difficult to ascertain. The hot water may quickly generate an insulating layer of steam or it may affect the triggering mechanism. The hot water has greater vapor pressure than does the cold water, and the presence of this gaseous phase may reduce the implosion that is a key step in the mechanism. In recovery furnace leaks, the water introduced into the smelt is invariably hot. In spite of this, some of the smelt-water exposures result in explosions. If the water were cold, probably a greater percentage of the exposures would result in explosions.

Synthetic Green-Liquor Experiments. Previous investigators of smelt-water exposures have noted that green liquor is more explosive than water when introduced into molten smelts. To investigate this effect under our conditions, experiments were performed with the piston-type injector (35 mg H_2O) operating at 150 psi. The molten-salt composition used in these experiments was $65\text{Na}_2\text{CO}_3\text{-}25\text{Na}_2\text{S}\text{-}10\text{NaCl}$, which has a normal explosion incidence of 50 percent with this injector. Synthetic green-liquor solutions containing from 4 to 16 weight percent Na_2CO_3 and from 1 to 4 weight percent Na_2S were injected into the molten salt. The explosion incidence was 100 percent in 50 injections with each composition. These results confirm the previous data and show that dissolved solids in the injected liquid increase the incidence of explosion, possibly because they enhance the heat transfer into the water.

ULTRASONIC MEASUREMENT OF VISCOSITY AND BULK MODULUS

The viscosity of a polyatomic liquid can be considered to consist of two components, a bulk viscosity and a shear viscosity. The ratio of the bulk viscosity to the shear viscosity is obtained from ultrasonic absorption measurements:

$$\eta_B/\eta_s = 4/3 (\alpha_{ex}/\alpha_{calc}-1) ,$$

where η_B is the bulk viscosity, η_s is the shear viscosity, α_{ex} is the experimentally measured attenuation of ultrasonic energy, and α_{calc} is the attenuation calculated from the density, shear viscosity, and sound velocity according to the classical work of Stokes⁽¹⁾. The bulk viscosity for some molten salts has been found to be five times as great as the ordinary shear viscosity. Measurement of the velocity of sound in the molten salts also permits calculation of the bulk modulus, K_b since

$$K_b = \rho c^2 / g,$$

where ρ is the density, c is the sound-propagation velocity, and g is the acceleration of gravity.

Apparatus and Procedure. An ultrasonic technique similar to one developed by Litovitz,⁽²⁾ in which comparator methods are used for measuring the velocity and attenuation of ultrasound in the medium under study was adapted for measurements on molten salts. A significant improvement over Litovitz's method was accomplished by using an electronic delay instead of the acoustical delay line (water) for the comparator. A block diagram of the apparatus is shown in Figure A-6. In the initial run, using 70 Na₂CO₃-30 Na₂S at 1500 F, the molten smelt etched

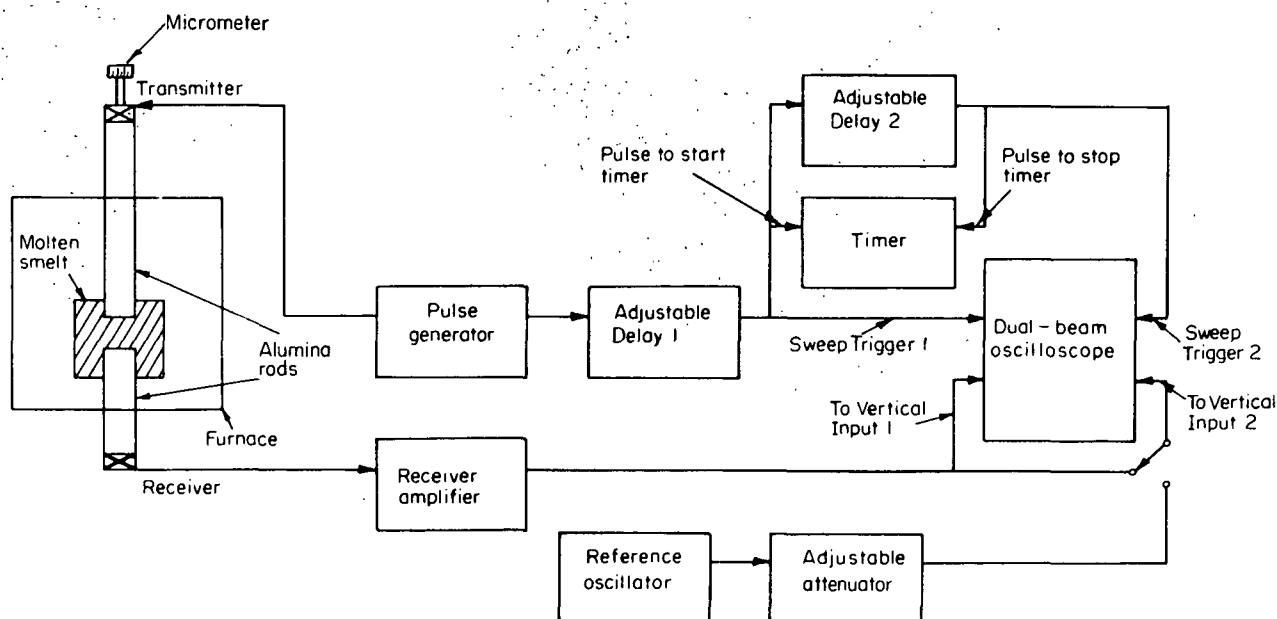


FIGURE A-6. SCHEMATIC OF APPARATUS FOR ULTRASONIC MEASUREMENTS

(1) Stokes, G. G., Trans. Cambridge Phil. Soc., 8, 287 (1845).

(2) Higgs, R. W., and Litovitz, T. A., J. Acoustical Soc. America, 32, 1108 (1960).

the fused-silica rods of the apparatus so rapidly that much of the ultrasonic energy was scattered by the roughened surfaces. As a result, no valid measurements could be made. The fused-silica rods were replaced by high-density alumina rods, and this problem was eliminated. A pulse generator supplies a 5-megahertz signal to the transmitter, a piezoelectric element bonded to the end of an alumina rod 20 mm in diameter and 24 in. long. The vertical position of this alumina rod is adjusted by a micrometer screw which is accurate to 25 μ in. The transmitted signal travels through the rod into the molten salt and from the salt through a second alumina rod (20 mm in diameter and 18 in. long) to the piezoelectric receiver. Simultaneously, a signal from the pulse generator is transmitted through Adjustable Delay 1, which is used to provide a convenient point in time for triggering the reference beam on the dual-beam oscilloscope (Sweep Trigger 1). This delay remains fixed throughout any series of measurements. The output from Adjustable Delay 1 also passes through Adjustable Delay 2 and triggers Sweep Trigger 2. The timer connected in parallel with Adjustable Delay 2 is started by the input signal to the delay and is stopped by the output signal from the delay, thus giving a direct reading of the delay time.

The receiver signal, corresponding to the ultrasonic pulse that has passed through the alumina rods and the molten salt, passes through the receiver amplifier directly to Vertical Inputs 1 and 2 of the oscilloscope. The signal corresponding to the receiver signal appears on Oscilloscope Trace 1 at a point corresponding to time t . In measuring velocity, Adjustable Delay 2 is varied to cause a second signal to appear on Trace 2 at the same time t . The amplitudes of the pulses displayed on the oscilloscope are measured by comparison with signals supplied by the reference oscillator through the adjustable attenuator. The procedure for measuring velocity and attenuation is as follows:

- (1) The distance between the ends of the alumina rods is set to a maximum and the micrometer reading x_1 is recorded.
- (2) Delay 2 is adjusted so that the position of the delayed signal coincides with that of the received signal on the oscilloscope. The time t_1 is read from the timer.
- (3) Vertical Input 2 is switched to receive a signal from the reference oscillator and attenuator. The attenuator setting is adjusted so that the amplitude of the oscillator signal appearing on the oscilloscope equals that of the received signal. The attenuator reading α_1 is recorded.
- (4) The upper quartz rod is moved vertically to a new position and the process is repeated, giving x_2 , t_2 , and α_2 .

Then, neglecting diffraction effects and assuming no interference between reverberations, the velocity of sound, c , and the attenuation, α , are given by:

$$c = \frac{x_1 - x_2}{t_1 - t_2} \quad \text{and} \quad \alpha = \frac{\alpha_2 - \alpha_1}{x_1 - x_2}$$

The measurements of the attenuation of the 5-megahertz ultrasonic waves in the molten-salt compositions showed that only a small fraction of a decibel was absorbed over the 1-in. pathlength employed. The results are presented in Table A-2. This change in attenuation is too small for accurate measurement. The viscosity of the smelt is too low to be an important factor in determining the manner in which acoustic waves are propagated in the smelt. However, the

viscosity could have an important influence on other factors that determine explosive tendency. For example, small differences in shear viscosity may, under certain circumstances, have a large effect on the rate of turbulent mixing of smelt and water, and, hence, on the rate of heat transfer into the water.

TABLE A-2. ATTENUATION OF ULTRASONIC ENERGY IN MOLTEN SALT COMPOSITIONS OVER A PATH LENGTH OF 1 INCH

	<u>Na₂CO₃</u>				
Temperature, F	1584	1657	1728	1778	1834
Attenuation, decibels	0.0	0.0	0.0	0.1	0.2
	<u>85Na₂CO₃-15Na₂S</u>				
Temperature, F	1570	1645	1717	1785	1860
Attenuation, decibels	0.2	0.6	0.4	0.4	0.5
	<u>70Na₂CO₃-30Na₂S</u>				
Temperature, F	1503	1580	1675	1740	1832
Attenuation, decibels	0.3	0.2	0.6	0.5	0.6
	<u>Na₂S</u>				
Temperature, F	1738	1795	1832	1905	1940
Attenuation, decibels	0.2	0.2	0.3	0.3	0.3
	<u>50Na₂CO₃-25Na₂S-25NaCl</u>				
Temperature, F	1580	1665	1737	1785	1835
Attenuation, decibels	0.3	0.5	0.2	0.2	0.5
	<u>NaCl</u>				
Temperature, F	1508	1645	1717	1775	1828
Attenuation, decibels	0.2	0.3	0.1	0.1	0.3
	<u>75Na₂CO₃-20Na₂S-5NaAlO₂</u>				
Temperature, F	1545	1615	1688	1760	1832
Attenuation, decibels	0.2	0.0	0.2	0.2	0.8
	<u>75Na₂CO₃-20Na₂S-5NaOH</u>				
Temperature, F	1545	1615	1688	1750	1828
Attenuation, decibels	0.2	0.0	0.2	0.2	0.8

CAVITATION EXPERIMENTS

The steam-cavitation model for initiation of smelt-water explosions, requires that very low pressure exist in the cavitation bubble at maximum expansion. The CO_2 formed by cavitation-induced decomposition of the Na_2CO_3 in molten smelt could provide gas pressure in the bubbles and thus inhibit the subsequent implosion of the bubbles. Consequently, smelt components that suppress the decomposition of Na_2CO_3 would act as explosion sensitizers, and those that enhance decomposition would be desensitizers.

Experiments to test this hypothesis were conducted by rapid stirring of smelt mixtures. A motor-driven stirrer capable of operating at speeds up to 10,000 rpm was used for these experiments. The high velocity at the stirrer tip which is required to obtain cavitation in a liquid was achieved by using as the stirrer a disk with four pins spaced 90 degrees apart around the circumference. Both stainless steel and graphite disks were used; the stainless steel was suitable for molten Na_2CO_3 , but when Na_2S was introduced into the mixture, the rapid corrosion of the metal required the use of graphite. The stainless steel disk was 1/2-in. diameter and 3/16 in. thick. Cylindrical pins, 1/8-in. diameter, with hemispherical ends, were welded to the edge of the disk, and they projected 1/8 in. from the disk. When graphite was used, the thickness of the disk was increased to 1/4 in. so that the pins could be threaded and screwed into the disk. The equipment assembly used for the cavitation experiments is shown in Figure A-7.

Preliminary to the molten salt experiments, the high-speed stirrer was used to induce cavitation in liquids having densities at room temperature in the range of those of molten smelt components, from 1 to 3 g/cc. Cavitation was detected visually by the formation of vapor bubbles in the liquid in the vicinity of the stirrer. These preliminary experiments were carried out with water, carbon tetrachloride, and bromoform at room temperature in glass containers. Cavitation was readily observed at stirring speeds of about 4000 rpm. The speed was measured with a stroboscopic tachometer.

When similar experiments were performed with the molten salts contained in an alumina crucible in the resistance furnace, observation of the cavitation-bubble phenomenon was uncertain. Consequently, an alternative method was adopted. The change in CO_2 concentration over the melt produced by the cavitation was monitored by a continuous-reading, nondispersive, infrared CO_2 analyzer.

There was a small background of CO_2 above the melt because of the normal atmospheric content and the slight decomposition pressure of Na_2CO_3 in the undisturbed melt. These sources gave rise to a blank reading of 0.1 percent by volume CO_2 on the analyzer. When the Na_2CO_3 melt was maintained at 1600 F and the stirring speed was increased slowly, a sudden change in the CO_2 concentration from 0.1 to 0.2 percent by volume was observed at a stirring speed of 3700 rpm. This observation of increase in CO_2 concentration was replicated in six such experiments. When the temperature of the molten Na_2CO_3 was raised to 1650 F, an identical increase in CO_2 concentration occurred at a stirring speed of 3900 rpm.

Similar experiments with two explosive smelt compositions, $70\text{Na}_2\text{CO}_3\text{-}30\text{Na}_2\text{S}$ and $50\text{Na}_2\text{CO}_3\text{-}25\text{Na}_2\text{S}\text{-}25\text{NaCl}$, under the same conditions as used for the Na_2CO_3 , showed no increase in the CO_2 concentration occurred at any stirring speed up to 10,000 rpm, the limit of the apparatus. This same negative result was obtained several times on different days when the experiments were repeated to verify the reproducibility.

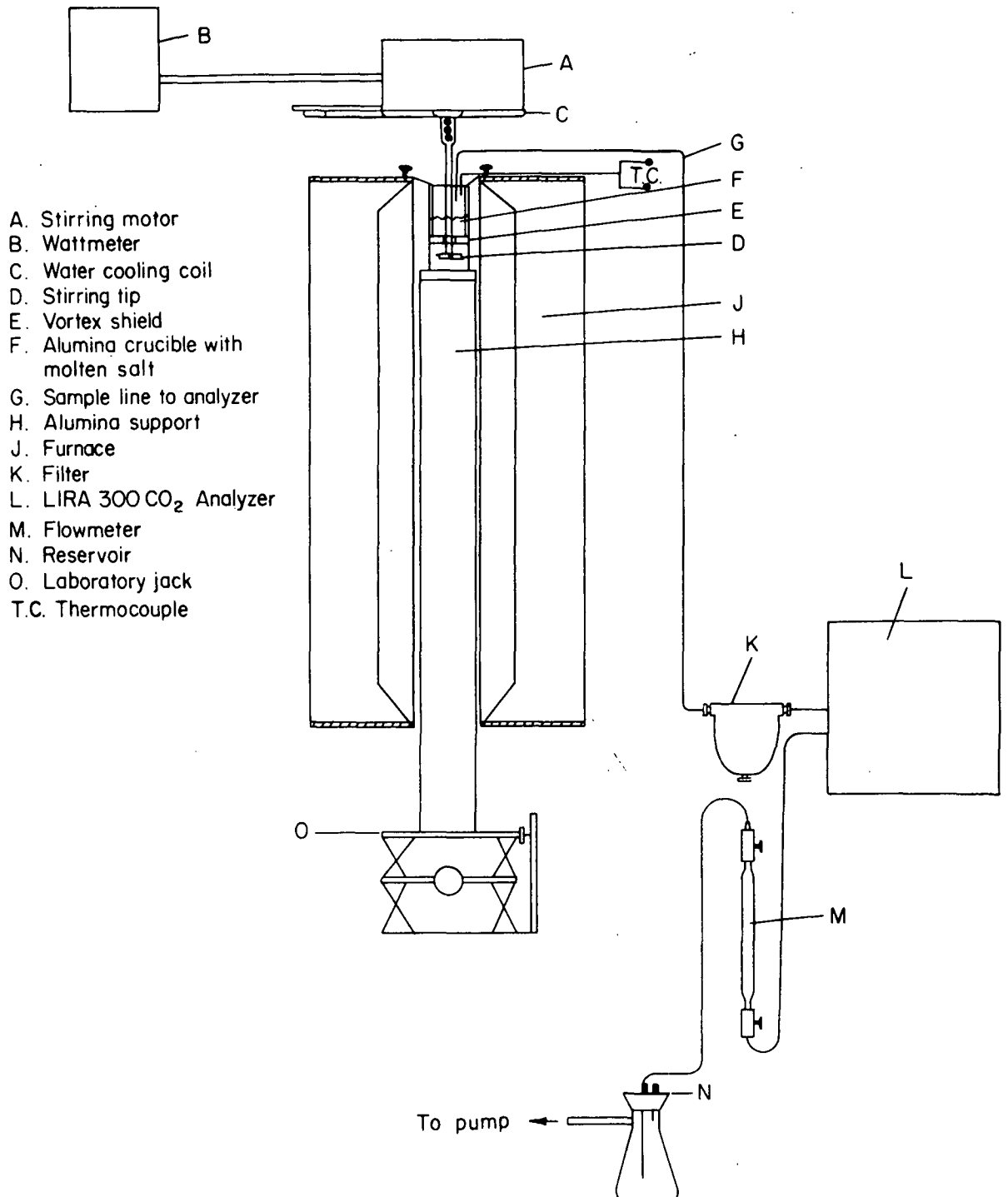


FIGURE A-7. APPARATUS USED FOR CAVITATION EXPERIMENTS

From this series of experiments it is concluded that the Na_2S and the NaCl , which are explosion-sensitizing components in smelt, inhibit the decomposition of Na_2CO_3 under the cavitation conditions.

VACUUM DECOMPOSITION STUDIES

The purpose of these experiments was to obtain quantitative information on the effects of explosion sensitizers on the rate of decomposition of Na_2CO_3 under near-vacuum conditions, such as would exist in a steam bubble at maximum expansion prior to cavitation.

These vacuum decomposition experiments were carried out by heating the molten salt in a closed system under vacuum. When the desired temperature was reached, the CO_2 produced by decomposition of the Na_2CO_3 was collected in a trap cooled to -320 F with liquid nitrogen. A schematic of the apparatus used for these experiments is shown in Figure A-8. The CO_2 collected was then transferred to a vacuum line and the amount obtained was measured.

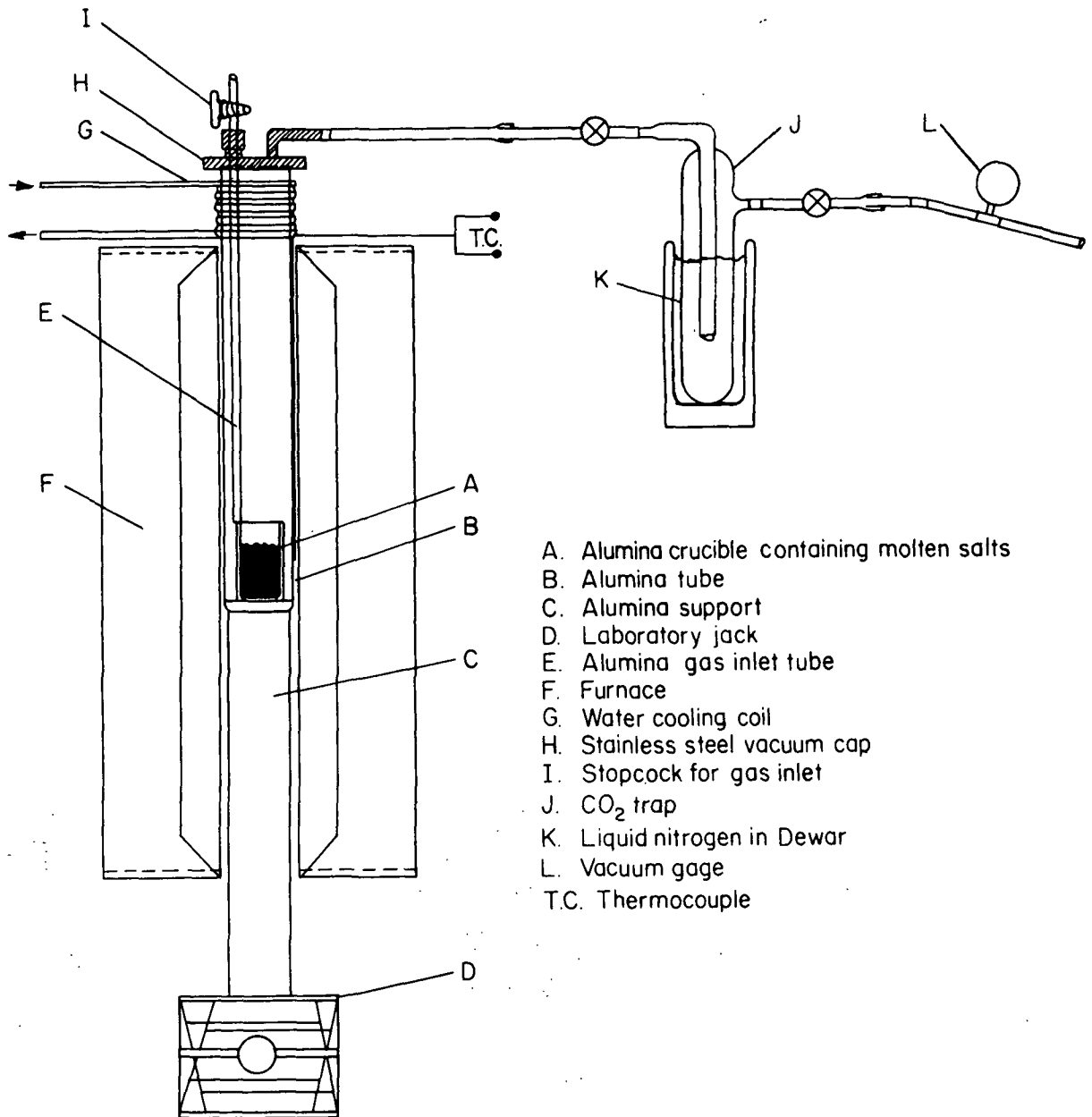
In the initial series of experiments, the alumina crucible which contained the molten salt was enclosed in a quartz tube. Seemingly consistent results were obtained for decomposition of Na_2CO_3 at different temperatures under these conditions. However, when explosion sensitizers such as Na_2S and NaCl were added to the system, relatively large amounts of CO_2 were obtained and the results were not reproducible. The source of the discrepancy was found to be reaction of the Na_2CO_3 vapor with the hot quartz tube to form CO_2 and Na_2SiO_3 . When the quartz outer tube was replaced with a high-density alumina tube, much less CO_2 was released, and reproducible results were obtained.

The data obtained with the alumina tube in use are presented in Table A-3. The CO_2 was collected for 1 hour to provide enough material for accurate measurement on the vacuum line. Some of the samples were recondensed from the vacuum line and analyzed by mass spectrometry to verify that the gas being measured was CO_2 . A typical volume percent analysis is:

CO_2	99.60
N_2	0.21
H_2	0.10
SO_2	0.08
O_2	<u>0.05</u>
	100.04

As shown in Table A-3, for any given composition the amount of CO_2 obtained at 1830 F was approximately 1.6 times that at 1740 F .

As part of the Na_2CO_3 was replaced with Na_2S , the amount of CO_2 formed decreased. When NaCl was substituted for additional Na_2CO_3 still less CO_2 was obtained. This result was to be expected because the mole fraction of Na_2CO_3 in the mixture was reduced by these substitutions. However, the amount by which the CO_2 yield was reduced was greater than would be anticipated, as shown in Table A-4. For the composition $70\text{Na}_2\text{CO}_3\text{-}30\text{Na}_2\text{S}$, the amount of CO_2 obtained experimentally was only 56 to 58 percent of that calculated on the basis of the



- A. Alumina crucible containing molten salts
- B. Alumina tube
- C. Alumina support
- D. Laboratory jack
- E. Alumina gas inlet tube
- F. Furnace
- G. Water cooling coil
- H. Stainless steel vacuum cap
- I. Stopcock for gas inlet
- J. CO₂ trap
- K. Liquid nitrogen in Dewar
- L. Vacuum gage
- T.C. Thermocouple

FIGURE A-8. APPARATUS FOR VACUUM DECOMPOSITION EXPERIMENTS

mole fraction of Na_2CO_3 in the mixture. With the mixture $50\text{Na}_2\text{CO}_3$ - $25\text{Na}_2\text{S}$ - 25NaCl , the CO_2 collected was 70 to 72 percent of the theoretical amount.

TABLE A-3. VACUUM DECOMPOSITION OF Na_2CO_3

Composition of Melt ^(a)	Temperature, F	Yield, cc-atm CO_2 , (STP)/hr	Weight of CO_2 , mg/hr
Na_2CO_3	1740	22.8	44.8
	1830	36.8	72.0
$70\text{Na}_2\text{CO}_3$ - $30\text{Na}_2\text{S}$	1740	8.4	16.4
	1830	13.6	26.8
$50\text{Na}_2\text{CO}_3$ - $25\text{Na}_2\text{S}$ - 25NaCl	1740	6.4	12.4
	1830	10.0	19.6

(a) 50 grams was used in each experiment.

TABLE A-4. REDUCTION OF Na_2CO_3 DECOMPOSITION BY SENSITIZERS

Composition of Melt	Mole Fraction Na_2CO_3	Temperature, F	Yield, mg CO_2 /hr (Experimental)	Yield, mg CO_2 /hr (Based on Mole Fraction)	Percent of Theoretical Decomposition
Na_2CO_3	1.00	1740	44.8	44.8	—
		1830	72.0	72.0	—
$70\text{Na}_2\text{CO}_3$ - $30\text{Na}_2\text{S}$	0.635	1740	16.4	29.1	56.5
		1830	26.8	45.7	58.6
$50\text{Na}_2\text{CO}_3$ - $25\text{Na}_2\text{S}$ - 25NaCl	0.385	1740	12.4	17.2	72.0
		1830	19.6	27.7	70.7

These experiments on the vacuum decomposition of Na_2CO_3 show that explosion sensitizers such as Na_2S and NaCl reduce the amount of CO_2 produced from molten mixtures of these components under vacuum conditions.

INFRARED STUDIES

Infrared absorption spectra were made of both mill smelts and synthetic smelts to determine whether or not there are compositional differences that can be detected in this fashion. Absorption bands were observed for carbonate, sulfate, sulfite, thiosulfate, and dithionate ($\text{S}_2\text{O}_6^{2-}$) in all of the samples run. The sulfide does not absorb in this region of the spectrum.

The same absorption bands occurred in the spectra of both the explosive and nonexplosive mixtures. Consequently, the infrared spectra do not provide any clues as to differences in the nature of the components in the various smelts. The infrared spectrum for Smelt K is shown in Figure A-9. This spectrum is typical of all the smelts examined. Because some chemical structures absorb infrared radiation more strongly than others, the relative intensities of the bands do not represent true quantitative relationships among the various components. The small amount of water observed, also in all of the blanks run, was attributed to moisture absorbed during handling of the sample in the KBr-disk technique.

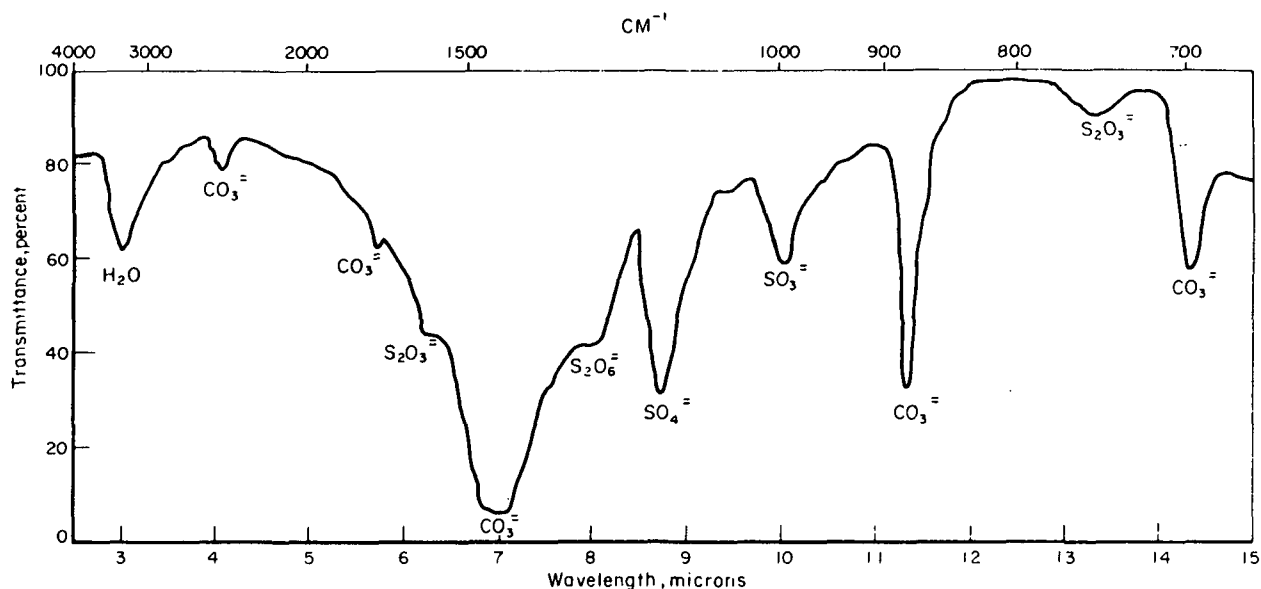


FIGURE A-9. INFRARED SPECTRUM OF TYPICAL KRAFT MILL SMELT
KBr Disk

According to the literature, NaOH has a sharp infrared absorption band at 2.75 microns (3637 cm^{-1}), which should be detectable in the smelt mixture, if sufficient NaOH is present. As there was no evidence for this absorption in the mill smelts examined, the titration results obtained previously, which showed only small amounts (less than 1 percent) of NaOH in two of the smelts, are supported by the infrared data.

PRESSURE-TRANSDUCER EXPERIMENTS

To compare the relative magnitudes of smelt-water explosions obtained under different laboratory conditions, and to obtain data on the explosion characteristics for the explosion model, pressure-transducer experiments were performed. In these experiments a piezoelectric transducer was coupled to the smelt via an alumina rod immersed in the molten salt. The pressure wave from the explosion was picked up by the rod, sensed by the transducer, recorded on an oscilloscope, and photographed. The electrical circuit employed is shown in Figure A-10.

The pulse from the square-wave generator provided a signal for external triggering of the oscilloscope sweep. The output of the transducer was fed to the oscilloscope (Tektronics 585) with a plug-in capable of reading a deflection of 5 mv/cm. In order to record the explosion on the fast sweep of the oscilloscope, a time delay had to be used. With the piston-type injector a 60-millisecond delay was required, and with the direct gas-pressure injector, a 13-millisecond delay was employed. By this means the entire explosion sequence could be recorded on the oscilloscope in a single photograph. A number of pressure pulses constituting the explosion occurred within a 2-millisecond interval. Typically, from 6 to 10 pulses can be detected. The amplitudes of the pressure waves vary. Most of them are of about 20-psi magnitude, but occasionally peaks up to 40 psi have been observed. These pressure-transducer experiments have demonstrated that when there is a high relative velocity of motion between water and smelt, the explosion occurs about 1 millisecond after the water-smelt contact. The duration of the explosion for the small amounts of water involved in our experiments (35 to 75 mg) was approximately 2 milliseconds.

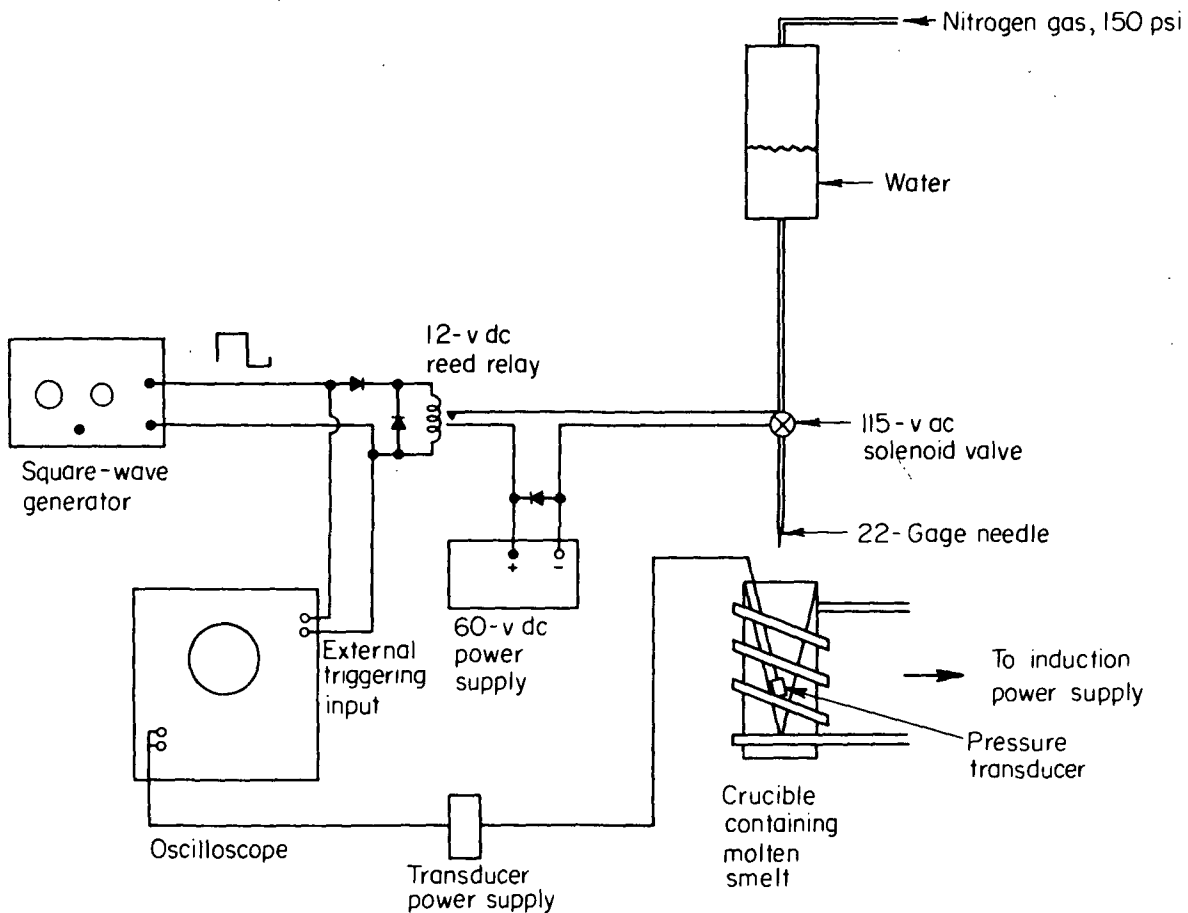


FIGURE A-10. APPARATUS FOR PRESSURE TRANSDUCER EXPERIMENTS

MEASUREMENT OF OTHER PHYSICAL PROPERTIES

The density of molten salts as a function of temperature can be measured by a variety of methods involving displacement, expansion, or liquid-level detection. The displacement method was used in this program because it provides a means of obtaining density and shear viscosity at the same time, and, with minor modification, it could also be used to determine surface tension. A typical arrangement of equipment for this method is shown in Figure A-11. Density is measured by application of Archimedes' principle, based on displacement of the molten salt by a weight suspended from the balance. By putting the bob in motion in the melt, shear viscosity can be determined from the rate of movement of the bob through a fixed distance in the melt. By calibrating the system with a liquid of known viscosity, the apparatus can serve to measure unknown viscosities.

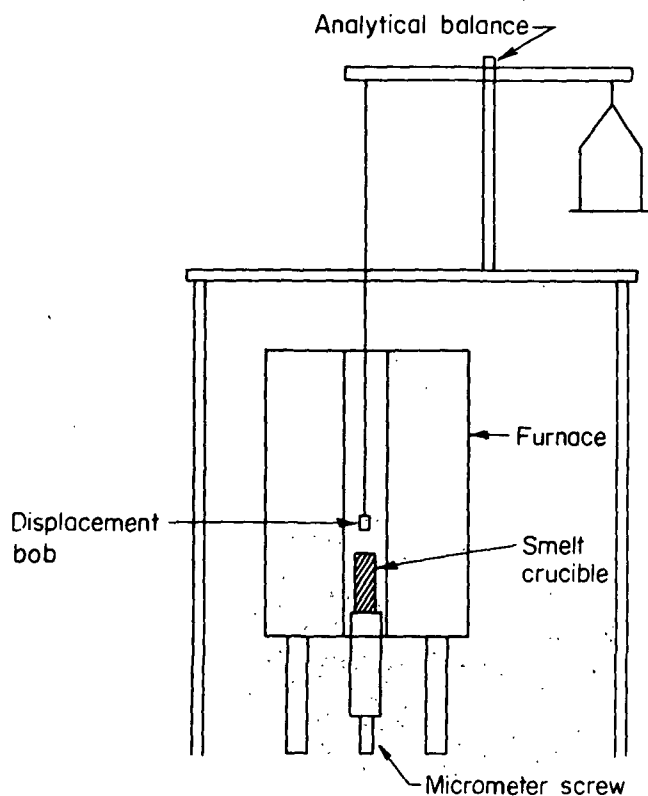


FIGURE A-11. SCHEMATIC OF APPARATUS FOR PHYSICAL-PROPERTY MEASUREMENTS

In addition to density and viscosity, it is also possible to measure surface tension with the same equipment. By modifying the bob so that it has a pin extending from the bottom, a measurement of the force required to pull the pin through the surface of the melt can be obtained. By using calibration liquids of known surface tension, the difference between the rest weight and the break-away weight of the bob can be used to determine the surface tension of the molten salt to be measured.

APPENDIX B

SMELT-WATER EXPLOSION MODEL COMPUTER PROGRAM

APPENDIX B

THE SMELT-WATER EXPLOSION MODEL COMPUTER PROGRAM

Description of Program

The latest version of the smelt-water explosion model computer program (in the FORTRAN Computer language) is listed in Table B-1. It consists of a main program, 7 subroutine-subprograms, and 10 function subprograms.

In the main program are introduced the necessary data regarding the values of the various constants and the initial conditions for each run (lines 180-330), including all necessary conversions to the CGS system of units used in the program. The initial values are then computed of the partial pressure of the gas (340), the steam fraction (350), radius of the globule (360), rate of heat input per unit mass of water (410), rate of gas input per unit mass of water (430), and the rates of rise of temperature (530), steam fraction (560), partial pressure of gas (570), partial pressure of steam (580), total globule pressure (590), and globule outer surface velocity (600).

After determining the initial value of the time-interval step used for the integration process (610), the time is increased by this step (640), and the solution begins. The actual integrations and computations of the new values of the rates of change are performed by calling upon subroutine SOLV (650), which is described later. After each such call, the main program checks to see if the computed steam fraction has exceeded unity (670). If it has not, the final values of the various dependent variables (indicated by a final B in the variable name) and of their rates of change (indicated by a final 2) are converted to the initial values (A and 1, respectively) for the following integration interval by subroutine ADV (700) and the integration process is repeated (710). Subroutine ADV also readjusts the value of the integration time interval in accordance with the previously computed rate of change of globule pressure and other considerations. If the computed steam fraction exceeds unity, subroutine SET (called at line 730) performs a linear interpolation to reset the values of the dependent variables and the time to the instant when 100 percent steam was reached. The main program then recomputes new initial values for the rates of change of the various dependent variables corresponding to the condition of 100 percent steam (lines 740-940). Integration subroutine SOLV now calls upon subroutine STEAM instead of subroutine BOIL.

Since recondensation of some of the steam may occur after the 100 percent steam condition is reached, line 980 of the main program checks if the computed steam partial pressure exceeds the equilibrium value corresponding to the steam vapor pressure at the temperature in question. If it has, all dependent variables and the time are reset to the instant when this occurs by linear interpolation (1050) and the new rates of change of all dependent variables computed (1060-1260). The problem reverts to the previous condition of part steam and part liquid water in the globule (1300) and then again to the 100 percent steam case if later warranted (670). The problem ends and input of new initial conditions for the next problem are requested when the globule pressure has gone through the ambient pressure value a specified number of times (see lines 250, 690, 1000, 2620-2630).

Ambient Pressure Variation Effects

The computer model was modified to include the possibility of superimposing a periodically varying pressure component on the ambient pressure. This would simulate the effects of the expansions and contractions of other globules in the smelt bed, located far enough away from the globule in question and oscillating at a low enough frequency so that gradients in the ambient pressure field of the latter would not be significant. It was conjectured that the main smelt-water explosion may be a cooperative phenomenon involving a fortuitous combination of amplitudes and phases of expansions and contractions of two or more oscillating globules. No single cavitation-collapse event could constitute the main explosion because of the excessively large maximum diameter of cavity expansion required for any but very small amounts of water before cavitation collapse commences.

The values of the following parameters of the variable component of the ambient sound field are adjustable:

- Pressure amplitude
- Frequency
- Initial phase
- Degree of distortion from sine wave.

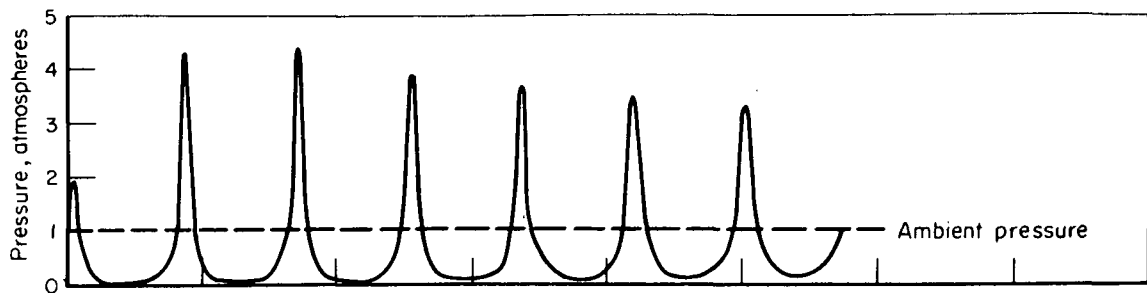
Computations were performed for many combinations of values of these parameters, with pressure amplitudes ranging from a fraction up to 1 atmosphere, frequencies from a fraction up to several times the frequency of globule pulsation (thus representing neighboring globules of different sizes), initial phases from -180 to +180 degrees, and for sinusoidal up to highly distorted waveforms of the "spiked" positive pulse variety.

Figure B-1b shows a typical result of these computations, for the case of a superimposed sinusoidal variation of 0.5 atmosphere amplitude, zero initial phase, and with a period four times as long as that of the pulsations for the steady ambient pressure case (Figure B-1a). It is seen that the initial expansion time for the globule is considerably longer, because of the lower resultant value of the ambient pressure which furnishes the restoring force that stops the expansion of the globule and initiates its collapse. The first collapse pressure pulse, when it does occur, is about 4.2 atmospheres, but the next two pulses are bunched closer together in time and are appreciably greater, both exceeding 5 atmospheres. The fourth is considerably reduced and then the fifth, following the long period of expansion, is again enhanced. The average pulse period is increased by the variable ambient pressure superposition in this case. It is to be noted that there are only five pulses in Figure B-1b in about the same time period as for the six pulses in Figure B-1a.

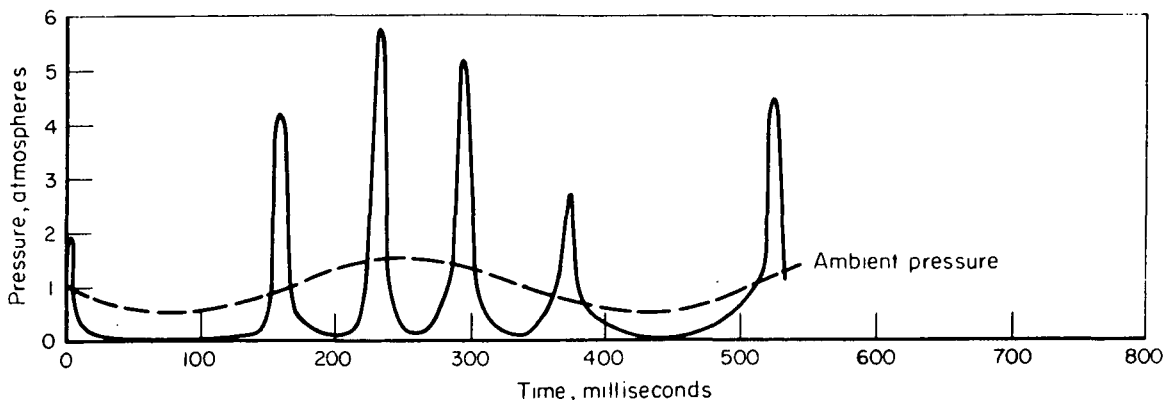
The above is typical of the results of practically all cases computed. Some pressure pulses are enhanced somewhat in magnitude and others diminished, as compared with the corresponding steady pressure amplitude case. The amount of the change in each pulse depends not only on the phase relationship between the ambient pressure variation and the particular pulse, but also on the amount and direction of the modification in the previous pulse produced by the ambient pressure variation. A higher pressure pulse would tend to produce a greater subsequent expansion of the globule, followed by a higher pressure pulse upon recollapsing, except as modified by heat-input changes, energy-damping sources, and the phase of the ambient pressure variation.

The searched-for fortuitous resonance-type of pulse amplitude buildup to account for the main explosion was never encountered for any combination of values of variable ambient pressure parameters. It does little good, for example, to introduce an ambient pressure variation of the same frequency as that of the steady ambient pressure pulse and of the proper phase to enhance the first peak. The greater the resultant amplitude of the first peak, the longer the time interval becomes until the second peak occurs (since the globule expands further before recollapse commences) and the sooner is this optimum phase relationship between the ambient variations and pulses destroyed. The best case of resonance buildup discovered in the course of the computations involved an ambient pressure variation frequency of three times the nominal pulse frequency. The first pulse peak registered properly with the third cycle of the ambient variation to receive a boost; the second pulse peak also registered in proper phase after four additional cycles to receive a further boost, and the third peak likewise registered after five additional cycles. Unfortunately, the fourth pulse peak occurred after 6-1/2 additional cycles, just at the wrong phase, and was diminished in amplitude.

Clearly, the action of the cavitation collapse pressure pulse as a trigger for the main explosion becomes more effective because of the ambient pressure fluctuation due to the expansion and collapse of neighboring globules. Although some pulses are enhanced and others diminished, perhaps leaving the average pulse amplitude about the same, it is reasonable to suppose that the highest amplitude pulse of a series would be the most effective trigger.



a. Constant Ambient Pressure of One Atmosphere



b. Superimposed Sinusoidal Variation of 0.5-Atmosphere Amplitude, Zero Initial Phase, and 340-Millisecond Period

FIGURE B-1. DIRECT AND CAVITATION-COLLAPSE PRESSURE PULSES FOR AMBIENT PRESSURE AND FOR A SUPERIMPOSED VARIABLE PRESSURE

TABLE B-1. (Continued)

```

00580 PSD1=C4*TD0T1
00590 PD0T1=PGD1+PSD1
00600 VD0T1=PD0T1/RH0C-1.5*VA**2/RA+(PA-PAM)/DSM/RA
00610 32 DELT=AMINI(PA/ABS(PD0T1),RA*SQRT(DSM/PA),GHZ)/MULT
00620 P1=PA
00630 S1=SIGN(1.,PD0T1)
00640 40 TIME=TIME+DELT
00650 CALL SOLV(B0IL,JSTOP)
00660 IF (JSTOP-3) 42,42,5
00670 42 IF (STFB-1.) 44,44,60
00680 44 CALL PRNT(1,PA,ACB,TIME,CLB,EMB,EMB/CLB,ACB,WGR,STFB,RB,FB,PB)
00690 IF (NSTOP-IND) 49,5,5
00700 49 CALL ADV
00710 60 T0 40
00720 60 FRAC=(1.-STFA)/(STFB-STFA)
00730 CALL SET(1,FRAC,C1,C2,C3,C4,C5,C6,C7,C8,C9,TABS)
00740 BETA=SQRT((BTS+WGA*BTG)/(1/BTS+WGA/BTG))/(1+WGA)
00750 Q1=Q0*(TSM-TA)/(TSM-T0)*BETA
00760 IF (VA) Q1=Q1*(1+Q0*DW0*(1+WGA)*R0**3/RA*AMAXI(VD0T1,0.)/Q0)
00770 DRD=3*Q1/R0/DW0/(1+WGA)*(RA/R0)**N0
00780 WGD1=ALPHA*(1-PGA/PA)/RA*SQRT(GSC/GMW*(TSM+TA+546.32)/2)
00790 TD0T1=(DRD+GSC/GMW/C6*WGD1*TABS+3*VA/RA*(RA/R0)**3/DW0/C6
00800 *(C3/C5*PSA-PGA))/CPST(PSA,TA)+C3**2/C5/C6*PSA/TABS
00810 +WGA*(CPG-GSC/GMW/C6))
00820 PSD1=PSA/C5*(3*VA/RA*(RA/R0)**3/DW0-C3/TABS*TD0T1)
00830 PGD1=PGA/TABS*(TD0T1-PGA/GSC/GMW/WGA*3*VA/RA*(RA/R0)**3/DW0
00840 +WGD1*TABS/WGA)
00850 PD0T1=PSD1+PGD1
00860 VD0T1=(PD0T1/RH0C*(1-VA/CSM)-1.5*VA**2/RA*(1-4/3.*VA/CSM)
00870 +(PA-PAM)/DSM/RA)/(1-2*VA/CSM)
00880 STFD0T1=0.
00890 IF (TIME-TIMEX) 110,110,69
00900 69 CALL PRNT(2,PA,ACB,TIME,CLA,EMA,EMA/CLA,ACA,WGA,STFA,RA,TA,PA)
00910 TIMEX=TIME
00920 DELT=AMINI(PA/ABS(PD0T1),RA*SQRT(DSM/PA),GHZ)/MULT
00930 P1=PA
00940 S1=SIGN(1.,PD0T1)
00950 80 TIME=TIME+DELT
00960 CALL SOLV(STEAM,JSTOP)
00970 IF (JSTOP-3) 82,82,5
00980 82 IF (PSB-PRW(TB)) 84,84,100
00990 84 CALL PRNT(1,PA,ACB,TIME,CLB,EMB,EMB/CLB,ACB,WGR,STFB,RB,FB,PB)
01000 IF (NSTOP-IND) 93,5,5
01010 93 CALL ADV
01020 60 T0 80
01030 97 STOP
01040 100 FRAC=(PSA-PRW(TA))/(PSA-PRW(TA)-PSB+PRW(TB))
01050 CALL SET(1,FRAC,C1,C2,C3,C4,C5,C6,C7,C8,C9,TABS)

```

TABLE B-1. LISTING OF MOLTEN SALTS - WATER EXPLOSION MODEL COMPUTER PROGRAM

```

00100 EXTERNAL B0IL,STEAM,PRW
00110 COMMON/A/PA,PSA,PGA,VA,RA,TA,STFA,WGA,CLA,EMA,ACA,
00120 PD0T1,PSD1,PGD1,VD0T1,T00T1,STFD0T1,WGD1,Q1
00130 COMMON/B/PSB,PRB,VR,RB,FB,STFB,WGR,CLB,EMB,ACB,
00140 PD0T2,PSD2,PGD2,VD0T2,T00T2,STFD0T2,WGD2,Q2
00150 COMMON/C/DELT,TIME,MULT,DSM,IN,N0,GHZ,BTS,BTG,ERR,J0
00160 COMMON/D/PHI,NPHI,AMP,PAM,P0,PAM0,RH0C,CSM,TSM,ALPHA,
00170 R0,T0,DW0,DRD,P1,S1,PSTP,PLIM,NSTOP,VADD,CPG,SHW,GSC,GMW
00180 DATA R0,TSM,GMW,CPG,SHW,VADD/1.,950.,44.,.2031,1.,1.01325E06/
00190 DATA ERR,PLIM,MULT,PSTP,GSC/.0005,.1,30,1.,8.3144E07/
00200 DATA PAM0,AMP,PHI0,GHZ/0.,0.,0.,1.E03/
00210 DATA P0,V0,DSM,CSM,BTS,BTG/1.,0.,1.86,1.985E05,.036,.036/
00220 CALL EQUATE(THZ,THZ/6283.1853,PAM0,VADD*PAM0,P0,VADD*P0,
00230 PHI,6.2831853/360*PHI0,RH0C,DSM*CSM,0,0,0,0,0,0,0)
00240 5 PRINT, ' J0,T0,WGA,ALPHA,Q0,N0,IND'
00250 ACCEPT, Q0,T0,WGA,ALPHA,Q0,N0,IND
00260 PRINT, ' TIME CAL MECH EFF ACOUS GASF STF RAD'
00270 * TEMP PRESS
00280 CALL EQUATE(Q0,.27123*Q0,PAM,P0-PAM0*SIN(PHI),CLA,0.,ACA,0.,
00290 EMA,0.,TIME,0.,TIMEX,0.,VA,V0,TA,T0,PSA,PRW(T0))
00300 NPHI=1+PHI0/90.
00310 DW0=DW(PAM,T0)
00320 NSTOP=0
00330 PA=PAM
00340 PGA=PA-PSA
00350 STFA=WGA/PGA/VST(PSA,TA)*GSC/GMW*(TA+273.16)
00360 RA=R0*(STFA*VST(PSA,TA)*DW0+1-STFA)**(1./3.)
00370 CALL PRNT(2,PA,ACB,TIME,CLA,EMA,0.,ACA,WGA,STFA,RA,TA,PA)
00380 VOL=1/(1+(1-STFA)/STFA/VST(PSA,TA)/DW(PA,TA))
00390 BETA=SQRT((STFA*BTS+WGA*BTG)/(STFA/BTS+WGA/BTG))/(STFA+WGA)
00400 Q1=Q0*SQRT((1-VOL*(1-BETA))/(1-VOL*(1-1/BETA)))
00410 DRD=3*Q1/R0/DW0/(1+WGA)*(RA/R0)**N0
00420 CALL SET(2,0.,C1,C2,C3,C4,C5,C6,C7,C8,C9,TABS)
00430 WGD1=ALPHA*(1-PGA/PA)/RA*SQRT(GSC/GMW*(TSM+TA+546.32)/2)
00440 A1=STFA+C7
00450 A2=PGA+C7
00460 A3=GSC/GMW*WGA-PGA*STFA*(C4*C5/PSA+C3/TABS)
00470 A4=GSC/GMW*WGD1*TABS
00480 R1=-(1-STFA)/C2/C8
00490 R2=1.
00500 R3=-STFA/C2*C1*(C5/PSA*C4+C3/TABS)+(1-STFA)/C2*(C4/C8-3*C9)
00510 R4=3*VA/RA*(RA/R0)**3*C1/C2/DW0
00520 DMAT=A1*R2-A2*R1
00530 TD0T1=(DRD-HVW(TA)*(A1*R4-A4*R1))/DMAT+STFA*C7/C6*(A4*R2-A2*R4)
00540 /DMAT)/(STFA*(CPST(PSA,TA)-C3*C4/C6)+(1-STFA)*SHW+WGA*CPG
00550 +HVW(TA)*(A1*R3-A3*R1))/DMAT-STFA*C7/C6*(A3*R2-A2*R3)/DMAT)
00560 STFD0T1=((A1*R3-A3*R1)*TD0T1+A1*R4-A4*R1)/DMAT
00570 PGD1=((A3*R2-A2*R3)*TD0T1+A1*R4-A4*R1)/DMAT

```

TABLE B-1. (Continued)

```

01060 BETA=SQRT((BTS+WGA*BTG)/(1/BTS+WGA/BTG))/(1+WGA)
01070 Q1=Q0*(TSM-TA)/(TSM-T0)*BETA
01080 IF (VA) Q1=Q1*(1+DN*DW0*(1+WGA)*R0**3/RA*AMAX1(VD0T1,0.)/Q0)
01090 ORD=3*Q1/R0/DW0/(1+WGA)*(RA/R0)**N)
01100 WGD1=ALPHA*(1-PGA/PA)/RA*SQRT(GSC/GMW*(TSM+TA+546.32)/2)
01110 A1=C7
01120 A2=PGA*C7
01130 A3=GSC/GMW*WGA-PGA*(C4*C5/PSA+C3/TABS)
01140 A4=GSC/GMW*WGD1*TABS
01150 B1=0.
01160 B2=1.
01170 B3=-C1/C2*(C5/PSA*C4+C3/TABS)
01180 B4=3*VA/RA*(RA/R0)**3*C1/C2/DW0
01190 TD0T1=(ORD-HVW(TA)*B4+(A4*B2-A2*B4)/C6)/(CPST(PSA,TA)-C3*C4/C6
01200 +WGA*CPG+HVW(TA)*B3-(A3*B2-A2*B3)/C6)
01210 PGD1=((A3*B2-A2*B3)*TD0T1+A4*B2-A2*B4)/C7
01220 PSD1=C4*TD0T1
01230 STFDT1=3*VA/RA*(1+1/C2)-C1/C2*TD0T1*(C3/TABS+C5/PSA*C4)
01240 PD0T1=PSD1+PGD1
01250 VD0T1=(PD0T1/RH0C*(1-VA/CSM)-1.5*VA**2*(1-4/3.*VA/CSM)/RA
01260 + (PA-PAM)/DSM/RA)/(1-2*VA/CSM)
01270 IF (TIME-TIMEX) 110,110,105
01280 105 CALL PRNT(2,PA,ACB,TIME,CLA,EMA,EMA/CLA,ACA,WGA,STFA,RA,TA,PA)
01290 TIMEX=TIME
01300 G0 T0 32
01310 110 PRINT 115,FRAC
01320 115 FORMAT(' FRAC=',F5.2)
01330 G0 T0 5
01340 END
01350 SUBROUTINE SOLV(STATE,,JSTOP)
01360 COMMON/A/PA,PSA,PGA,VA,RA,TA,STFA,WGA,CLA,EMA,ACA,
01370 PD0T1,PSD1,PGD1,VD0T1,TD0T1,STFDT1,WGD1,,1
01380 COMMON/B/P,PSB,PGB,V,R,T,STF,WGB,CLB,EMB,ACB,
01390 PD0T2,PSD2,PGD2,VD0T2,TD0T2,STFDT2,WGD2,,2
01400 COMMON/C/DT,TIME,MULT,DSM,DN,N0,GHZ,BTS,BTG,ERR,J0
01410 COMMON/D/PHI,NPHI,AMP,PAM,P0,PAM0,RH0C,CSM,TSM,ALPHA,
01420 R0,T0,DW0,ORD,P1,S1,PSTP,PLIM,NSTOP,VADD,CPG,SHW,GSC,GMW
01430 JSTOP=0
01440 5 I=0
01450 P=PA+PD0T1*DT
01460 V=VA+VD0T1*DT
01470 R=RA+.5*(V+VA)*DT
01480 T=TA+TD0T1*DT
01490 STF=STFA+STFDT1*DT
01500 PSB=PSA+PSD1*DT
01510 PGB=PGA+PGD1*DT
01520 WGB=WGA+WGD1*DT
01530 PHI=PHI+DT/(GHZ/(1+AMP*51N(PHI)))

```

TABLE B-1. (Continued)

```

01540 PAM=PA-PAM7*SIN(PHI)
01550 PDOT2=PDOT1
01560 10 VDOT2=(PDOT2/RHOC*(1-V/CSM)-1.5*V**2/R*(1-4/3.*V/CSM)
01570) +(P-PAM)/DSM/R/(1-2*V/CSM)
01580 V=VA+.5*(VDOT1+VDOT2)*DT
01590 R=RA+.5*(V+VA)*DT
01600 VOL=1/(1+(1-STF)/STF/VST(PSB,T)/DW(P,T))
01610 BETA=SQRT((STF*BTS+WGB*BTG)/(STF/BTS+WGB/BTG))/(STF+WGB)
01620 Q2=Q0*SQRT((1-VOL*(1-BETA))/(1-VOL*(1-1/BETA)))*(TSM-T)/(TSM-T0)
01630 IF (V) Q2=Q2*(1+JN*DW0*(1+WGB)*R0**3/R*4MAX1(VDOT2,0.)/Q0)
01640 JRD=3*Q2/RQ/DW0/(1+WGB)*(R/R0)**N0
01650 WGD2=ALPHA*(1-PGB/P)/R*SQRT(GSC/GMW*(TSM+T+546.32)/2)
01660 WGB=WGA+(WGD1+WGD2)/2*DT
01670 CALL STATE
01680 PDOT2=PGD2+PSD2
01690 T=TA+(TDOT1+TDOT2)/2*DT
01700 PGB=PGA+(PGD1+PGD2)/2*DT
01710 PSB=PSA+(PSD1+PSD2)/2*DT
01720 PBI=PSB+PGB
01730 IF (I-1) 13,17,17
01740 13 I=I+1
01750 P=PBI
01760 G0 T0 10
01770 17 IF (ABS(P/PBI-1.)-ERR) 100,100,20
01780 20 IF (I-20) 40,25,25
01790 25 JSTOP=JSTOP+1
01800 DT=DT/3
01810 IF (JSTOP-3) 5,5,30
01820 30 PRINT, 'POOR SOLUTION, I=',I,' JSTOP=',JSTOP
01830 G0 T0 100
01840 40 I=1+MOD(I,2)
01850 G0 T0 (60,50),J
01860 50 RT1=P/PBI
01870 I=I+1
01880 P=PBI
01890 G0 T0 10
01900 60 RT2=P/PBI
01910 I=I+1
01920 IF (ABS(RT2-RT1)-1.E-08) 65,70,70
01930 65 JSTOP=5
01940 G0 T0 30
01950 70 P=PBI*(1.+RT1*(RT2-1.))*2/(RT2-RT1)
01960 G0 T0 10
01970 100 P=PBI
01980 CLB=CLA+(C1*RA**N0+J2*R**N0)/2*DT
01990 ACB=ACA+DT/RHOC/2*(((P-PAM)*R)**2+((PA-PAM)*RA)**2)
0200 EM9=.5*DSM*R*(V*R)**2
0210 RETURN

```

TABLE B-1. (Continued)

```

02020 END
02030 SUBROUTINE BOIL
02040 EXTERNAL DW,VST,TDTVST,DTPBW,PDVST,BMW,FEW
02050 COMMON/B/P,PSB,PG3,V,R,T,STF,WGB,CLB,EMB,ACB,
02060 PDOT2,PSD2,PGD2,VDOT2,TDOT2,STFDOT2,WGD2,D2
02070 COMMON/D/PHI,NPHI,AMP,PAM,P3,PAM0,RH0C,CSM,FSM,ALPHA,
02080 R0,T0,DW0,DRD,P1,S1,PSTP,PLIM,NST0P,VADD,CPG,SHW,GSC,GMW
02090 CALL EQUATE(C1,DW(P,T),C2,DW(P,T)*VST(PSB,T)-1.,C3,TDTVST(PSB,T),
02100 C4,DTPBW(T),C5,PDVST(PSB,T),C6,4.186E07,C7,VST(PSB,T),
02110 C8,BMW(P),C9,FEW(T),TABS,T+273.16)
02120 A1=STF*C7
02130 A2=PGB*C7
02140 A3=GSC/GMW*WGB-PGB*STF*(C4*C5/PSB+C3/TABS)
02150 A4=GSC/GMW*WGD2*TABS
02160 B1=- (1-STF)/C2/BMW(P)
02170 B2=1.
02180 B3=-STF/C2*C1*(C5/PSB+C4+C3/TABS)+(1-STF)/C2*(C4/BMW(P)-3*FEW(T))
02190 B4=3*V/R*(R/R0)**3*C1/C2/DW0
02200 DMAT=A1*B2-A2*B1
02210 TDOT2=(DRD-HVW(T)*(A1*B4-A4*B1))/DMAT+STF*C7/C6*(A4*B2-A2*B4)
02220 /DMAT)/(STF*(CPST(PSB,T)-C3*C4/C6)+(1-STF)*SHW+WGB*CPG+HVW(T)
02230 *(A1*B3-A3*B1))/DMAT-STF*C7/C6*(A3*B2-A2*B3)/DMAT)
02240 STFDOT2=((A1*B3-A3*B1)*TDOT2+A1*B4-A4*B1)/DMAT
02250 PGD2=((A3*B2-A2*B3)*TDOT2+A4*B2-A2*B4)/DMAT
02260 PSD2=C4*TDOT2
02270 STF=(C1/DW0*(R/R0)**3-1.)/C2
02280 RETURN
02290 END
02300 SUBROUTINE STEAM
02310 COMMON/B/P,PSB,PG3,V,R,T,STF,WGB,CLB,EMB,ACB,
02320 PDOT2,PSD2,PGD2,VDOT2,TDOT2,STFDOT2,WGD2,D2
02330 COMMON/D/PHI,NPHI,AMP,PAM,P3,PAM0,RH0C,CSM,FSM,ALPHA,
02340 R0,T0,DW0,DRD,P1,S1,PSTP,PLIM,NST0P,VADD,CPG,SHW,GSC,GMW
02350 C3=TDTVST(PSB,T)
02360 C5=PDVST(PSB,T)
02370 C6=4.186E07
02380 C7=VST(PSB,T)
02390 TABS=T+273.16
02400 TDOT2=(DRD+GSC/GMW/C6*WGD2*TABS+3*V/R*(R/R0)**3/DW0/C6
02410 *(C3/C5*PSB-PGB))/(CPST(PSB,T)+C3**2/C5/C6*PSB/TABS
02420 +WGB*(CPG-GSC/GMW/C6))
02430 STFDOT2=0.
02440 PSD2=PSB/C5*(3*V/R*(R/R0)**3/DW0-C3/TABS*TDOT2)
02450 PGD2=PGB/TABS*(TDOT2-PGB/GSC/GMW/WGB*3*V/R*(R/R0)**3/DW0
02460 +WGD2*TABS/WGB)
02470 STF=1.
02480 RETURN
02490 END

```

TABLE B-1. (Continued)

```

02500 SUBROUTINE PRNT(N,PA,ACB,X1,X2,X3,X4,X5,X6,X7,X8,X9,X10)
02510 COMMON/D/PHI,NPHI,AMP,PAM,P3,PAM3,RHOC,CSM,FSM,ALPHA,
02520& R3,T0,DW0,TRD,P1,S1,PSIP,PLIM,NSTOP,VA0D,CPG,SHW,GSC,GMW
02530 G0 T0 (S,R5), N
02540 S PMAX=AMAX1(PA,P1)
02550 PMIN=AMIN1(PA,P1)
02560 IF (ABS(ALOG(X10/P1))-PSIP) 7,80,80
02570 7 IF (PA/PMAX-1+PLIM) 30,10,10
02580 10 IF (PMIN/PA-1+PLIM) 30,70,70
02590 30 IF (S1+SIGN(1.,X10-PA)) 50,40,50
02600 40 S1=-S1
02610 G0 T0 80
02620 50 IF ((PA-PAM)*(X10-PAM)) 55,55,70
02630 55 NSTOP=NSTOP+1
02640 G0 T0 85
02650 70 IF (PHI-NPHI*1.5707963) 100,100,75
02660 75 NPHI=NPHI+1
02670 G0 T0 85
02680 80 P1=PA
02690 85 CALL EQUATE(Y1,1000*X1,Y2,12.56637*X2,Y3,12.56637E-07*X3,
02700& Y4,X4/4.186E05,Y5,12.56637E-07*X5,Y6,100*X6,Y7,100*X7,Y8,X8/R3,
02710& Y9,X9,Y10,X10/VA0D)
02720 PRINT 90, Y1,Y2,Y3,Y4,Y5,Y6,Y7,Y8,Y9,Y10
02730 90 FORMAT(F8.2,2F7.0,5F7.2,F7.1,F7.2)
02740 IF ((PA-PAM)*(X10-PAM)) ACB=0.
02750 100 RETURN
02760 END
02770 SUBROUTINE EQUATE(Y1,X1,Y2,X2,Y3,X3,Y4,X4,Y5,X5,Y6,X6,Y7,X7,
02780& Y8,X8,Y9,X9,Y10,X10)
02790 Y1=X1
02800 Y2=X2
02810 Y3=X3
02820 Y4=X4
02830 Y5=X5
02840 Y6=X6
02850 Y7=X7
02860 Y8=X8
02870 Y9=X9
02880 Y10=X10
02890 RETURN
02900 END
02910 SUBROUTINE ADV
02920 COMMON/A/PA,PSA,PGA,VA,RA,TA,STFA,WGA,CLA,EMA,ACA,
02930& PD0T1,PSD1,PGD1,VD0T1,TD0T1,STFD1,WGD1,J1
02940 COMMON/B/PB,PSB,PGB,VB,RB,FB,STFB,WGB,CLB,EMB,ACB,
02950& PD0T2,PSD2,PGD2,VD0T2,TD0T2,STFD2,WGD2,J2
02960 COMMON/C/DELT,TIME,MULT,DSM,IN,NO,THZ,BFS,BTG,ERR,00
02970 PORA=MULT/2.*ABS(PD0T2)/PB

```

TABLE B-1. (Continued)

```

02980 P3R3=MULT/2.*ABS(PD0T2-PD0T1)/DELT/PA
02990 DELT=1/(P3RA+SQR(T(P3RA**2+P3RB)))
03000 DELT=AMINI(DELT,RB*SQR(DSM/PB)/MULT,THZ/MULT)
03010 CALL EQUATE(PA,P9,PSA,PSB,PGA,PGB,VA,VB,RA,RB,TA,TB,STFA,STFB,
03020 WGA,WGB,CLA,CLB,EMA,EMB)
03030 CALL EQUATE(ACA,ACB,PD0T1,PD0T2,PSD1,PSD2,PGD1,PGD2,VD0T1,VD0T2,
03040 TD0T1,TD0T2,STFD0T1,STFD0T2,WGD1,WGD2,01,02,0,0)
03050 RETURN
03060 END
03070 SUBROUTINE SET(IG,FRAC,C1,C2,C3,C4,C5,C6,C7,C8,C9,TA8S)
03080 EXTERNAL DW,VST,DTVST,DTPBW,PDPVST,BMW,TEW
03090 COMMON/A/PA,PSA,PGA,VA,RA,TA,STFA,WGA,CLA,EMA,ACA,
03100 PD0T1,PSD1,PGD1,VD0T1,TD0T1,STFD0T1,WGD1,01
03110 COMMON/B/PB,PSB,PGB,VB,RB,TB,STFB,WGB,CLB,EMB,ACB,
03120 PD0T2,PSD2,PGD2,VD0T2,TD0T2,STFD0T2,WGD2,02
03030 COMMON/C/DELT,TIME,MULT,DSM,ON,N0,THZ,BIS,BIG,ERR,00
03140 F(X,Y)=X+FRAC*(Y-X)
03150 GO TO (10,20),IG
03160 10 CALL EQUATE(VA,F(VA,VB),RA,F(RA,RB),TA,F(TA,TB),PGA,F(PGA,PGB),
03170 WGA,F(WGA,WGB),CLA,F(CLA,CLB),EMA,F(EMA,EMB),ACA,F(ACA,ACB),
03180 STFA,1.,TIME,TIME-(1-FRAC)*DELT)
03190 PSA=PBW(TA)
03200 PA=PSA+PGA
03210 20 CALL EQUATE(C1,DW(PA,TA),C2,DW(PA,TA)*VST(PSA,TA)-1.,
03220 C3,DTVST(PSA,TA),C4,DTPBW(TA),C5,PDPVST(PSA,TA),C6,4.186E07,
03230 C7,VST(PSA,TA),C8,BMW(PA),C9,TEW(TA),TA8S,TA+273.16)
03240 RETURN
03250 END
03260 FUNCTION TEW(T)
03270 A=T-3.98
03280 B=T+273.16
03290 C=EXP(93301.6/B**2)
03300 TEW=1.5399E-06*A*C*(1.-93301.6*A/B**3)/(1.-2.30986E-06*A**2+C)
03310 RETURN
03320 END
03330 FUNCTION BMW(P)
03340 BMW=(30.0E08+P)/.1362
03350 RETURN
03360 END
03370 FUNCTION DW(P,T)
03380 DW=(1.-2.3098E-06*(T-3.98)**2*EXP(93301.6/(T+273.16)**2))*
03390 (1.+(P-1.01325E06)/BMW(.5*(P+1.01325E06)))
03400 RETURN
03410 END
03420 FUNCTION PRW(T)
03430 R=-6104.0774/(T+273.16)
03440 PRW=5.0241171E11*EXP(R*(1.+R*(.0313919+R*(.0015673+.0000234*R))))
03450 RETURN

```

TABLE B-1. (Continued)

```

03460 END
03470 FUNCTION DTPRW(T)
03480 B=-6104.0774/(T+273.16)
03490 C=-B/(T+273.16)
03500 DTPRW=PRW(T)*C*(1.+B*(.0627638+B*(.0047019+.0000952*B)))
03510 RETURN
03520 END
03530 FUNCTION HVW(T)
03540 HVW=595.4-T*(.50667+T*(.000450+T*1.53E-06))
03550 RETURN
03560 END
03570 FUNCTION VST(P,T)
03580 B=(T+273.16)/100
03590 C=P/98.0665
03600 VST=47.06E05*B/C-917.2/B**2.82
03610 IF (T-1200.) 10,10,20
03620 10 VST=VST-C**2*(.13088/B**14.+4.379E10/B**31.6)
03630 20 RETURN
03640 END
03650 FUNCTION TDTVST(P,T)
03660 B=(T+273.16)/100
03670 C=P/98.0665
03680 TDTVST=47.06E05*B/C+2.82*917.2/B**2.82
03690 IF (T-1200.) 10,10,20
03700 10 TDTVST=TDTVST+C**2*(14.*.13088/B**14.+31.6*4.379E10/B**31.6)
03710 20 RETURN
03720 END
03730 FUNCTION PDPVST(P,T)
03740 B=(T+273.16)/100
03750 C=P/98.0665
03760 PDPVST=-47.06E05*B/C
03770 IF (T-1200.) 10,10,20
03780 10 PDPVST=PDPVST-2*C**2*(.13088/B**14.+4.379E10/B**31.6)
03790 20 RETURN
03800 END
03810 FUNCTION CPST(P,T)
03820 B=(T+273.16)/100
03830 C=P/98.0665
03840 CPST=.45493-.0091513*B+.002151*B**2+3.82*6.0575E-05*C/B**3.82
03850 IF (T-1200.) 10,10,20
03860 10 CPST=CPST+C**3*(15.*1.43041E-08/B**15.+32.6*1.08024E04/B**32.6)
03870 20 RETURN
03880 END

```

APPENDIX C

LIMITATIONS OF THE PRESENT MODEL

APPENDIX C**LIMITATIONS OF THE PRESENT MODEL****Introduction**

As pointed out in the text, any computer model of a physical process is an idealization. It is presumed that the deviations of the model from reality are not serious enough to preclude the usefulness of the model for the purpose of investigating the sensitivity of the system behavior to various assumed changes in the system variables. This presumption necessitates making some assessments as to how serious these deviations are, and whether or not it would be worthwhile to modify the model in future work to correct for the significant deviations.

The idealized assumptions made in devising the model are listed below, then discussed individually.

- Uniformity within the globule of
 - Temperature
 - Pressure
 - Composition.
- Radial symmetry
 - Spherical globule
 - Effectively infinite smelt pool.
- Heat and gas input rates chosen, not computed.

Temperature Uniformity

The assumption of the uniformity of temperature at all times throughout the globule was made to facilitate the analysis. For this assumption to be justified, the various components and phases in the globule would at all times have to be in a state of continual and thorough mixing. For the main explosion, thorough and rapid mixing with injected smelt is presumed to be the mechanism for obtaining the needed high initial rate of heat input. The continuation of strong convective mixing would be required to maintain temperature uniformity throughout the development of the model main explosion and also of the triggering mechanism. It is not known how valid is the assumption of the existence of sufficient mixing to maintain temperature uniformity and temperature equilibrium between the various components and phases of the globule contents throughout the entire time span of interest.

The ordinary processes of heat conduction are far too slow to obtain temperature homogeneity throughout the globule. The thermal diffusivity of water (ratio of thermal conductivity to density times specific heat) is only $0.0014 \text{ cm}^2/\text{sec}$. For changes that occur on a

millisecond time scale, temperature uniformity would exist only on the distance scale of 1.2×10^{-3} cm. For both steam and for CO_2 gas at atmospheric pressure, the value of the thermal diffusivity is about 110 times that for liquid water. In the expanded phase of the small triggering globule the time scale for temperature changes is about 50 milliseconds for a 1-cm-radius globule and the average pressure is about 0.5 atmosphere. The thermal diffusivity under these conditions is about $0.3 \text{ cm}^2/\text{sec}$. Heat conduction would then be rapid enough to result in temperature uniformity on a scale of only about 0.12 cm. The situation is better for smaller globules since the time scale of events is proportional to the globule size and the diffusion length varies as the square root of the time scale. Exchange of heat by thermal radiation is also nowhere nearly rapid enough at the temperatures involved to ensure temperature uniformity.

The obvious improvement in the model needed to take into account the possibility that temperature is a function of distance from the globule center is to set up a layered shell structure for the model. The model would have to include some assumptions as to the mechanism, largely convective, by which heat, mass, and momentum are transferred from one layer to the next. The complexity and cost of the computations with the improved model would be considerably increased.

Pressure Uniformity

As to the propagation of acoustic waves, pressure uniformity is a reasonably fair assumption. The speed of sound propagation in water is about 1.5×10^5 cm/sec. It takes only tens of microseconds for sound to traverse globules of the size range of interest, hence acoustic wave effects in the globule can be ignored as long as the globule essentially consists of liquid water. The speed of sound propagation in steam is 0.4×10^5 cm/sec, and in CO_2 it is 0.3×10^5 cm/sec. Even though the globules are larger when they consist wholly of steam and CO_2 , sound-propagation effects can still be ignored because of the increased time scale of temperature and pressure changes when the globules are larger.

When the globule consists of only a few percent steam or gas, the sound-propagation velocity can be very much lower than for pure liquid or gas alone. This is because the average density is about the same as that of the liquid phase but the average bulk modulus is close to that of the gas or vapor phase. Anomalously high values of sound absorption can also occur in this region for certain frequencies, depending upon the size distributions of the gas or vapor bubbles. As the globule traverses the region of part steam and gas and part water, it may well be a poor assumption to ignore sound-wave-propagation effects.

Unlike the interior of the globule, sound-wave-propagation effects in the smelt are explicitly taken into account in the model. However, these effects make only a few percent difference in the radial acceleration of the globule surface; in other words, the smelt may be considered to be incompressible in the time scales of interest.

The superposition of the acoustic pressure waves within the globule as they reflect partially from the globule periphery results in a radial pressure distribution, given sufficient time for these multiple reflections to occur compared to the time scale of changing events, determined by the inertial reaction of the globule material to radial acceleration. This resultant pressure distribution would be uniform only if this inertial reaction were negligible. The model neglects inertia effects for the globule materials, although taking them into account for the surrounding smelt.

If the globule were macroscopically homogeneous (that is, each shell contained the same proportions of liquid water, steam, and gas) and if it expanded and contracted uniformly (no appreciable acoustic wave-propagation effects, as discussed above), the radial acceleration of any element of globule material would be proportional to its radial position. A pressure gradient equal to $-\rho_g a_s r/r_s$ would exist within the globule, where ρ_g is the average density of the globule material, and a_s is the value of the acceleration at the periphery of the globule, of radius r_s . The pressure distribution within the globule would then be given by

$$p = p_s + (\rho_g a_s r_s/2) (1 - r^2/r_s^2) \quad (C-1)$$

The pressure at the center of the globule would then be greater than that at the periphery by the amount $\rho_g a_s r_s/2$. The value of a_s , as given by lines 1560-1570 of the computer program, is

$$a_s = (p_s - p_o)/\rho r_s - 1.5 v_s^2/r_s \quad (C-2)$$

where p_o is the ambient pressure, ρ the smelt density and v_s the radial velocity of the globule periphery. Hence, the difference in pressure between the center and outer surface of the globule

$$\Delta p_g = .5(\rho_g/\rho) (p_s - p_o) - .75 \rho_g v_s^2 \quad (C-3)$$

It is to be noted that Δp_g is independent of the globule radius.

For the first (resistance to water expansion) pulse of Figure 9, v_s is negligible and the pressure at the center of the globule exceeds that at its periphery by about one fourth of the difference between the peripheral pressure and ambient, since ρ_g/ρ is about 1/2. Δp_g can thus be as great as 12 atmospheres for this pulse. However, although the assumption of pressure uniformity in the globule is a very poor one at this time, it makes no essential difference in the dynamics of the problem because of the high bulk modulus of water. At the other extreme, when 100 percent steam is reached at 7.2 milliseconds, Δp_g is only -0.013 atmosphere because of the low density of steam, even if $p_s = 7.5$ atmospheres. The assumption of pressure uniformity is seen to be good when the globule is all steam and gas.

The assumption of pressure uniformity is poorest for the intermediate case, when the globule is part liquid water and part vapor and gas. At the computed pressure peak of 130 atmospheres in Figure 9, $\Delta p_g = 14$ atmospheres. Steam would be formed much more rapidly at the periphery of the globule than at its center because of the difference in boiling points between these two locations. The assumptions of temperature and composition uniformity would also necessarily be invalid in this intermediate situation.

Composition Uniformity

The question of composition uniformity throughout the globule has essentially been considered in the above discussions of pressure and temperature uniformity. Composition uniformity would ordinarily be a poor assumption for the intermediate case when the globule consists of part liquid water and part water vapor and gas.

One other aspect of composition of the globule is not taken into account in the model. As a result of the model computations for the main explosion, it was concluded that rapid injection

December 5, 1973

✓ Project 2419

Dear Malcolm:

Thanks kindly for forwarding to us a copy of the Battelle Institute report completed earlier this year at the conclusion of their Smelt-Water Explosion Research program. This will be helpful to our staff here and particularly if we are called upon to do any further work in this area. I expect to meet with Rodney Boren today, and I will be interested in learning from him the subsequent action that FKI believes should be taken. I note that your committee recommended additional work for the future.

Sincerely,

John C. Wollwage
Vice President-Research

Dr. M. L. Taylor
Chairman, FKI Smelt-Water
Technical Committee
c/o Union Camp Corporation
1600 Valley Road
Wayne, New Jersey 07470

JCW/cmb

YS: Strange, Holm, Brezinski

of a pound of smelt into a pound of water is required to obtain the needed high initial rate of best input. However, the model does not take into account the effects of this internal smelt content on the dynamics of the globule.

Radial Symmetry of Globule Motion

Only radial expansion and contractions of the globule are considered in the model. The action of the presumed triggering mechanism, however, depends upon the instability of radial motion that can become significant in the latter stages of the collapse phase. The model takes no account of the effects on globule dynamics of departure from radial symmetry. The model does include, however, some provision for an increase in heat input rate at the critical instability stage (lines 760, 1080, and 1630 of the computer program) because of the expected increase in surface-contact area with the smelt resulting from the shape distortions and turbulence.

The limitation of the model to radial expansion and contraction does not permit computation of the effects of rectilinear motion of the globule superimposed on these radial expansions and contractions. Such a rectilinear motion would result, for example, from the bouyant force on a submerged globule. A globule of water on the upper free surface of the smelt would also not be in the form of a sphere unless it were extremely small.

Infinite Smelt Bed Approximation

The assumption that the globule is surrounded by an effectively infinite pool of smelt makes the effect of the smelt on the globule dynamics comparatively easy to compute. However, it is a poor assumption except for extremely small globules immersed in an actual smelt bed.

Figures 9 and 10 present some basic information regarding the dynamics of the main explosion, obtained on the infinite smelt bed assumption. The text includes qualitative discussion as to the possible modifications in the results because of proximity to the globule of the free surface of the smelt and of the bottom and sides of the container, specifically regarding the rate of heat input needed to obtain an explosion and the severity of the resultant explosion. The tacit assumption is made in this procedure that the free surface and container effects are of second order. However, this is not the case for a 3.75-in.-diam globule. The free surface and container boundary conditions on the smelt would begin to affect the globule dynamics appreciably at a very early stage of the computations. As a consequence, it would be wrong to attempt to relate the results of the model computations quantitatively to actual cases of smelt-water explosions. The basic physical phenomena, the sequence of events, and the order of magnitudes of the results predicted by the model are, however, expected to be applicable to the actual situation.

Heat and Gas Input Rates

In the present model, the initial heat- and gas-input rates are arbitrarily selected prior to computing instead of being determined by the physical and chemical considerations of the

APPENDIX D

FORMULATION OF DIMENSIONLESS PARAMETERS

APPENDIX D

FORMULATION OF DIMENSIONLESS PARAMETERS

Conservation of Energy Equation

This equation describes how the heat input to the steam-water-gas globule is apportioned among the enthalpy increases of these components and the conversion of water to steam, as follows:

$$(3/R_o \rho_{w_o}) Q = q_s + q_w + q_g + L_w(T) \cdot \dot{F}_s \quad (D-1)$$

Q is the rate of heat input to the globule per unit initial apparent outer surface area. The quantity on the left side of Equation (D-1) thus represents the rate of heat input per unit total mass of H₂O, the constant sum of the liquid water and steam masses. R_o is the initial radius of the globule and ρ_{w_o} is the initial water density. The quantities q_s, q_w, and q_g are, respectively, the rates of increase of enthalpy (internal heat plus mechanical energy) of the steam, liquid water and gas components, each per unit total mass of H₂O. The last term on the right is the rate of heat input to the process of conversion of liquid water to steam, where L_w(T) is the latent heat of water as a function of temperature T and \dot{F}_s is the time rate of change of the steam fraction F_s, the mass fraction of the H₂O in the vapor phase.

The quantity q_s is given by the well-known thermodynamic relationship:

$$q_s = F_s \{ C_{ps}(P_s, T) \dot{T} - T [\partial V_s(P_s, T)/\partial T]_p \dot{P}_s/J \} \quad (D-2)$$

where C_{ps}(P_s, T) is the constant pressure specific heat of steam as a function of the steam partial pressure P_s and T. \dot{T} is the rate of increase of temperature of the globule; all components and phases in the globule are assumed to be in thermal equilibrium at all times. $[\partial V_s(P_s, T)/\partial T]_p$ is the temperature derivative at constant pressure of the volume per unit mass of steam (reciprocal density) as a function of P_s and T. \dot{P}_s is the time rate of change of P_s and J is the mechanical equivalent of heat.

The quantity q_w is given by

$$q_w = (1 - F_s) \cdot C_{pw} \dot{T} \quad (D-3)$$

where C_{pw} is the specific heat of liquid water. The rate of work done in expanding the water is also included in the computer program for the sake of completeness but is omitted in these dimensional analysis considerations because it is negligibly small by comparison with C_{pw} \dot{T} .

Finally, the quantity q_g is given by

$$q_g = w_g \{ C_{pg} \dot{T} + V_g(P_g, T) \dot{P}_g/J \} \quad (D-4)$$

where w_g is the ratio of the mass of gas (CO_2) in the system to the total mass of H_2O . C_{pg} is the (constant) specific heat of the gas at constant pressure and $V_g(P_g, T)$ is the reciprocal density of the gas as a function of the gas partial pressure P_g and T . Equation (D-4) is the special form of the thermodynamic relation expressed by Equation (D-2) that is applicable to an ideal gas. The CO_2 in the globule was assumed to be an ideal gas at the temperatures and pressures in question whereas the actual equations of state of steam were used in the computer analysis.

Each computational case begins with the selected initial values Q_o , T_o , P_o , R_o , and w_{go} of the corresponding variables. The computer determines the initial partial pressures of CO_2 and of steam and the initial steam fraction corresponding to P_o , T_o , and w_{go} . As time progresses, Q is programmed to depart from Q_o by a factor that depends upon the temperature difference between the smelt and the globule and to decrease with increases in w_g and F_s . As gas enters the globule, the total mass of material in the globule at any time becomes $(1 + w_g)$ times the constant total mass of H_2O .

The initial values Q_o , T_o , P_o , and R_o are convenient and meaningful scale factors for rendering the dependent variables Q , T , P , and R , respectively, dimensionless. The dependent variables w_g and F_s are already dimensionless. The suitable scale factor for the independent variable, the time t , is a characteristic time constant given by

$$t_c = R_o \sqrt{\rho_{sm}/P_o} \quad (\text{D-5})$$

where ρ_{sm} is the density of the smelt. The quantity t_c is obtained from the conservation of momentum equation discussed later. It is to be noted that t_c is proportional to R_o and inversely proportional to the square root of P_o . The quantity ρ_{sm} varies little from one smelt composition to the next. For $R_o = 1 \text{ cm}$, $\rho_{sm} = 2.0 \text{ gm/cm}^3$ and $P_o = 10^6 \text{ dynes/cm}^2$ (1 atmosphere), $t_c = 1.414$ milliseconds.

In terms of $\tau = t/t_c$, Equation (D-1) becomes

$$\begin{aligned} (3 Q_o/R_o \rho_{wo}) (Q/Q_o) = F_s \left\{ (C_{ps} T_o/t_c) \frac{\partial}{\partial \tau} \left(\frac{T}{T_o} \right) - T \left(\frac{\partial V_s}{\partial T} \right)_p (P_o/t_c J) \frac{\partial}{\partial \tau} \left(\frac{P_s}{P_o} \right) \right\} \\ + (1 - F_s) (C_{pw} T_o/t_c) \frac{\partial}{\partial \tau} \left(\frac{T}{T_o} \right) \\ + (w_g \left\{ (C_{pg} T_o/t_c) \frac{\partial}{\partial \tau} \left(\frac{T}{T_o} \right) + V_g (P_o/t_c J) \frac{\partial}{\partial \tau} \left(\frac{P_g}{P_o} \right) \right\}) \\ + \left\{ L_w(T)/t_c \right\} \frac{\partial}{\partial \tau} (F_s) \quad (\text{D-6}) \end{aligned}$$

Equation (D-6) would become dimensionless by dividing both sides by any one of the coefficients of the τ derivatives of the scaled dependent variables. The most significant term on the right side for the main explosion is presumably the last one, since it represents the rate at which heat energy is used to generate steam. Dividing through by the initial value of its coefficient, $L_w(T_o)/t_c$ and using Equation (D-5) for t_c results in:

$$\begin{aligned}
\{3 Q_o \sqrt{\rho_{sm}/P_o}/\rho_{wo} L_w(T_o)\} \left(\frac{Q}{Q_o}\right) &= [T_o/L_w(T_o)] \cdot [F_s C_{ps} + (1 - F_s) C_{pw} \\
&+ w_g C_{pg}] \frac{\partial}{\partial \tau} \left(\frac{T}{T_o}\right) + [P_o/J L_w(T_o)] \\
&\cdot \left[-T \left(\frac{\partial v_s}{\partial T}\right)_p \frac{\partial}{\partial \tau} \left(\frac{P_s}{P_o}\right) + v_g \frac{\partial}{\partial \tau} \left(\frac{P_g}{P_o}\right) \right] \\
&+ [L_w(T)/L_w(T_o)] \left(\frac{\partial F_s}{\partial \tau}\right) \quad (D-7)
\end{aligned}$$

The bracketed coefficient of the (Q/Q_o) term on the left,

$$A = 3 Q_o \sqrt{\rho_{sm}/P_o}/\rho_{wo} L_w(T_o) \quad (D-8)$$

is a significant dimensionless parameter for the model explosion. The several other dimensionless coefficients of the dimensionless dependent variables and their t derivatives on the right, for example, the first one $[T_o/L_w(T_o)] \cdot C_{ps}(P_s, T)$ are parameters that represent dimensionless ratios of various properties of liquid water, steam, and the gas as functions of partial pressure and temperature.

Conservation of Momentum Equation

This equation describes the radial motion of the globule wall in response to the pressure changes in the globule, as follows:

$$\dot{v} = \dot{P}/\rho_{sm} c_{sm} + (P - P_o)/\rho_{sm} R - \frac{3}{2} v^2/R \quad (D-9)$$

where \dot{v} is the time rate of change of the radial velocity v , \dot{P} is the time rate of change of the pressure $P = P_s + P_g$, and $c_{sm} = \sqrt{K_{sm}/\rho_{sm}}$ is the velocity of propagation of an acoustic pressure wave in the smelt. K_{sm} is the bulk modulus of the smelt.

The first term on the right represents a contribution to the acceleration that is in phase with the rate of change of pressure. This term is responsible for the acoustic energy that is radiated into the "far-field" and is not returned to the globule. The second term represents an acceleration that is proportional to the pressure change. The resultant "near-field" kinetic energy is exchanged back and forth with the potential energy in the globule as the latter expands and collapses. The third, nonlinear, term represents a deceleration resulting from the redistribution of near-field energy in the smelt as the globule expands and contracts. Certain minor terms involving the small ratio v/c_{sm} , the Mach number, have been omitted in Equation (D-9) for simplicity but not omitted in the computer model.

The results of many computations made with the computer model over wide ranges of conditions have shown the maximum values of the second term to be two to three orders of magnitude greater than those of the first term. Division by $P_o/\rho_{sm} R_o$ is thus indicated to be the proper way to render Equation (D-9) dimensionless. This results in

$$\dot{v}_{sm} R_o/P_o = \dot{P} R_o/P_o c_{sm} + (P/P_o - 1) (R_o/R) - v^2 \rho_{sm} R_o/R P_o \quad (D-10)$$

Since \dot{v} has the physical dimensions of length/(time)², and R_o is the proper scale factor for length, then the suitable scale factor for time, as obtained from the conservation of momentum equation, is t_c given by Equation (D-5). In terms of $\tau = t/t_c$ Equation (D-10) becomes

$$\frac{\partial}{\partial \tau} \left(\frac{vt_c}{R_o} \right) = \sqrt{\frac{P_o}{K_{sm}}} \cdot \frac{\partial}{\partial \tau} \left(\frac{P}{P_o} \right) + (P/P_o - 1) (R_o/R) - \left(\frac{vt_c}{R_o} \right)^2 (R_o/R) \quad (D-11)$$

Conservation of momentum considerations have thus yielded not only the proper scaling factor for time but also another dimensionless parameter $\sqrt{P_o/K_{sm}}$. This numerically small quantity does not constitute a significant parameter, since in all practical applications of interest P_o would be close to atmospheric pressure and $K_s = \rho_{sm} c_{sm}^2$ does not vary a great deal from one melt composition to the next.

Conservation of Mass Equation

The conservation of mass equation is expressed in the form:

$$\frac{F_s \cdot V_s(P_s, T) + (1-F_s)/D_w(P, T)}{F_s \cdot V_s(P_{s0}, T_o) + (1-F_{s0})/D_w(P_o, T_o)} = \left(\frac{R}{R_o} \right)^3 \quad (D-12)$$

Multiplication of both the numerator and denominator of Equation (D-12) by the constant total mass of water results in

$$\frac{\text{Volume of steam} + \text{Volume of liquid water (at time } t)}{\text{Volume of steam} + \text{Volume of liquid water (initially)}} = \left(\frac{R}{R_o} \right)^3$$

Equation (D-12) is explicitly independent of w_g , since the gas occupies the same volume as the steam. In other words,

$$F_s \cdot V_s(P_s, T) = w_g V_g(P_g, T) \quad (D-13)$$

The pressure $P = P_s + P_g$.

The time derivatives of Equations (D-12) and (D-13) are used by the computer to relate the quantities \dot{F}_s , \dot{w}_g , \dot{P}_s , \dot{P}_g , \dot{T} , and \dot{v} . Denoting the denominator of Equation (D-12) by D_{A12} , we have

$$\left(V_s - \frac{1}{D_w} \right) \dot{F}_s + \left[F_s \frac{\partial V_s}{\partial T} - \frac{(1-F_s)}{D_w^2} \frac{\partial D_w}{\partial T} \right] \dot{T} + F_s \frac{\partial V_s}{\partial P_s} \dot{P}_s - \frac{(1-F_s)}{D_w^2} \frac{\partial D_w}{\partial P} \dot{P} = 3 \left(\frac{R}{R_o} \right)^2 \frac{v}{R_o} \quad (D-14)$$

$$V_s \dot{F}_s + F_s \left(\frac{\partial V_s}{\partial T} \dot{T} + \frac{\partial V_s}{\partial P_s} \dot{P}_s \right) = V_g \dot{w}_g + w_g \left(\frac{\partial V_g}{\partial T} \dot{T} + \frac{\partial V_g}{\partial P_g} \dot{P}_g \right) \quad (D-15)$$

The quantities $\partial D_w/\partial T$ and $\partial D_w/\partial P$ are readily expressible in terms of the thermal expansion coefficient and bulk modulus of water. The temperature and pressure derivatives of V_s and V_g are obtainable from the equations of state described in the following section of this report. Of course, as long as any liquid water remains in the globule in thermal equilibrium with the steam, P_s is a function of T and \dot{P}_s and \dot{T} are related through the temperature derivative of this function.

Equations (D-14) and (D-15) are readily expressible in dimensionless forms by application of the scaling factors on the various dependent variables and on the independent variable (time) previously discussed. A number of dimensionless parameters of relatively minor significance are obtained thereby; they represent ratios of various properties of steam, liquid water, and gas. However, since \dot{w}_g in Equation (D-15) is not a computed dependent variable but a specified input to the computer program, the dimensionless parameter

$$B = \dot{w}_g t_c = \dot{w}_g R_o \sqrt{\rho_{sm}/P_o} \quad (D-16)$$

is significant. It represents the mass of gas admitted to the globule in the characteristic time period t_c relative to the total mass of H_2O in the globule.

Constitutive Equations

The constitutive equations are the equations of state of liquid water and steam, the relationships among density, pressure, and temperature discussed in Appendix B, including the P-T characteristic for steam and water in thermal equilibrium. Also discussed in Appendix B is the equation of state for the CO_2 gas that enters the globule from the smelt. No significant dimensionless parameters were obtained by expressing the various constitutive equations in dimensionless form.